

Responsive polymer photonics

Citation for published version (APA):

Stumpel, J. E. (2014). *Responsive polymer photonics*. [Phd Thesis 1 (Research TU/e / Graduation TU/e), Chemical Engineering and Chemistry]. Technische Universiteit Eindhoven. <https://doi.org/10.6100/IR780943>

DOI:

[10.6100/IR780943](https://doi.org/10.6100/IR780943)

Document status and date:

Published: 01/01/2014

Document Version:

Publisher's PDF, also known as Version of Record (includes final page, issue and volume numbers)

Please check the document version of this publication:

- A submitted manuscript is the version of the article upon submission and before peer-review. There can be important differences between the submitted version and the official published version of record. People interested in the research are advised to contact the author for the final version of the publication, or visit the DOI to the publisher's website.
- The final author version and the galley proof are versions of the publication after peer review.
- The final published version features the final layout of the paper including the volume, issue and page numbers.

[Link to publication](#)

General rights

Copyright and moral rights for the publications made accessible in the public portal are retained by the authors and/or other copyright owners and it is a condition of accessing publications that users recognise and abide by the legal requirements associated with these rights.

- Users may download and print one copy of any publication from the public portal for the purpose of private study or research.
- You may not further distribute the material or use it for any profit-making activity or commercial gain
- You may freely distribute the URL identifying the publication in the public portal.

If the publication is distributed under the terms of Article 25fa of the Dutch Copyright Act, indicated by the "Taverne" license above, please follow below link for the End User Agreement:

www.tue.nl/taverne

Take down policy

If you believe that this document breaches copyright please contact us at:

openaccess@tue.nl

providing details and we will investigate your claim.

Responsive polymer photonics

PROEFSCHRIFT

ter verkrijging van de graad van doctor aan de Technische Universiteit Eindhoven, op gezag van de rector magnificus prof.dr.ir. C.J. van Duijn, voor een commissie aangewezen door het College voor Promoties, in het openbaar te verdedigen op donderdag 6 november 2014 om 16:00 uur

door

Jelle Eduard Stumpel

geboren te Tilburg

Dit proefschrift is goedgekeurd door de promotoren en de samenstelling van de promotiecommissie is als volgt:

voorzitter:	prof.dr.ir. J.C. Schouten
1 ^e promotor:	prof.dr. A.P.H.J. Schenning
2 ^e promotor:	prof.dr. D.J. Broer
leden:	prof.dr. D. Diamond (Dublin City University) dr. N. Katsonis (University of Twente) prof.dr.ir. J.M.J. den Toonder prof.dr.ing. C.W.M. Bastiaansen (Queen Mary University of London)
adviseur:	dr. A.C.C. Esteves

Er zijn veel mooie spreuken, maar je moet ze wel weten te vinden
- Veronica Huisman, levensgenietster -

A catalogue record is available from the Eindhoven University of Technology
Library

ISBN: 978-90-386-3706-8

Copyright © 2014 by Jelle Eduard Stumpel

The research described in this thesis has been financially supported by the
Netherlands Organisation for Scientific Research, Chemical Sciences (NWO-CW),
file number 700.57.444

Table of contents

Summary	IX
Chapter 1 Introduction	- 1 -
1.1 Introduction	- 2 -
1.2 Photoresponsive polymer coatings	- 3 -
1.2.1 <i>Photoresponsive surface topographies</i>	- 3 -
1.2.2 <i>Photoresponsive wettability</i>	- 7 -
1.2.3 <i>Photoresponsive cell adhesion</i>	- 9 -
1.3 Polymer coatings with responsive optical properties	- 9 -
1.3.1 <i>Chemically responsive photonic polymers</i>	- 10 -
1.3.2 <i>Humidity-responsive photonic polymers</i>	- 14 -
1.3.3 <i>pH-responsive photonic polymers</i>	- 15 -
1.3.4 <i>Temperature-responsive photonic polymers</i>	- 16 -
1.4 Aim and outline of this thesis	- 17 -
References	- 20 -
Chapter 2 Photoresponsive hydrogel surface topographies in an acidic environment	- 25 -
2.1 Introduction	- 26 -
2.2 Results and discussion	- 27 -
2.2.1 <i>Synthesis and copolymerisation of spiropyran monoacrylate (SPA)</i>	- 27 -
2.2.2 <i>Photoresponse of the linear copolymer PNS</i>	- 28 -
2.2.3 <i>Preparation and photoresponse of freestanding crosslinked polymer network films</i>	- 29 -
2.2.4 <i>Preparation and photoresponse of substrate-attached surface topographies</i>	- 34 -
2.3 Conclusion	- 37 -
Experimental section	- 37 -
References	- 42 -

Chapter 3	Photoresponsive hydrogel ratchet topographies in a neutral environment	- 45 -
3.1	Introduction	- 46 -
3.2	Results and discussion	- 47 -
3.2.1	<i>Preparation and photoresponse of surface-constrained hydrogel films</i>	- 47 -
3.2.2	<i>Symmetric, photoresponsive surface topographies by polymerisation-induced diffusion</i>	- 51 -
3.2.3	<i>Asymmetric, photoresponsive surface topographies on pre-structured substrates</i>	- 52 -
3.3	Conclusion	- 55 -
	Experimental section	- 55 -
	References	- 58 -
Chapter 4	Water-responsive optical surface topographies based on cholesteric liquid crystals	- 61 -
4.1	Introduction	- 62 -
4.1.1	<i>Cholesteric liquid crystals</i>	- 62 -
4.2	Results and discussion	- 65 -
4.2.1	<i>Preparation and characterisation of water-responsive CLC polymer salt coatings</i>	- 65 -
4.2.2	<i>Preparation and characterisation of patterned isotropic-CLC polymer coatings</i>	- 68 -
4.2.3	<i>Preparation and characterisation of bicoloured CLC polymer coatings</i>	- 71 -
4.3	Conclusion	- 73 -
	Experimental section	- 74 -
	References	- 76 -
Chapter 5	Humidity-responsive optical surface topographies based on interpenetrating polymer networks	- 79 -
5.1	Introduction	- 80 -
5.2	Results and discussion	- 82 -
5.2.1	<i>Prerequisites for the preparation of a sequential cholesteric IPN</i>	- 82 -
5.2.2	<i>Formation and activation of a cholesteric IPN</i>	- 85 -
5.2.3	<i>Response of the activated cholesteric IPN to humidity</i>	- 89 -
5.2.4	<i>Patterned cholesteric IPN coatings</i>	- 90 -
5.3	Conclusion	- 93 -
	Experimental section	- 93 -
	References	- 96 -

Chapter 6	Amine-responsive hydrogen-bonded cholesteric liquid crystal coatings as a sensor	- 99 -
6.1	Introduction	- 100 -
6.2	Results and discussion	- 101 -
6.2.1	<i>Preparation and characterisation of inkjet-printed CLC coatings</i>	- 101 -
6.2.2	<i>Control experiment: response of the CLC sensor to pure water vapour</i>	- 103 -
6.2.3	<i>Response of the CLC sensor to pure TMA</i>	- 103 -
6.2.4	<i>Response of the CLC sensor to TMA at high humidity</i>	- 106 -
6.2.5	<i>Proof of principle: detecting fish decay</i>	- 108 -
6.3	Conclusion	- 109 -
	Experimental section	- 109 -
	References	- 111 -
Chapter 7	Technology assessment	- 115 -
7.1	Introduction	- 116 -
7.2	Photoresponsive hydrogel surface topographies	- 116 -
7.2.1	<i>Microfluidics</i>	- 116 -
7.2.2	<i>Cell culturing</i>	- 117 -
7.3	Responsive cholesteric coatings	- 118 -
7.3.1	<i>Enantioselective sensing</i>	- 118 -
7.3.2	<i>Analyte-selective sensing (molecular imprinting)</i>	- 120 -
7.4	Spiropyran derivatives for other applications	- 121 -
7.5	Conclusion	- 123 -
	References	- 124 -
	Samenvatting	- 127 -
	List of publications	- 131 -
	Acknowledgements/dankwoord	- 133 -
	Curriculum Vitae	- 137 -

Summary

Responsive polymer photonics

Polymer coatings are of major importance in everyday life. Most of the surfaces that we use daily have been modified with a protective or aesthetic coating. However, the majority of these coatings are static. In other words, they are not responsive to external influences. It is expected that responsive coatings will play an important role in meeting social challenges in the fields of sustainable energy, health care and food safety.

The research described in this thesis focuses on the development of responsive materials that operate in a reversible way. Photoresponsive and stimulus-responsive photonic coatings were prepared. The first type of coating undergoes photo-induced topographical alterations; coatings in the second category change colour upon exposure to a specific stimulus. Both types are based on liquid crystal or hydrogel-based materials and, in both cases, the response is a dimensional alteration that leads to changes in the initial surface topography and/or colour. Chapter 1 gives an overview of the stimuli-responsive photonic coatings that have been produced in the past.

Chapter 2 describes the use of light-induced topographical changes in a crosslinked poly(*N*-isopropylacrylamide)-spiropyran hydrogel coating. When this coating is placed in an acidic environment, the spiropyran derivative spontaneously changes into its protonated merocyanine isomer. Exposure to visible light then results in back-isomerisation into the spiropyran form. The protonated merocyanine species is hydrophilic and its spiropyran isomer is hydrophobic. Spiropyran-based polyNIPAAm hydrogels therefore undergo a light-induced hydrophilicity change, resulting in an alteration in the dimensions of the hydrogel. The degree of swelling and shrinkage in the hydrogel depends on the crosslink density of the material. Polymerisation-induced diffusion was used to control the spatial crosslink density in a hydrogel coating. This results in a corrugated structure after the material was swelled in a slightly acidic aqueous solution. Photo-exposure resulted in a reversible reduction of the height of this surface topography.

Chapter 3 describes photoresponsive hydrogels that operate at neutral pH. In these hydrogels, acrylic acid acts as an internal proton source, resulting in a hydrogel coating that is photoresponsive in a neutral environment. Polymerisation-induced diffusion was used to obtain responsive surface topographies of the kind described in Chapter 2. Moreover, asymmetric ratchet-like structures were prepared using a pre-structured substrate. In this system, the asymmetric change of the surface topography is a result of variation in the thickness of the hydrogel. The extent of the photo-induced alteration of the coating can be controlled by adjusting the crosslink density of the hydrogel.

Chapter 4 reports on responsive photonic coatings based on cholesteric liquid crystals (CLCs). In this liquid crystalline phase, an alternating refractive index change through the material results in the partial reflection of the incident light. Water-responsive surface topographies were prepared in which the hydrogen-bonded supramolecular polymer coating had alternating regions with a CLC or an isotropic alignment. Treatment with an alkaline solution led to the disruption of the hydrogen bonds and the formation of carboxylates. Due to the hygroscopic nature of these moieties, the materials swelled when placed in water. Interestingly, the isotropic areas swelled uniformly, while the CLC areas mostly swelled unidirectionally. The structure of the surface topography was therefore accentuated after placement in water. A change in the helical pitch of the CLC region also led to a different reflected colour, while the isotropic areas are colourless in both the dry and the swollen state. Additionally, coatings were prepared that underwent dual-coloured patterned changes when placed in water. A novel approach was used to produce the humidity-responsive optical sensors with a broad operational range presented in Chapter 5. An interpenetrating polymer network (IPN) which combines CLC-based materials with hydrogels was used for this coating. A cholesteric polymer network was swollen with an acrylic acid-based mixture which was subsequently photopolymerised. The activation of this coating with an alkaline solution led to the formation of a hygroscopic potassium polyacrylate network in the CLC scaffold. Humidity-dependent volumetric changes in this IPN network led to a relative large colour change. Moreover, an IPN with a responsive surface topography was prepared. This coating consisted of regions containing both responsive potassium acrylate areas

and static polystyrene areas. Depending on the relative humidity, the surface became flat or structured.

Chapter 6 presents the fabrication of a hydrogen-bonded CLC coating which responds to gaseous trimethylamine (TMA), a substance produced by decay in fish. Like the alkaline treatment, TMA deprotonates the carboxylic acids in the material and carboxylate salts are formed. Under anhydrous conditions, this salt formation causes a decrease in the molecular order that results in a colour loss. However, the coating swells under humid conditions, resulting in a clearly visible colour change from green to red.

Overall, this thesis shows that responsive photonic coatings can be produced that are of interest for a range of applications. The technology assessment in Chapter 7 discusses some of these applications in greater detail. The development of photoresponsive coatings has considerable potential for applications ranging from microfluidic devices to cell culturing. Turning to the use of responsive photonic coatings as sensors, preliminary results are presented which are expected to improve the selectivity of the sensor. Finally, the photochromic behaviour of spiropyran is discussed as a way of preparing smart windows and writable optical materials.

Chapter 1

Introduction

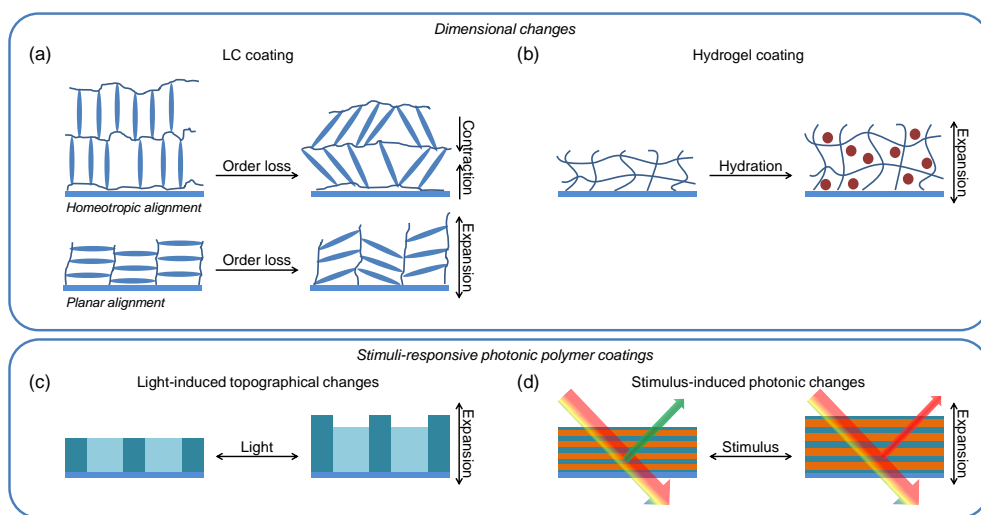
Abstract

This thesis discusses innovative approaches to polymer-based photonic coatings, with the present chapter presenting an overview of developments in this field. The coatings in question can change their topological properties in a reversible, dynamic way when exposed to an external stimulus. This thesis will first describe photoresponsive coatings that change their surface topography and therefore their functional properties, such as wettability, upon exposure to light. Photonic coatings in which exposure to a certain trigger leads to an optical response will then be discussed. A change in the dimensions of these coatings triggered by a stimulus results in an alteration of their photonic properties. These two kinds of materials have a shared property: a stimulus leads to a volumetric and/or dimensional change. The final section of the present chapter sets out the aims of the research and the structure of this thesis.

This chapter is partially reproduced from: J. E. Stumpel, D. J. Broer and A. P. H. J. Schenning, *Chemical Communications*, 2014, Accepted manuscript.

1.1 Introduction

Polymer coatings play an important role in our society. They protect everyday objects from environmental influences. Coatings are also widely used for aesthetic purposes, adhesion-promotion/reduction, anti-reflection or anti-fouling. These functional properties are often determined by the surface topography. Recently, the development of stimulus-responsive polymer coatings which have dynamic rather than static properties has been a focus of considerable attention.¹⁻⁶ In this category of coatings, the properties change in response to an external stimulus. The functional properties can be adjusted autonomously depending on user needs or on environmental changes. It is expected that coatings of this type will play an important role in meeting social challenges in the fields of sustainable energy, health care and food safety.



Scheme 1.1 Schematic representations of dimensional changes in polymer networks and coatings. (a) Molecular changes arise in an LC material after loss of order. The direction of the contraction or expansion depends on the alignment of the material. (b) Expansion occurs after the hydration (swelling) of a hydrogel. (c) The structural alteration of a photoresponsive polymer coating with patterned regions that have a different molecular order or crosslink density. In this case, the largest alterations occur in the dark areas. (d) A stimulus-responsive photonic coating with, for instance alternating layers of high- and low-refractive indices leads to the selective reflection of light.

This introductory chapter focuses on responsive photonic coatings in which the response is a dimensional and/or volumetric change which can be observed as a variation in surface topography or an alteration in reflected colour

(Scheme 1.1c, d). The first part of this chapter looks at coatings in which the volumetrical and dimensional response is stimulated by light. The second part will turn to photonic coatings in which exposure to a stimulus leads to an optical change in the polymer films. Stimulus-responsive polymer materials and shape-memory materials other than photonic coatings, and responsive coatings based on fluorescence or absorption processes, are outside the scope of this thesis.

1.2 Photoresponsive polymer coatings

Using light to induce dimensional or structural changes is appealing since it can be done locally without contact and without changing the immediate chemical environment of the polymer coatings or the integration of electrodes. Photo-exposure can lead to the structural modification of a polymeric network, resulting in a change in the surface topography. In particular, photo-induced alterations in the surface roughness or the hydrophilicity of materials are of interest since they cause changes in their wettability and/or changes in their adhesion properties.^{3,7,8} Coatings that respond to sunlight could be useful in the development of sun-tracking materials or materials with self-cleaning properties involving structural changes. A photochromic dye is usually incorporated in the coating to make a polymer photoresponsive.^{7,9,10} When exposed to light of a certain wavelength, this dye isomerises into a different form. The most commonly used dyes are azobenzene derivatives,¹¹⁻¹³ which undergo cis-trans isomerisation, and hydrophobic spiropyran derivatives,¹⁴⁻¹⁶ which isomerise into the hydrophilic merocyanine form. Isomerisation of the photochromic dye leads to an alteration of the functional properties of the polymer coating as a result of topological changes. Usually, the materials for such coatings are based on liquid crystalline (LC) polymers or hydrogels and solvent gels.¹⁷⁻¹⁹ Small changes in the molecular order of LC materials can lead to large dimensional changes.^{20,21} Volumetric and dimensional changes in gels are based on differences in swelling and shrinkage due to the adsorption or desorption of a solvent (Scheme 1.1).

1.2.1 *Photoresponsive surface topographies*

An interesting application for photoresponsive polymer coatings is an alterable surface topography. In some of these coatings, local photo-exposure leads to the expansion or compression of the exposed area of the surface topography. In other

coatings, the pattern is imprinted in the polymer film and the response is non-uniform, leading to the formation or enlargement of protrusions.²²

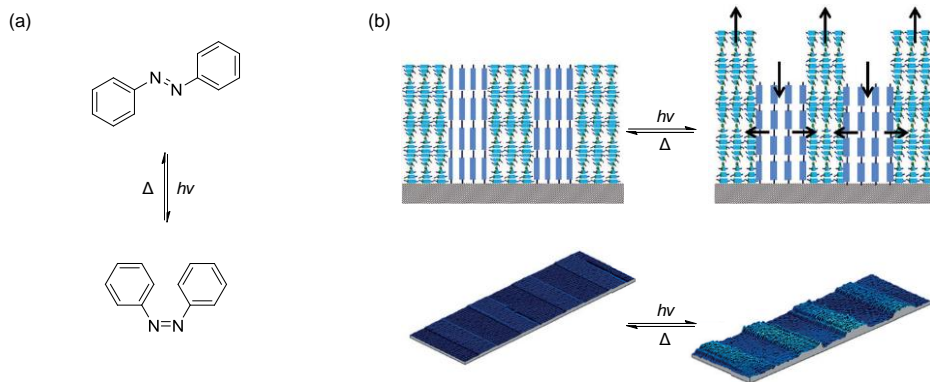


Figure 1.1 (a) Cis-trans isomerisation of the azobenzene moiety upon exposure to light. (b) Schematic representation of an azobenzene-based liquid-crystal network containing striped patterns of alternating areas with chiral nematic order and homeotropic orientation. Upon exposure the chiral nematic areas expand perpendicularly to the plane of the film and the homeotropic areas contract in the perpendicular direction. (c) 3D images of surface topographies in the initial state and during illumination with UV light. Adapted from reference 22 (Figure 1.1b, c). Copyright © 2012 WILEY-VCH Verlag GmbH & Co. KGaA, Weinheim.

Cholesteric liquid crystal (CLC) polymer coatings (which will be explained in more detail in Chapter 4) containing azobenzene moieties have been used to obtain photoswitchable surfaces.^{20,22,23} Due to the helical organisation of the molecular building blocks in the cholesteric material, expansion is usually in the direction perpendicular to the chiral nematic alignment (Figure 1.1). Protrusions are formed by exposing the polymer coating to light through a mask.²³ The polymer network behaves in a fully elastic way and the deformation is reversible. Permanent deformations can be formed by the addition of chain transfer agents to control the kinetic chain length and allow the out-of-plane reorientation of the azobenzene moieties and a corresponding molecular order loss. Subsequent studies have been reported involving coatings in which the pattern is already present in the material before light exposure.²² Films with alternating cholesteric and homeotropically aligned regions have been prepared. Photo-exposure leads to the appearance of a relief structure since the expansion of the cholesteric areas is predominantly perpendicular to the plane of the film; the expansion of the homeotropic region is

mostly parallel to the plane of the film (Figure 1.1, Scheme 1.1). Recently, an even more straightforward, innovative approach has been reported.²⁴ It was shown that, when a cholesteric polymer network is applied to a homeotropic alignment layer, worm-like fingerprint textures are obtained without any photomask being required. When illuminated with UV light, these protrusions are enhanced, leading to changes in the friction and adhesion properties of the material.

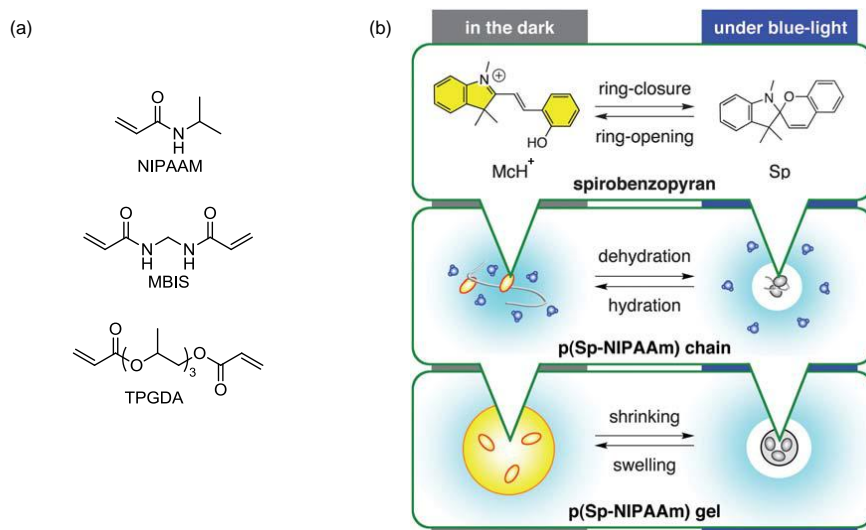


Figure 1.2 (a) *N*-isopropylacrylamide and two common crosslink agents: *N,N'*-methylenebis(acrylamide) and tri(propylene glycol) diacrylate. (b) Relations between the isomerisation of spiropyran into protonated merocyanine, the hydration behaviour of a p(Sp-NIPAAm) chain and the volumetric change in a p(Sp-NIPAAm) gel in an acidic aqueous solution. Adapted from reference 25 (Figure 1.2b) with permission from The Royal Society of Chemistry.

A popular monomer for the preparation of responsive polymer hydrogel networks is *N*-isopropylacrylamide (abbreviated as NIPAAm, Figure 1.2a), which possesses well-studied thermoresponsive volumetrical changes.²⁶ When polyNIPAAm is above its lower critical solution temperature (LCST) of 30–35 °C, a macromolecular transition from a hydrophilic to a hydrophobic structure of the polymer chain takes place, causing a collapse due to the release of water. Hydrogel coatings have been prepared on a substrate with light-absorbing patterns which convert light into heat.²⁷ In these materials, photo-exposure leads to the partial shrinkage of the films and in turn to changes in the surface topography.

To make a hydrogel which is photoresponsive in itself, a photochromic dye can be incorporated in the polymer network. Early investigations of the incorporation of spiropyran in NIPAAAM polymers in slightly acidic media have led to the development of photoresponsive hydrogel coatings.^{28,29} The working mechanism for the swelling and shrinkage observed in the hydrogel is shown schematically in Figure 1.2b.²⁵ In an acidic environment, the hydrophobic spiropyran (Sp) spontaneously isomerises into hydrophilic protonated merocyanine (McH⁺). Exposure to visible light leads to the formation of Sp. When the irradiation is stopped, the more stable McH⁺ is formed again. Upon incorporation in a linear NIPAAAM polymer chain, Sp and McH⁺ can induce the dehydration and hydration of the polymer chain because of the large difference in hydrophilicity between the two isomers. A crosslinker can be used to obtain polymer network coatings which operate as hydrogels. The light-induced hydration and dehydration mentioned here results in the reversible swelling or shrinkage of the entire hydrogel. In the dark, the gels are fully swollen; light exposure leads to the shrinkage of the gels. The photochromic behaviour of spiropyran can be fine-tuned by substituting electron-donating or electron-withdrawing groups on the benzene rings of the molecule or by making adjustments in the molecular composition of the hydrogels.^{25,30,31}

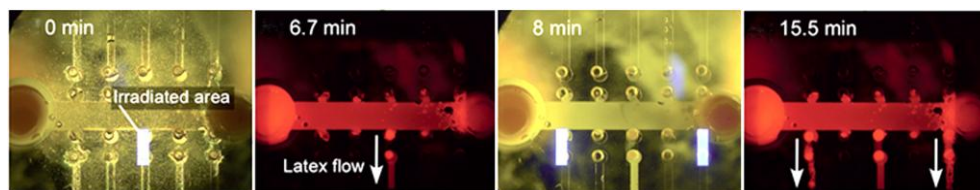


Figure 1.3 Independent and parallel flow control in the PDMS microchannel network equipped with 10 photoresponsive microvalves created from a p(Sp-*co*-NIPAAAM) hydrogel sheet. White arrows indicate the flow direction of the latex bead suspension. Independent control of a single microvalve was obtained by local light irradiation, as shown by the latex bead suspension flow after irradiation (real dimensions of the image are $13.8 \times 10.6 \text{ mm}^2$). Adapted from reference 32 with permission from The Royal Society of Chemistry.

Sheet-like hydrogel coatings exposed locally to light to obtain restricted shrinkage have also been reported. This technique has been used to move objects over a hydrogel surface or to form microchannels or microvalves in microfluidic systems on demand (Figure 1.3).^{25,32} Photoresponsive valves have been manufactured which can be opened or closed by local exposure to blue light.³³ Due to the

thermoreponsive behaviour of pNIPAAm, it is also possible to control the valves using temperature changes. Ionic liquids have been incorporated to prepare ionogel-based valves, which are more rigid.³⁰ Due to the low vapour pressure of ionic liquids and their thermal and chemical resistance, the resulting gels have a larger rigidity. Furthermore, it is possible to control the response time in these systems by varying the ionic liquid.

1.2.2 Photoresponsive wettability

When the structures of a surface topography are in the micrometre size regime, they influence the wettability of the surface. When water fills the cavities, the wetting is in the Wenzel-type wetting regime. Depending on the topography, air pockets can also be formed, creating a superhydrophobic coating (Cassie state).^{34,35} Consequently, the surface roughness plays a decisive role in the wettability of the surface.^{36,37}

Most polymer coatings with photoresponsive wettability behaviour are based on rough surfaces which are modified to make them more hydrophilic or hydrophobic upon light exposure. Covalent attachment of azobenzene-functionalised poly(acryl amides) to a rough surface has led to extremely large contact angle (CA) differences ($\Delta\theta = 140^\circ$ in the advancing CA at the transition from Wenzel wetting to superwetting or more than 175° in the receding CA at the transition from superhydrophobic to Wenzel wetting).³⁸ The coated surfaces can be reversibly switched between different wetting regimes as a result of changes in surface energy induced by the isomerisation of azobenzene.

Another way of preparing surfaces with photoresponsive wettability is to apply a photoresponsive polymer coating to structured surfaces with micropillar arrays.^{39,40} After the activation of a patterned silicon wafer, polymers containing azobenzene can be spin coated or dip coated onto the surface. The isomerisation of trans-azobenzene into the cis-isomer leads to large changes in wettability depending on the spacing of the micropillars. The optimum for 10- μm -square pillars is a spacing of 40 μm , where a reversible photo-induced change in the contact angle of 66° is seen. This is about 33 times larger than for the same coating on a flat substrate (Figure 1.4).³⁹ Interestingly, when coatings of similar azobenzene-based polymers are applied to much smaller features, no hydrophobicity change is observed after photo-exposure since the microstructure determines the superhydrophobicity of

the system. However, photo-exposure leads to a change in the adhesive force of these materials.⁴⁰ Water droplets can be pinned onto the hydrophobic surface using UV light illumination, and visible light exposure reduces adhesion so that the droplet rolls off the surface.

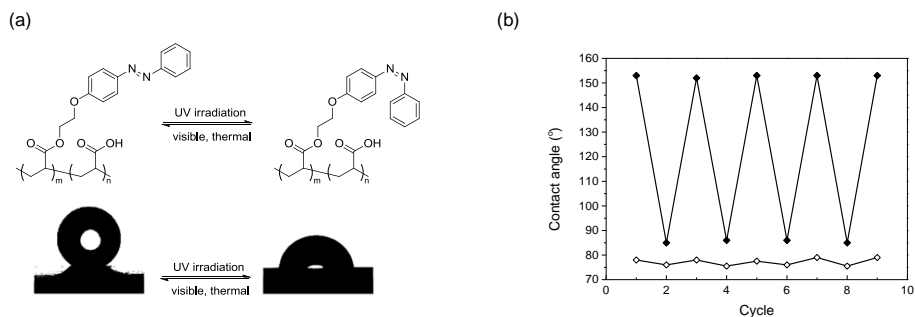


Figure 1.4 (a) Chemical structure of the photochromic polymer. (b) Optical images of the shape of water drops on a substrate with 40 μm pillar spacing coated with azobenzene-containing polymer upon UV and Vis irradiation. (c) Reversible wettability behaviour by UV and Vis irradiation: represents CA on a flat silicon wafer; ♦ represents CA on a patterned substrate with 40 μm pillar spacing. Adapted from reference 39 (Figure 1.4b, c) with permission from The Royal Society of Chemistry.

As stated before, spiropyran is a photochromic dye which undergoes a hydrophilicity change itself upon isomerisation (Figure 1.2a). This behaviour has also been used for photoresponsive wettability. Soft moulding lithography has been used to prepare a poly(ethyl methacrylate)-*co*-poly(methyl acrylate) film doped with nitrospiropyran.⁴¹ Even though the spiropyran molecule is not incorporated in the polymer backbone, isomerisation leads to changes in the hydrophilicity of the flat surface. Due to the formation of air pockets and an increase in the hydrophobicity of the substrate, the photo-induced reversible changes in the contact angle of a spiropyran-dispersed polymer film surface can also be enlarged by a factor of 3 compared to a flat surface when the surface is micropatterned.

More recently, coatings based on hydrogels which can change between a superhydrophilic and moderate hydrophobic state have been developed. The hydrogels are prepared from crosslinked copolymer films made with spiropyran and NIPAAm.⁴² Photoisomerisation of McH^+ into Sp leads to dehydration and a hydrophilicity change in the hydrogel obtained (Figure 1.2b). When these

copolymers are grafted from a structured surface (nanorods), a light-induced change from 5° to 123° can be achieved in the static contact angle.

1.2.3 *Photoresponsive cell adhesion*

There is also interest in responsive materials for biomedical applications.^{4,9,43} Spiropyran-NIPAAm hydrogel coatings have been reported that can be used to control cell adhesion.⁴⁴ The spiropyran form is most stable at equilibrium in neutral pH conditions. UV exposure leads to the isomerisation of spiropyran into merocyanine. Micropatterned illumination results in a difference in cell adhesion in the different areas. After a subsequent washing step, the majority of the cells are left on the UV-exposed areas of the surface and the cell population is 20 times higher than in the non-exposed areas. This effect is most probably caused by the zwitterionic merocyanine causing more hydrophilic regions, which have a higher affinity for cells, although the exact mechanism is not yet fully understood. Cell adhesion properties can therefore be initialised by illumination with visible light while unwanted cells can be easily removed from their substrate with this technique.

1.3 **Polymer coatings with responsive optical properties**

In photonic coatings, a structural change may, for instance, lead to a colour change. Stimulus-responsive photonic coatings are interesting as optical sensing materials which change their colour autonomously in response to environmental changes or an analyte. In photonic materials, shape and volumetric changes alter the optical properties.⁴⁵ The advantages of polymeric sensors are their low cost, ease of fabrication and the fact that they might be operated battery-free. Most coatings with responsive optical properties are based on materials which operate as Bragg reflectors. Typical Bragg reflectors contain alternating layers of materials with high- and low-refractive indices that reflect light of a specific wavelength (Scheme 1.1d). Liquid crystals have been used for various kinds of optically responsive coatings.^{46,47} In the chiral nematic phase (or cholesteric liquid crystals, CLCs), the mesogens are aligned in a helical structure due to the periodic director axis. The anisotropy in the system leads to changes in the refractive index across the material, resulting in a one-dimensional photonic coating and causing the selective reflection of light.⁴⁸ Another way to prepare colour-reflecting materials

involves using colloidal photonic crystals or inverse-opal structures in which spheres are periodically positioned in a hydrogel or an elastic matrix. This leads to the selective reflection of light that varies depending on differences in the properties of the spheres and the matrix. The positioning of the colloids alters when the material expands or contracts, resulting in a change in the reflection band.

1.3.1 Chemically responsive photonic polymers

The most simple material composition for polymeric photonic coatings is a 1D Bragg reflector consisting of alternating layers of high and low refractive index polymers. Block copolymers which form a lamellar gel have been used to produce polymers of this kind. An optical sensor for detecting various counterions has been developed.⁴⁹ The material acts as an ordinary Bragg reflector with alternating layers of polystyrene (PS) and 2-vinylpyridine (2-PVP). The response of the gel is due to the quaternisation of 2-PVP by bromoethane. Various kinds of anions have the ability to bind to the obtained pyridinium cations. Differences in the hydration energy of charged pyridine counterions lead to ion-specific swelling of the 2-PVP areas, whilst the PS remains unaffected. Originally the thickness of both layers was 24 nm. However the thickness of the 2-PVP areas varied from 24 to 220 nm depending on the particularly coordinated counterion. This results in a change in the reflection band (Figure 1.5 displays the mechanism and the colour change as a result of binding of various anions). An optical sensor for the detection of anions can be constructed in this way.

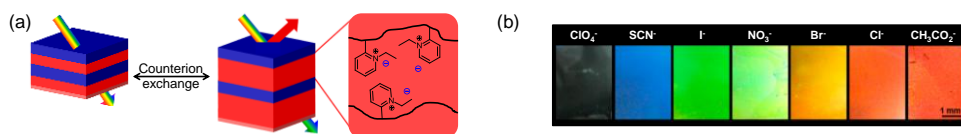


Figure 1.5 (a) Schematic representation of the mechanism for the colour change in the PS-*block*-QP2VP photonic lamellar gels by counterion exchange. (b) Colour change of the photonic gel films quaternised for 36 hours with a direct exchange of counterions. The colour of the photonic gel films shifts from transparent to blue, green, and red as counterion hydration energy increases. The counterions were exchanged using a 10 mM solution of a variety of tetrabutylammonium salts. Adapted with permission from ACS Nano 2012, 6, 8933. Copyright (2012) American Chemical Society.

An exciting class of materials for responsive photonic properties consists of colloidal particles embedded in a responsive polymer network. The swelling of this type of coating in various liquids results in a spectral shift in the band gap. A colloid-based coating which can be used as photonic paper has been presented.^{50,51} Writing on the paper involves swelling the film locally with silicone liquids (Figure 1.6). The degree of swelling (to which the colour change is related) is dependent on the molecular weight of the liquid. On an initial purple film, blue, green and red areas can be obtained by swelling using silicone liquids with a decreasing molecular weight.

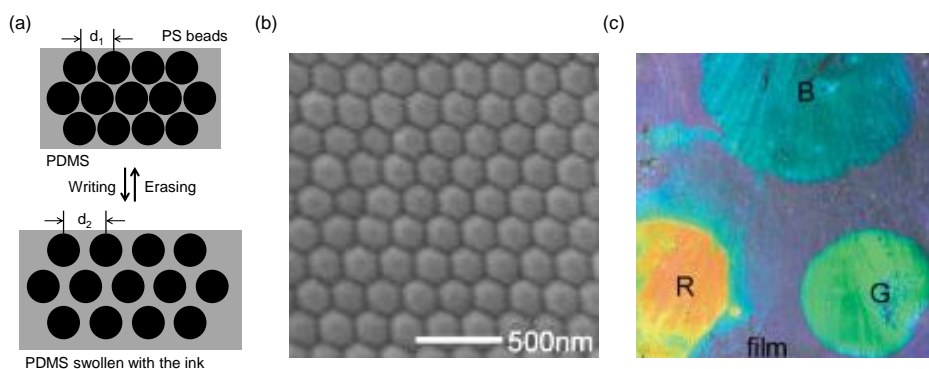


Figure 1.6 (a) A schematic representation of the mechanism for a colloid-based material upon solvent uptake. (b) SEM image of the matrix. (c) Blue, red and green dots written on the same colloidal crystal using silicone liquids with molecular weights of 3780, 770 and 162 g/mol respectively. Adapted from reference 51. Copyright © 2003 WILEY-VCH Verlag GmbH & Co. KGaA, Weinheim.

Molecular imprinting has led to a colloidal crystal hydrogel sensor for bisphenol A.⁵² The coating responds selectively to the target molecule through a loss in reflectance. In other words, there is a colourless shift. Interestingly, in control experiments where the sensor was exposed to reference compounds with chemical structure similar to bisphenol A, the initial reflection band remained unaltered. The production of a colloidal hydrogel in which boronic acid is incorporated in the polymer backbone leads to materials which can detect high glucose concentrations.⁵³ The system is not limited to the detection of organic analytes. For instance, the functionalisation of the system with 5-amino-8-hydroxyquinoline led to a similar sensor which can detect free Ni²⁺ concentration in the presence of human plasma.⁵⁴ Different colloidal crystal hydrogel ion-sensors

based on crown ethers have also been reported.^{55,56} This system responds selectively to Pb^{2+} ions with a remarkably low detection limit ($0.1 \mu\text{M}$, 40 ppb). When a proper chelation agent is selected, this method can also be used for other ionic species.

Another type of band gap material that can be subjected to triggered metal-sensing is CLC, which was mentioned above. This material self-organises in a periodic rotation of the predominant orientation of the molecules.⁵⁷ The pitch determines the position of the band gap in the spectrum and therefore the colour of the material. When there is fixed alignment at the boundaries of the film, a change in volume normally results in a change of colour. Polymer-stabilised CLC metal sensors have been developed in which the incorporation of a crown ether in the polymer backbone leads to the ability to bind and detect metal ions.⁵⁸ Barium and potassium were detected successfully on the basis of a blue shift in the colour of the material (Figure 1.7). The binding constant for bivalent barium was higher than for monovalent potassium ions. The exact mechanism underlying the blue shift is unclear. It is most probably caused by an increase in the isotropisation temperature. However, this shift could also be the result of a focal conic deformation of the planar organisation or shrinkage due to interaction between charged crown ethers.

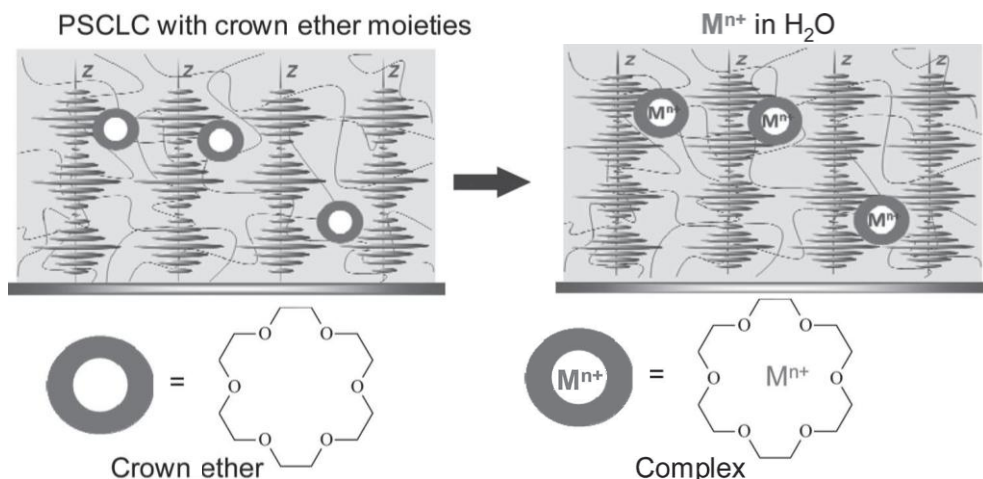


Figure 1.7 The general working principle of PSCLC materials containing crown ether moieties for sensors on metal ions. Adapted from reference 58. Copyright © 2012 WILEY-VCH Verlag GmbH & Co. KGaA, Weinheim.

CLCs have also been used to discriminate between methanol and ethanol (Figure 1.8b).^{59,60} The porosity of the film allowed both solvents to penetrate into the material. Due to the difference in the molecular affinity of the film's interior with the solvent, it was possible to detect methanol in water. When the material comes into contact with an aqueous solution of ethanol, there is a larger red shift than when methanol is mixed in. This sensor is of interest for detecting trace amounts of methanol in wine or other alcoholic drinks. Hydrogen-bonded CLC materials have also been used for the detection of amino acids (Figure 1.8).⁶¹ Arginine, lysine and histidine in solution could be detected by a change in the reflected colour. Due to the alkaline nature of the amino acid (especially arginine, which has a basic guanidinium group), the hydrogen bonds are disrupted, leading to carboxylate moieties. These hygroscopic moieties absorb water from the solution, causing swelling and therefore a red shift in the reflection band of the film.

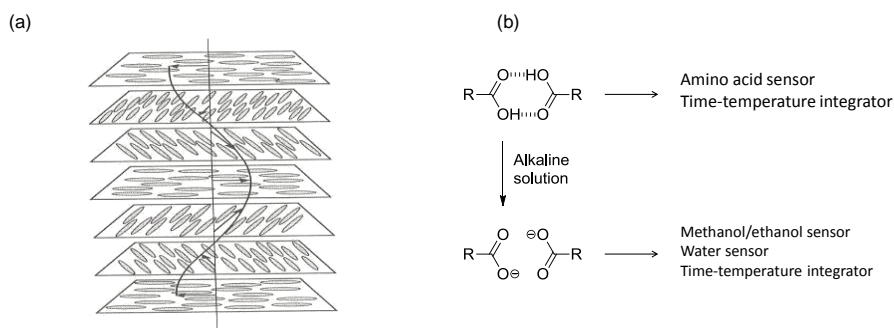


Figure 1.8 (a) Schematic representation of the organisation of the mesogens in a CLC. (b) The use of hydrogen-bonded CLC materials for various applications

In addition to detection in solutions, the detection of gaseous compounds has also been reported.⁶² An amine-responsive polymer-stabilised CLC mixture based on cholesteryl derivatives has been produced.⁶³ Due to the functionalisation of the cholesteryl unit with trifluoroacetyl groups which can form a hemiaminal, the coating is amine-responsive. The material is most sensitive to primary amines, such as 1-butylamine, since they are less sterically hindered than, for instance, secondary amines.

1.3.2 Humidity-responsive photonic polymers

Materials which can autonomously detect differences in relative humidity (RH) have attracted a great deal of attention in applications in the medical and food industry.⁶⁴ A sensor based on hygroscopic CLC polymers, which can absorb water from the surroundings, has been reported (Figure 1.8).⁶⁵ Upon water uptake, the helical pitch increases and so light with a longer wavelength is reflected. The shift of 40 nm between a RH of 3% and 83% can be easily observed by the human eye. Small humidity changes are more challenging to observe. Another type of coating uses the holographic patterning of polymer-dispersed liquid crystals to form polymeric photonic crystals based on non-porous and nanoporous regions.⁶⁶ This leads to rapidly-responding (1.5-second response time) humidity sensors. Upon water uptake by the nanoporous regions, their refractive index changes whilst the non-porous areas remain unchanged. The contrast in refractive index between the different regions therefore decreases, leading to a red shift in the reflection band.

Nanoporous polymer humidity-responsive coatings with a colloid-like structure have also been made using silica nanoparticles dispersed in a photocurable poly(ethylene glycol diacrylate).⁶⁷ After polymerisation, the nanoparticles were removed in an etching procedure. Subsequent activation of the obtained inverse-opal structures with O₂-plasma treatment led to an increase of the hydrophilicity of the coating. Humidity-dependent water uptake of the cavities led to a clearly visible colour shift. Other kinds of colloid-based sensors have been produced in which the colloids are still present in the responsive coating.^{68,69} The entire polymer matrix is made of hydrogel material, resulting in increased swelling with increasing humidity. The spacing between the 3D colloidal structure therefore increases and a red shift is seen. These systems are often based on inorganic colloidal particles such as Fe₃O₄ nanoparticles. But fully polymeric systems have also been reported in which the refractive index of the polymer particle is different enough from that of the polymer matrix to stimulate Bragg reflection. In these systems, colour changes up to 240 nm have been reported resulting from the concerted action of changes in index and periodicity as the matrix is taking up the water. (Figure 1.9 shows the colour changes in such a system at a relative humidity between 20% and 100%).⁶⁸ The system consists of monodisperse latex spheres of poly(styrene-*co*-methyl methacrylate-*co*-acrylic acid) in a poly(acrylamide-bis(acrylamide)) matrix. A similar material was prepared by embedding a

poly(styrene sulfonate-*co*-methylbutylene) copolymer, which forms a cylindrical morphology, in a poly(styrene sulfonate) (PSS) matrix in which the PSS areas expand under the influence of water.⁶⁴ The hexagonal organisation of the cylinders results in short diffusion pathways of water molecules, leading to a response time of just a few seconds.

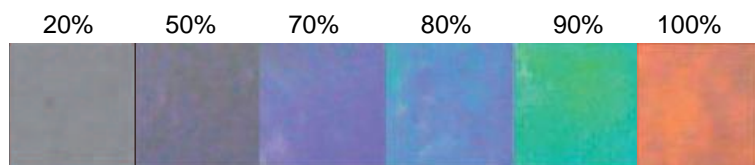


Figure 1.9 Reversible changes of the colour of a photonic crystal hydrogel as a response to changes in the relative humidity. Photographs of the as-prepared PC hydrogel corresponding to a relative humidity of 20%, 50%, 70%, 80%, 90% and 100%, respectively. Adapted from reference 68 with permission from The Royal Society of Chemistry.

1.3.3 *pH-responsive photonic polymers*

Photonic polymers can be used as optical pH sensors which react in a reversible way. Coatings in which the actual colour is pH-dependent have been reported. A polymerised crystalline colloidal array consisting of a poly(acrylamide) hydrogel with embedded polystyrene colloids and a colour shift of 300 nm has been reported.⁷⁰ The investigation of a similar system from which the colloidal particles had been removed resulted in an inverse-opal structure. This led to pH-sensitive materials in which the sensitivity depends on the amount of acrylic acid incorporated.⁷¹ However, the response times of this system (~1200 seconds) need to be optimised for the development of real-time sensors. A different approach to preparing photonic pH sensors involves the use of carboxylic acid-based CLCs.^{72,73} At a pH of 7, there is almost no response in the polymer film and a higher pH leads to the deprotonation of the carboxylic acid and therefore the formation of the carboxylate ions. The hygroscopic properties of this species lead to the absorption of water and a shift in the reflection band. The response becomes faster as the pH increases. Interestingly, the film can also be used to detect amino acids.^{61,73} Three thermoresponsive photonic polymers of which the intensity of the colour depends on the pH value are described in the next section.⁷⁴⁻⁷⁶

1.3.4 Temperature-responsive photonic polymers

A well-studied stimulus for obtaining colour changes in polymeric coatings is temperature.⁷⁷ A Bragg-type reflector has been reported that covers the entire visible spectrum when the temperature is between 20 and 50 °C.⁷⁸ The coating was made by spin coating alternating layers of poly(methylstyrene-*co*-acrylamidobenzophenone) and poly(NIPAAM-*co*-acrylic acid-*co*-acrylamidobenzophenone). The system was crosslinked by UV exposure of the photosensitive benzophenone groups. When immersed in water, the volume of the layers containing NIPAAM changes in a temperature-dependent way while the other layers remain unaffected.

A mechanically embossed polymer-network CLC-based temperature sensor which returns non-reversibly to its original state when heated above the glass transition temperature can be employed as a single use time-temperature integrator.⁷⁹ Unlike real time sensors, integrators change permanently when the variable to be detected crosses a given limit. Self-assembled hydrogen-bonded CLC polymers result in coatings which respond to temperature changes and can be used as thermally addressable reflective colour paper.⁸⁰ An image (the letter "T") can be written clearly using a hot pen (Figure 1.10). The local increase in temperature leads to the disruption of the hydrogen bonds. After three hours, the image fades away as a result of the strengthening of the H-bond interactions.

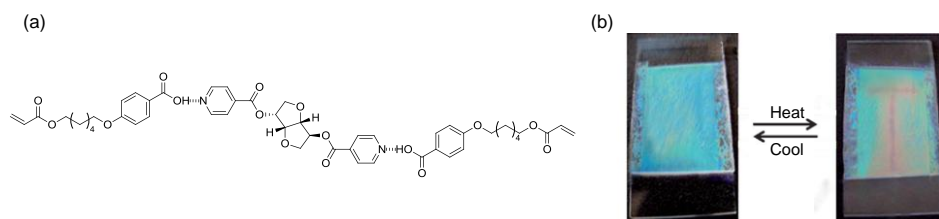


Figure 1.10 (a) The hydrogen-bonded building block for a temperature-responsive coating and (b) photographs of the polymer stabilised cholesteric liquid crystal film after polymerisation and the letter "T" applied thermally to the film. Adapted from reference 80 (Figure 1.10b) with permission from The Royal Society of Chemistry.

In addition to photonic coatings which respond solely to temperature, materials have been prepared with dual responses. The hydrogen-bonded system described above has been further improved to respond to pH as well.⁷⁶ In this case, increasing pH leads to the formation of carboxylate groups and the subsequent

swelling of the CLC network. When a proper polymer matrix is selected, more materials which are both temperature- and pH-responsive have been prepared.^{74,75,81} An inverse-opal gel consisting of 2-hydroxyethyl methacrylate, acrylic acid and ethylene glycol dimethacrylate, and filled with thermosensitive gel particles, results in materials of this kind.⁷⁵ The position of the reflection band of these coatings can be regulated thermally, whilst intensity depends on the pH of the surroundings. A similar copolymer network of NIPAAm, acrylic acid and a crosslinker has been developed.⁷⁴ A porous inverse-opal structure leads to comparable results. Another porous gel with azobenzene moieties incorporated in the polymer backbone with thermochromic properties has also been fabricated.⁸² The material reflects light in the entire visible spectrum in a temperature-dependent way. Furthermore, due to the presence of the azobenzene derivatives, UV exposure leads to changes in the reflected colour when the temperature remains constant (Figure 1.11).

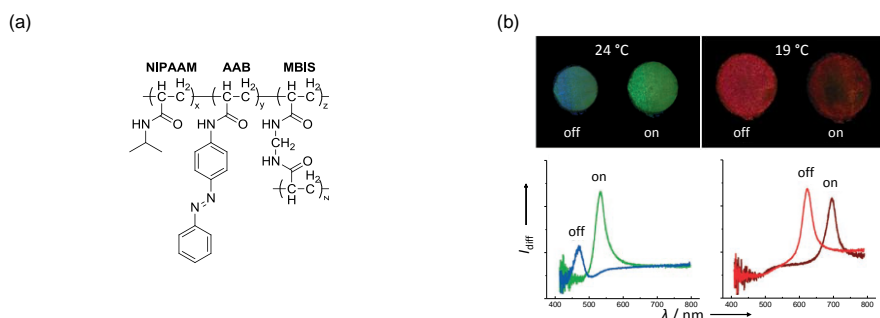


Figure 1.11 Multicolour photochromic behaviour of a porous poly(NIPAAm-co-4-acryloylaminoazobenzene) gel in water at 19, 21, and 24 °C before UV irradiation and after the equilibrium degree of swelling had been reached in response to the UV irradiation (366 nm, 8.0 mWcm⁻²). The chemical structure of the material is depicted on the left (the ratio of monomers in the feed is $x:y:z = 95:3:2$). Adapted from reference 82. Copyright © 2007 WILEY-VCH Verlag GmbH & Co. KGaA, Weinheim.

1.4 Aim and outline of this thesis

A variety of responsive coatings have been produced which have the ability to translate small molecular changes in the polymer network into large deformations of the macroscopic polymer material. However, the materials used for the development of photonic responsive coatings are rather limited. There is a need to

extend the toolbox of available molecules and polymers in order to produce photonic organic coatings with new properties and enhanced responses. Furthermore, new preparation methods and topographies could lead to materials with improved properties or new applications.

The aim of the work described in this thesis was to produce novel responsive photonic polymer coatings that can be applied as responsive topographical coatings and optical sensors. New molecular building blocks were synthesised and novel production methods were developed to prepare these coatings. All these coatings have a common feature: they undergo reversible volumetric changes when a stimulus is applied. These dimensional alterations lead to a deformation in the surface topography or a colour change involving different mechanisms. It is expected that the coatings investigated will be used in microfluidic devices, self-cleaning surfaces or optical sensors.

Chapter 2 looks at photoresponsive hydrogel coatings which operate in a slightly acidic environment. A novel spiropyran derivative was copolymerised with *N*-isopropylacrylamide and a crosslinker to give hydrogels with a spatial variation in the crosslink density. Upon illumination with visible light they undergo non-uniform deformation. This results in a coating with reversible photo-induced alterations in the surface topography. Chapter 3 reports on a slightly different approach which made the material operational in a pH-neutral environment as well. Coatings with an asymmetric, ratchet-like surface topography were prepared. Upon photo-exposure, flat or even inverse ratchet structures were obtained.

Water-responsive surface topographies are described in Chapter 4. These coatings are based on chiral nematic (cholesteric) liquid crystal polymers. Patterned coatings with alternating cholesteric and isotropic regions were produced, with the formation of a corrugated surface as a result. In addition to the profile change, a colour change was also seen in the cholesteric liquid crystalline areas. Chapter 5 describes how this optical behaviour was exploited in humidity-responsive coatings based on interpenetrating polymer networks (IPNs). Here, the properties of hydrogels and cholesteric liquid crystals were combined. The reflected colour of these materials is dependent on the relative humidity. Chapter 6 reports on a cholesteric polymer coating which is responsive to gaseous trimethylamine. Exposure to the gas in an inert environment leads to the reduced intensity of the

reflection band, while exposure to the gas in the presence of water vapour leads to a clearly observable colour change.

Finally, Chapter 7 explores the practical use of the coatings described in this thesis, addressing the prospects for the developed materials and improvements in the coatings.

References

- 1 C. Alexander and K. M. Shakesheff, *Adv. Mater.*, 2006, **18**, 3321-3328.
- 2 R. Blossey, *Nat. Mater.*, 2003, **2**, 301-306.
- 3 R. Byrne, F. Benito-Lopez and D. Diamond, *Mater. Today*, 2010, **13**, 16-23.
- 4 T. Sun and G. Qing, *Adv. Mater.*, 2011, **23**, H57-H77.
- 5 F. D. Jochum and P. Theato, *Chem. Soc. Rev.*, 2013, **42**, 7468-7483.
- 6 J.-H. Lee, C. Y. Koh, J. P. Singer, S.-J. Jeon, M. Maldovan, O. Stein and E. L. Thomas, *Adv. Mater.*, 2014, **26**, 532-569.
- 7 F. Ercole, T. P. Davis and R. A. Evans, *Polym. Chem.*, 2010, **1**, 37-54.
- 8 J. Zhang, Q. Zou and H. Tian, *Adv Mater*, 2013, **25**, 378-399.
- 9 H. G. Börner and J.-F. Lutz, *Bioactive Surfaces*, Springer Berlin Heidelberg, 2011.
- 10 M. M. Russew and S. Hecht, *Adv. Mater.*, 2010, **22**, 3348-3360.
- 11 E. Merino and M. Ribagorda, *Beilstein J. Org. Chem*, 2012, **8**, 1071-1090.
- 12 K. G. Yager and C. J. Barrett, in *Intelligent Materials*, The Royal Society of Chemistry, 2008, pp. 424-446.
- 13 Z. Mahimwalla, K. G. Yager, J.-i. Mamiya, A. Shishido, A. Priimagi and C. J. Barrett, *Polym. Bull.*, 2012, **69**, 967-1006.
- 14 V. I. Minkin, *Chem. Rev.*, 2004, **104**, 2751-2776.
- 15 L. Florea, D. Diamond and F. Benito-Lopez, *Macromol. Mater. Eng.*, 2012, **297**, 1148-1159.
- 16 R. Klajn, *Chem. Soc. Rev.*, 2014, **43**, 148-184.
- 17 J. Wei and Y. Yu, *Soft Matter*, 2012, **8**, 8050-8059.
- 18 A. Priimagi, C. J. Barrett and A. Shishido, *J. Mater. Chem. C*, 2014, **2**, 7155-7162.
- 19 T. Seki, *Macromol. Rapid Commun.*, 2014, **35**, 271-290.
- 20 D. Liu and D. J. Broer, *Langmuir*, 2014, Article ASAP.
- 21 D. Liu and D. J. Broer, *Liq. Cryst. Rev.*, 2013, **1**, 20-28.
- 22 D. Liu, C. W. M. Bastiaansen, J. M. J. den Toonder and D. J. Broer, *Angew. Chem., Int. Ed.*, 2012, **51**, 892-896.
- 23 D. Liu, C. W. M. Bastiaansen, J. M. J. den Toonder and D. J. Broer, *Macromolecules*, 2012, **45**, 8008-8012.
- 24 D. Liu and D. J. Broer, *Angew. Chem., Int. Ed.*, 2014, **53**, 4542-4546.
- 25 T. Satoh, K. Sumaru, T. Takagi and T. Kanamori, *Soft Matter*, 2011, **7**, 8030-8034.
- 26 H. G. Schild, *Prog. Polym. Sci.*, 1992, **17**, 163-249.
- 27 D. Liu, C. W. M. Bastiaansen, J. M. J. den Toonder and D. J. Broer, *Langmuir*, 2013, **29**, 5622-5629.

-
- 28 K. Sumaru, M. Kameda, T. Kanamori and T. Shinbo, *Macromolecules*, 2004, **37**, 4949-4955.
- 29 K. Sumaru, K. Ohi, T. Takagi, T. Kanamori and T. Shinbo, *Langmuir*, 2006, **22**, 4353-4356.
- 30 F. Benito-Lopez, R. Byrne, A. M. Raduta, N. E. Vrana, G. McGuinness and D. Diamond, *Lab Chip*, 2010, **10**, 195-201.
- 31 T. Satoh, K. Sumaru, T. Takagi, K. Takai and T. Kanamori, *Phys. Chem. Chem. Phys.*, 2011, **13**, 7322-7329.
- 32 S. Sugiura, A. Szilagyi, K. Sumaru, K. Hattori, T. Takagi, G. Filipcsei, M. Zrinyi and T. Kanamori, *Lab Chip*, 2009, **9**, 196-198.
- 33 S. Sugiura, K. Sumaru, K. Ohi, K. Hiroki, T. Takagi and T. Kanamori, *Sens. Actuators, A*, 2007, **140**, 176-184.
- 34 R. N. Wenzel, *Ind. Eng. Chem.*, 1936, **28**, 988-994.
- 35 A. B. D. Cassie and S. Baxter, *Trans. Faraday Soc.*, 1944, **40**, 546-551.
- 36 S. Wang, Y. Song and L. Jiang, *J. Photochem. Photobiol., C*, 2007, **8**, 18-29.
- 37 B. Xin and J. Hao, *Chem. Soc. Rev.*, 2010, **39**, 769-782.
- 38 J. Groten, C. Bunte and J. R uhe, *Langmuir*, 2012, **28**, 15038-15046.
- 39 W. Jiang, G. Wang, Y. He, X. Wang, Y. An, Y. Song and L. Jiang, *Chem. Commun.*, 2005, **0**, 3550-3552.
- 40 C. Li, Y. Zhang, J. Ju, F. Cheng, M. Liu, L. Jiang and Y. Yu, *Adv. Funct. Mater.*, 2012, **22**, 760-763.
- 41 A. Athanassiou, M. I. Lygeraki, D. Pisignano, K. Lakiotaki, M. Varda, E. Mele, C. Fotakis, R. Cingolani and S. H. Anastasiadis, *Langmuir*, 2006, **22**, 2329-2333.
- 42 G. Joseph, J. Pichardo and G. Chen, *Analyst*, 2010, **135**, 2303-2308.
- 43 P. M. Mendes, *Chem. Soc. Rev.*, 2008, **37**, 2512-2529.
- 44 J.-i. Edahiro, K. Sumaru, Y. Tada, K. Ohi, T. Takagi, M. Kameda, T. Shinbo, T. Kanamori and Y. Yoshimi, *Biomacromolecules*, 2005, **6**, 970-974.
- 45 J. Ge and Y. Yin, *Angew. Chem., Int. Ed.*, 2011, **50**, 1492-1522.
- 46 R. J. Carlton, J. T. Hunter, D. S. Miller, R. Abbasi, P. C. Mushenheim, L. N. Tan and N. L. Abbott, *Liq. Cryst. Rev.*, 2013, **1**, 29-51.
- 47 D.-J. Mulder, A. P. H. J. Schenning and C. W. M. Bastiaansen, *J. Mater. Chem. C*, 2014, Accepted Manuscript.
- 48 R. Eelkema and B. L. Feringa, *Org. Biomol. Chem.*, 2006, **4**, 3729-3745.
- 49 H. S. Lim, J.-H. Lee, J. J. Walish and E. L. Thomas, *ACS Nano*, 2012, **6**, 8933-8939.
- 50 H. Fudouzi and Y. Xia, *Langmuir*, 2003, **19**, 9653-9660.
- 51 H. Fudouzi and Y. Xia, *Adv. Mater.*, 2003, **15**, 892-896.

- 52 C. Guo, C. Zhou, N. Sai, B. Ning, M. Liu, H. Chen and Z. Gao, *Sens. Actuators, B*, 2012, **166–167**, 17-23.
- 53 M. M. Ward Muscatello, L. E. Stunja and S. A. Asher, *Anal. Chem.*, 2009, **81**, 4978-4986.
- 54 J. T. Baca, D. N. Finegold and S. A. Asher, *Analyst*, 2008, **133**, 385-390.
- 55 J. H. Holtz and S. A. Asher, *Nature*, 1997, **389**, 829-832.
- 56 C. E. Reese and S. A. Asher, *Anal. Chem.*, 2003, **75**, 3915-3918.
- 57 T. Geelhaar, K. Griesar and B. Reckmann, *Angew. Chem., Int. Ed.*, 2013, **52**, 8798-8809.
- 58 V. Stroganov, A. Ryabchun, A. Bobrovsky and V. Shibaev, *Macromol. Rapid Commun.*, 2012, **33**, 1875-1881.
- 59 C.-K. Chang, C. M. W. Bastiaansen, D. J. Broer and H.-L. Kuo, *Adv. Funct. Mater.*, 2012, **22**, 2855-2859.
- 60 C.-K. Chang, C. W. M. Bastiaansen, D. J. Broer and H.-L. Kuo, *Macromolecules*, 2012, **45**, 4550-4555.
- 61 P. V. Shibaev, D. Chiappetta, R. L. Sanford, P. Palffy-Muhoray, M. Moreira, W. Cao and M. M. Green, *Macromolecules*, 2006, **39**, 3986-3992.
- 62 H. Xu, P. Wu, C. Zhu, A. Elbaz and Z. Z. Gu, *J. Mater. Chem. C*, 2013, **1**, 6087-6098.
- 63 N. Kirchner, L. Zedler, T. G. Mayerhofer and G. J. Mohr, *Chem. Commun.*, 2006, 1512-1514.
- 64 E. Kim, S. Y. Kim, G. Jo, S. Kim and M. J. Park, *ACS Appl. Mater. Interfaces*, 2012, **4**, 5179-5187.
- 65 N. Herzer, H. Guneyasu, D. J. D. Davies, D. Yildirim, A. R. Vaccaro, D. J. Broer, C. W. M. Bastiaansen and A. P. H. J. Schenning, *J. Am. Chem. Soc.*, 2012, **134**, 7608-7611.
- 66 J. Shi, V. K. S. Hsiao, T. R. Walker and T. J. Huang, *Sens. Actuators, B*, 2008, **129**, 391-396.
- 67 J. H. Kim, J. H. Moon, S.-Y. Lee and J. Park, *Appl. Phys. Lett.*, 2010, **97**, 103701.
- 68 E. Tian, J. Wang, Y. Zheng, Y. Song, L. Jiang and D. Zhu, *J. Mater. Chem.*, 2008, **18**, 1116-1122.
- 69 H. Hu, Q.-W. Chen, K. Cheng and J. Tang, *J. Mater. Chem.*, 2012, **22**, 1021-1027.
- 70 K. Lee and S. A. Asher, *J. Am. Chem. Soc.*, 2000, **122**, 9534-9537.
- 71 Y. J. Lee and P. V. Braun, *Adv. Mater.*, 2003, **15**, 563-566.
- 72 P. V. Shibaev, K. Schaumburg and V. Plaksin, *Chem. Mater.*, 2002, **14**, 959-961.

-
- 73 P. V. Shibaev, R. L. Sanford, D. Chiappetta and P. Rivera, *Mol. Cryst. Liq. Cryst.*, 2007, **479**, 161/[1199]-167/[1205].
- 74 K. Ueno, K. Matsubara, M. Watanabe and Y. Takeoka, *Adv. Mater.*, 2007, **19**, 2807-2812.
- 75 M. Honda, T. Seki and Y. Takeoka, *Adv. Mater.*, 2009, **21**, 1801-1804.
- 76 F.-j. Chen, J.-b. Guo, O.-y. Jin and J. Wei, *Chin. J. Polym. Sci.*, 2013, **31**, 630-640.
- 77 A. Seeboth, D. Löttsch, R. Ruhmann and O. Muehling, *Chem. Rev.*, 2014, **114**, 3037-3068.
- 78 M. C. Chiappelli and R. C. Hayward, *Adv. Mater.*, 2012, **24**, 6100-6104.
- 79 D. J. D. Davies, A. R. Vaccaro, S. M. Morris, N. Herzer, A. P. H. J. Schenning and C. W. M. Bastiaansen, *Adv. Funct. Mater.*, 2013, **23**, 2723-2727.
- 80 F. Chen, J. Guo, Z. Qu and J. Wei, *J. Mater. Chem.*, 2011, **21**, 8574-8582.
- 81 J. Shin, S. G. Han and W. Lee, *Sens. Actuators, B*, 2012, **168**, 20-26.
- 82 K. Matsubara, M. Watanabe and Y. Takeoka, *Angew. Chem.*, 2007, **119**, 1718-1722.

Chapter 2

Photoresponsive hydrogel surface topographies in an acidic environment

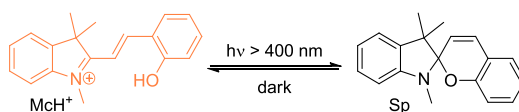
Abstract

This chapter describes the preparation of patterned photoresponsive hydrogels using a straightforward method. The polymer network hydrogel coating consists of *N*-isopropylacrylamide (NIPAAM), the crosslinking agent tripropylene glycol diacrylate (TPGDA) and a novel synthesised photochromic spiropyran monoacrylate. In an initial experiment, a linear NIPAAM copolymer (without TPGDA) containing the spiropyran dye was synthesised which showed relatively fast photoswitching behaviour. Freestanding hydrogel polymer networks were then prepared by photopolymerisation of a similar monomer mixture with TPGDA. The light-induced isomerisation of protonated merocyanine into neutral spiropyran under slightly acidic conditions resulted in macroscopic changes in the hydrophilicity of the entire polymer film, i.e. shrinkage of the hydrogel. The degree of shrinkage could be controlled by changing the crosslink density of the polymer network. A hydrogel film with a spatially modulated crosslink density was then fabricated by polymerisation-induced diffusion using a patterned photomask. The resulting patterned smooth hydrogel coating swelled in slightly acidic media, with maximum swelling in the regions with lower crosslink density, yielding a corrugated surface. Upon exposure to visible light, the surface topography flattened again, showing that a hydrogel coating can be created of which the topography can be controlled by light.

This chapter is partially reproduced from: J. E. Stumpel, D. Liu, D. J. Broer and A. P. H. J. Schenning, *Chemistry - A European Journal*, 2013, **19**, 10922-10927.

2.1 Introduction

There is considerable interest in responsive materials which can change their shape in a reversible and controllable way.^{1,2} Different stimuli can be used, such as temperature, pH or light, to switch these materials.^{3,4} Photoresponsive materials are particularly appealing since they can be approached without making contact and the stimulus can be turned on or off immediately, generally inducing a rapid response.^{5,6} These materials can be used for a wide range of applications ranging from solar-driven valves to biomedical release systems.⁷⁻¹²



Scheme 2.1 Isomerisation behaviour of protonated merocyanine (McH⁺) into spiropyran (Sp) upon visible light exposure at pH = 2.7

Spiropyran derivatives are a class of photochromic dyes which are frequently used in a range of stimuli-responsive materials.^{13,14} Incorporating these dyes in a hydrogel (a crosslinked polymer network which can absorb a large amount of water) results in responsive polymers that change geometry upon exposure to light.¹⁵⁻²¹ For example, Sumaru and co-workers fabricated photoresponsive hydrogels based on *N*-isopropylacrylamide (NIPAAm) which shrink upon visible light exposure due to the switching of the protonated merocyanine (McH⁺) into the spiropyran (Sp) form (Scheme 2.1, Figure 1.2b).²²⁻²⁵ When irradiation is stopped, Sp converts back to the more stable McH⁺ form. The hydrophobic spiropyran form induces dehydration of the NIPAAm polymer while the ionic McH⁺ form is more hydrophilic, promoting the uptake of water, as explained in more detail in Chapter 1.

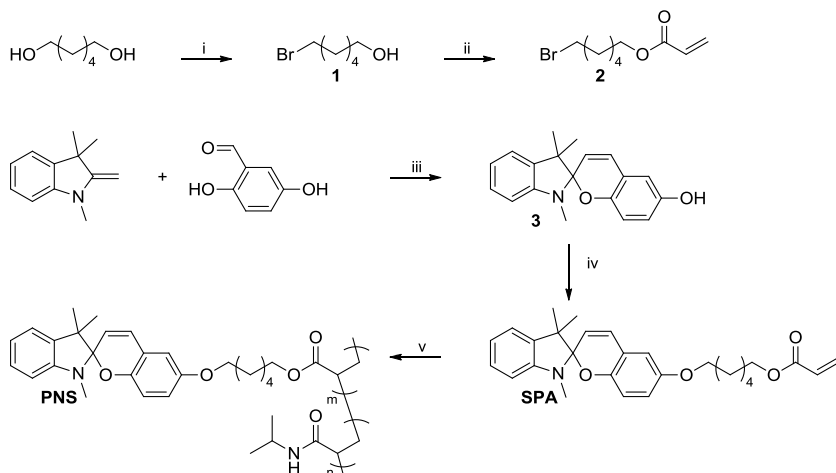
Patterned responsive hydrogels have been reported in which prescribed three-dimensional shape deformations are observed using temperature or pH as a stimulus.^{3,26} So far, patterned photoresponsive hydrogels have not been reported. Such films are of interest for photocontrolled mixing and flow in microfluidic devices, self-cleaning surfaces and smart surfaces for biological applications.^{27,28} Recently, photoswitchable surface topographies based on cholesteric liquid crystalline polymer coatings have been reported.²⁹ The preparation of these films required patterned indium tin oxide cells for proper alignment. Another study has

shown that patterned pH responsive hydrogels coatings could be made using a straightforward method based on polymerisation-induced diffusion that takes place during the formation of the polymer film by photopolymerisation.³ The current chapter reports on patterned photoresponsive hydrogel films with a changeable surface relief structure produced using this technique.³⁰ A photoreactive acrylate mixture consisting of NIPAAm^{31,32}, spiropyran acrylate and a diacrylate crosslinker was UV-exposed through a line photomask. The monomer mixture was polymerised exclusively in the exposed regions of the sample. Due to the depletion of the more reactive diacrylate, the diacrylate diffuses from the non-exposed area to the exposed area driven by a gradient in its concentration. After the removal of the mask the entire film was exposed to UV light, resulting in a fully polymerised film with a modulated crosslink density aiming to enable the spatial variation of hydrogel swelling with light as stimulus.

2.2 Results and discussion

2.2.1 Synthesis and copolymerisation of spiropyran monoacrylate (SPA)

For the preparation of photoresponsive hydrogels, an acrylate-bearing spiropyran **SPA** was synthesised that has an electron-donating alkoxy group at the 6-position in order to have a fast switching behaviour (Scheme 2.2).²² 1,6-Hexanediol was monobrominated with 48% HBr solution in toluene under reflux conditions to yield 6-bromohexan-1-ol (**1**).³³ Subsequent esterification with acryloyl chloride and triethylamine leads to 6-bromohexyl acrylate (**2**). Hydroxyspiropyran 1',3',3'-trimethylspiro[chromene-2,2'-indolin]-6-ol (**3**) was prepared by coupling 1,3,3-trimethyl-2-methyleneindoline and 2,5-dihydroxybenzaldehyde in ethanol at reflux temperature.³⁴ **SPA** was obtained after a potassium-iodide-catalysed Williamson ether synthesis of **2** with **3**. The novel monomer was fully characterised using ¹H-NMR, ¹³C-NMR and MALDI TOF MS analysis.³⁵ ¹H-NMR spectroscopy in CDCl₃ showed that **SPA** was completely in its spiropyran form. However, after the addition of a drop of 1 M HCl to the NMR-tube, the solution turned yellow and additional signals appeared in the aromatic region of the NMR spectrum, indicating the formation of the protonated merocyanine (MCH⁺) species.³⁶



Scheme 2.2 Synthetic route towards monoacrylate functionalised spiroopyran **SPA** and copolymer **PNS**. (i) 48% aq. HBr, toluene, reflux, 16 h; (ii) acryloyl chloride, TEA, DCM, 0 °C → RT, 18 h; (iii) EtOH, reflux, 2 h; (iv) 2, K₂CO₃, KI[cat], MEK, reflux, 40 h; v) NIPAAm, AIBN, THF, reflux, 19h.

In order to study the photoswitching of **SPA** in solution, a random linear copolymer (**PNS**, Scheme 2.2) was synthesised. Using azobisisobutyronitrile (AIBN) as a thermal initiator, this copolymer was prepared using a mixture of **SPA** and NIPAAm in a molar ratio of 3 : 97.²³ The molecular weight and monomer composition of the copolymer were determined using GPC ($M_w \approx 15000$, PDI ≈ 2.4) and ¹H-NMR spectroscopy (spiroopyran content in the polymer is roughly 2-3 mol%, similar to the monomeric feed).³⁷

2.2.2 Photoresponse of the linear copolymer **PNS**

UV/Vis spectroscopy was used to study the kinetics of the photoresponse of **PNS**.²⁵ In neutral solution, an absorption band at $\lambda_{\max} = 333$ nm was visible, corresponding to the closed spiroopyran form whereas, in an acidic solution (2 mM HCl, pH = 2.7), the protonated merocyanine species was present, as shown by the absorption band at $\lambda = 454$ nm (Figure 2.1a). After the illumination of **PNS** in a 2 mM HCl solution with visible light (> 400 nm) for five minutes, a decrease in the intensity of the absorption band of McH⁺ was observed, indicating isomerisation into neutral Sp. The solution became hazy, indicating a change in hydrophilicity, i.e. a lower critical solution temperature (LCST), of the thermoresponsive polymer, leading to the precipitation of the polymer even at room temperature.²⁴

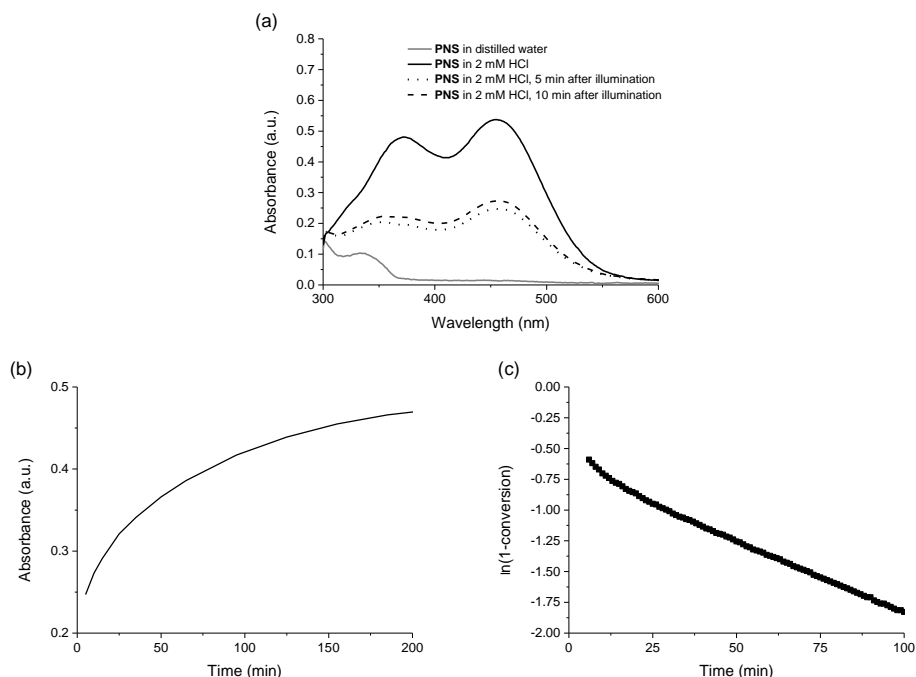


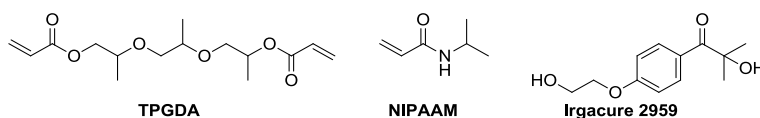
Figure 2.1 (a) UV/Vis spectra for 1.7 mM PNS in distilled water and in 2 mM HCl solution and the recovery of the spiropyran into protonated merocyanine after illumination. (b) Back-isomerisation in the dark over time, measured at $\lambda = 454$ nm. (c) Logarithmic plot of the recovery shows a linear relation between absorbance and time, indicating first-order reaction rate kinetics.

Time-resolved UV/Vis spectrometry was used to monitor the back-isomerisation of Sp into its McH^+ form as soon as the solution became clear again (after ~ 5 minutes) and revealed first-order reaction rate kinetics (Figure 2.1b, c). The back-isomerisation of spiropyran into protonated merocyanine after illumination with visible light has a $t_{1/2}$ of 9.5 min, which is in the same order of magnitude as reported previously for spiropyran-based hydrogels bearing electron-donating groups.²² These results show that a photoresponsive polymer can be synthesised based on SPA that has relatively fast switching behaviour.

2.2.3 Preparation and photoresponse of freestanding crosslinked polymer network films

Since polymerisation-induced diffusion is based on photopolymerisation processes, the initial step was to determine whether it is possible to prepare freestanding polymer network films containing the photochromic dye SPA by means of photopolymerisation. Hydrogels were prepared using a mixture of

97 mol% of NIPAAM, 1 mol% of SPA, 1 mol% of tripropylene glycol diacrylate (TPGDA) crosslinking agent and 1 mol% of Irgacure 2959 as the photoinitiator (Scheme 2.3). A cell with a spacing of $\sim 55 \mu\text{m}$ was filled with the acrylate mixture and exposed to UV light for 5 minutes at 110°C , resulting in a freestanding film after the opening of the cell. It should be noted that spiropyran also absorbs in the UV range, and that this could cause a gradient in UV intensity through the film thickness, resulting in a gradient in crosslink density.³



Scheme 2.3 Materials used for the preparation of photoresponsive crosslinked polymer hydrogel networks

A control experiment was performed using a polymer film prepared with equal amounts of NIPAAM and TPGDA. The total UV absorption through this entire freestanding polymer film of $\sim 55 \mu\text{m}$ was 25% only (i.e. the lower side of the film receives 75% of the intensity of the UV dose that the upper side receives). As the photopolymerisation at the used dose is faster than the vertical migration of the components, no gradient in crosslink density is expected. Reflection IR spectroscopy showed analogous spectra for the top and bottom sides of the film (Figure 2.2a), confirming that the chemical composition on either side is the same.

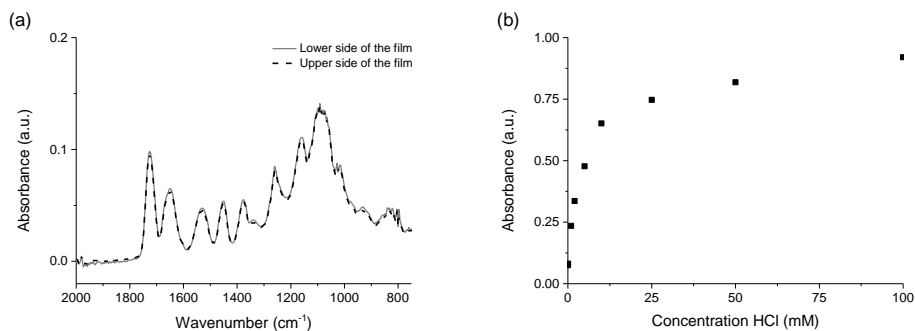


Figure 2.2 (a) FT-IR data for the polymer film prepared with equal amounts of TPGDA and NIPAAM, showing a homogeneous chemical composition throughout the z-direction of the film. (b) Absorbance at $\lambda = 470 \text{ nm}$ of a freestanding hydrogel film (composed of NIPAAM, TPGDA, SPA and Irgacure 2959, respectively 97, 1, 1, 1 mol%) as a function of HCl concentration.

When the hydrogel film was placed in demineralised water at room temperature, the colourless film swelled by a factor of 1.5 in every direction. It should be noted that the hydrogel films did not bend, indicating that crosslink density is uniform across the thickness of the film (see above).³ When subsequently moved to an acidic environment, the swollen film turned orange due to the formation and stabilisation of the protonated merocyanine form, and no additional swelling was observed. HCl titration experiments in which the isomerisation of Sp into McH⁺ was monitored as a function of acidity revealed that the specie is completely in its McH⁺ form when a higher concentration than 100 mM HCl is used (Figure 2.2b).

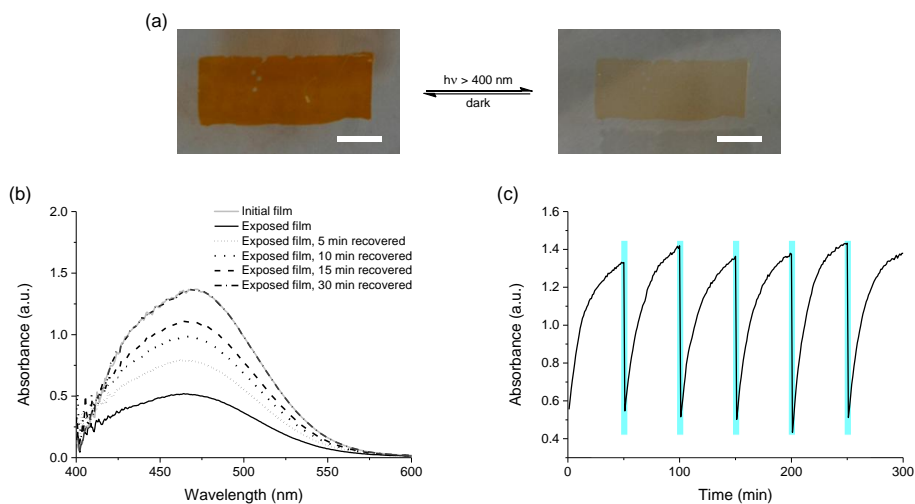


Figure 2.3 (a) Photographs of freestanding hydrogel films in 2 mM HCl solution before and after illumination with visible light (scale bar represents 1 cm), (b) the corresponding UV/Vis spectra for the recovery of spiropyran into protonated merocyanine after light exposure and (c) its reversible photoresponsive behaviour. Absorption at 470 nm is depicted after six subsequent illumination steps (blue lines represent light exposure).

Optimisation experiments were performed to identify the ideal acidity. After equilibrium was attained at a given pH, the hydrogel film was irradiated with visible light (> 400 nm, 5 min) to observe back-isomerisation of the McH⁺ into its Sp isomer. When the HCl concentration is below 1 mM, the recovery of Sp into McH⁺ is rather slow. However, if the concentration is higher than 5 mM HCl, Sp instantly isomerises back into McH⁺, without there being enough time for a proper measurement. The photoresponse of the films was therefore determined while they were immersed in a 2 mM HCl solution (pH = 2.7) in order to make a reliable

observation of recovery and to link the data to data obtained from the linear copolymer **PNS** study. When equilibrated at this concentration, around 25% of the species is in the McH^+ form (Figure 2.2b).

The reversibility of the photoresponse of the films was determined while the films were immersed in a 2 mM HCl solution (pH = 2.7). UV/Vis spectroscopy showed the typical absorption band for protonated merocyanine ($\lambda_{\text{max}} = 460 \text{ nm}$, Figure 2.3b). As with the measurements conducted on the linear copolymer, the film became colourless (Sp) upon exposure to visible light ($> 400 \text{ nm}$, 5 min). Moreover, an isotropic shrinkage of the size of the gel by 20% was observed (Figure 2.3a, Table 2.1, entry 1). UV/Vis spectroscopy indicated less absorption related to McH^+ . The back-isomerisation of Sp into protonated McH^+ in hydrogel films has a $t_{1/2}$ of ~13 minutes, which is slightly slower than the linear polymer. The difference in recovery between the copolymer and the hydrogel is probably related to the fact that the swelling agent needs to diffuse into the hydrogel film, while the **PNS** macromolecule is completely dissolved as it is a non-crosslinked linear copolymer.

Table 2.1 Variation in the composition of the films with different swelling behaviour; all mixtures contained 1 mol% of the photoinitiator Irgacure 2959

Sample	NIPAAM (mol%)	TPGDA (mol%)	SPA (mol%)	Relative size after light exposure (%) ^[a]
1	97	1	1	80
2	97.5	0.5	1	75
3	96	2	1	91
4	96	1	2	88
5	98	1	0	100
6 ^[b]	97	1	0 ^[b]	100

[a] Relative size = size of film after illumination (5 min, 100 mW/cm² in the range of 395–445 nm) / size of fully swollen film × 100. [b] Mixture containing 1 mol% dye K160 instead of **SPA**.

The time it takes for the polymer film to swell to its initial dimensions matches the time scale for the back-isomerisation of spiropyran into protonated merocyanine, indicating that the swelling of the hydrogel film is directly related to the photoswitching behaviour of the spiropyran dye.²⁵ Interestingly, the photoresponsive behaviour of the hydrogel film is fully reversible, and swelling and shrinkage can be repeated multiple times. Six repeated cycles switching

between McH^+ and Sp revealed that the absorption intensities were unaltered (Figure 2.3c).

Wettability measurements show that the initial swollen films have a water contact angle of 90° , which changes to 95° upon light exposure (Figure 2.4). This indicates that the hydrophobicity of the surface increases slightly due to the isomerisation of McH^+ into Sp . These somewhat surprising high contact angles obtained can be ascribed to the perfluorodecyltriethoxysilane functionalised glass which was used for the preparation of the thin films which determines orientation of the most apolar moieties of the hydrogel to the interface. Furthermore, as stated above, 75% of **SPA** is in its hydrophobic Sp form.

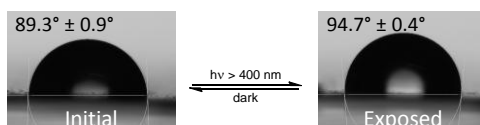


Figure 2.4 Change in wettability of the flat hydrogel film upon visible light exposure

To exclude the possibility that the shrinkage of the films after illumination results from the heating of the sample, two control experiments were performed (Table 2.1, entries 5 and 6). The volume of a freestanding film without **SPA** did not change after light exposure. Furthermore, a film containing a non-photochromic commercial dye instead of **SPA**, and which had a similar absorption spectrum (K160 , $\lambda_{\text{max}} = 450 \text{ nm}$)³⁸, did not shrink upon light illumination either. This behaviour indicates that the shrinkage of the **SPA** hydrogels is not a result of absorbed light being converted into heat, but that it is related to the photoresponsive change in the hydrophobicity of the spiropyran dye.

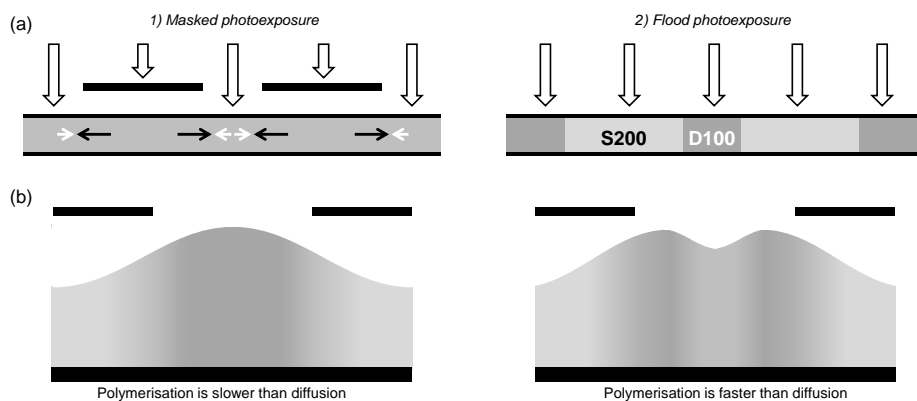
The effect of varying the quantities of crosslinker in the monomer mixture was studied before preparing the patterned hydrogel films. As expected, an increase in the amount of crosslinker TPGDA resulted in films which shrink less since the network is more tightly interwoven and rigid (9% shrinkage, Table 2.1, entry 3). More shrinkage (25%, Table 2.1, entry 2) was observed when the amount of crosslinker was reduced. Without the presence of the crosslinker TPGDA, the polymerised structures completely dissolved when placed in water. Interestingly, an increasing **SPA** content leads to a reduction of the shrinkage of the hydrogel film. It is probable that the incorporation of **SPA**, and its non-polar, hydrophobic

characteristics, results in a material that is more hydrophobic overall. Furthermore, as discussed above, only 25% of the spiropyran is in its hydrophilic protonated merocyanine form at pH 2.7.

2.2.4 Preparation and photoresponse of substrate-attached surface topographies

In order to prepare surface relief structures in photopatterned hydrogels, the hydrogels need to be attached to glass substrates. Methacrylate functionalised glass was used to achieve covalent bonding between the hydrogel and its substrate. Glass cells with a spacing of 55 μm filled with the same acrylate mixture (97 mol% NIPAAM, 1 mol% of **SPA**, 1 mol% TPGDA and 1 mol% of Irgacure 2959) as used before for the preparation of freestanding films were exposed to UV light using a line mask with dark lines of 200 μm and a pitch of 300 μm . The mask was then removed and flood exposure ensured the formation of a polymer film over the entire surface area (Scheme 2.4a). In order to obtain well-defined relief structures, the intensity and the exposure time of the UV light source were optimised. The best results were obtained using a mask exposure step with 13.5 mW/cm^2 intensity in the range of 320-390 nm for 50 seconds and subsequent full exposure for 300 seconds (48 mW/cm^2 intensity in the range 320-390 nm).

Interferometry measurements showed a relatively flat (100 nm difference in height for a total height of 55 μm), patterned surface in which the double exposed lines with a width of 100 μm (**D100**) were slightly thicker than the single exposed lines with a width 200 μm (**S200**, Figure 2.5a, b, such differences in height were typically found for samples prepared in a similar fashion).³ Furthermore, two additional peaks were observed at the edges between **D100** and **S200**. This structure is most likely formed by the accumulation and subsequent polymerisation of monomers, especially in the case of the more reactive TPGDA diacrylate, at the edges of the double exposed areas.^{30,39} The polymerisation occurs faster than the diffusion. The diffusion of unreacted monomers towards the centre of the exposed parts is therefore inhibited since polymerisation is faster. The right-hand image in Scheme 2.4b shows the crosslink density in a film of this kind schematically. This behaviour is already familiar in samples prepared by polymerisation-induced diffusion. When using masks with a different pitch or with different polymerisation conditions, it was possible to make surface topographies in which it was possible to prevent the formation of these peaks.



Scheme 2.4 (a) Schematic representation of the polymerisation-induced diffusion process (darker grey scale corresponds to a higher crosslink density). The more reactive diacrylate (TPGDA) diffuses towards the exposed area during the first masked photopolymerisation (indicated by black arrows), whilst the less reactive monomers diffuse towards the non-exposed area (indicated by white arrows). Subsequent flood exposure ensures full polymerisation. As a result, double exposed areas (**D100**, 100 correspond to 100 μm width) achieve a higher crosslink density, while the other regions (**S200**) have a lower crosslink density. (b) Exaggerated representations of cross-sections of polymer films after two possible diffusion scenarios at the position of the **D100** sections are shown: when the polymerisation is slower than the diffusion, two distinct areas are obtained, with a gradual transition at the interface; when the polymerisation is faster than the diffusion and so monomer accumulates towards the edges.

When the sample was immersed in an acidic solution, the film changed from colourless to orange and swelled significantly in the z -direction (the swollen film has a thickness of 100 μm). Afterwards, a relief structure could be clearly observed. The profile of the surface topography changed dramatically compared to the film before swelling (Figure 2.5b, d). Additional protrusions between the two regions were formed. These are a result of the monomer accumulation which occurred during the first polymerisation step. The **S200** regions were more swollen than the **D100** areas, which is the inverse pattern by comparison with the film in its dry state. On the basis of the data for the freestanding films, it can be concluded that the crosslink density is higher in the double exposed areas than in the single exposed areas, leading to different swelling behaviour in the different parts of the films.³ The more reactive TPGDA diacrylate migrates towards the exposed area during the first photopolymerisation step. The height difference between the centres of the two regions with different crosslink density is $\sim 6 \mu\text{m}$, which is 60 times more than the height difference in the dry state (Figure 2.5b, d).

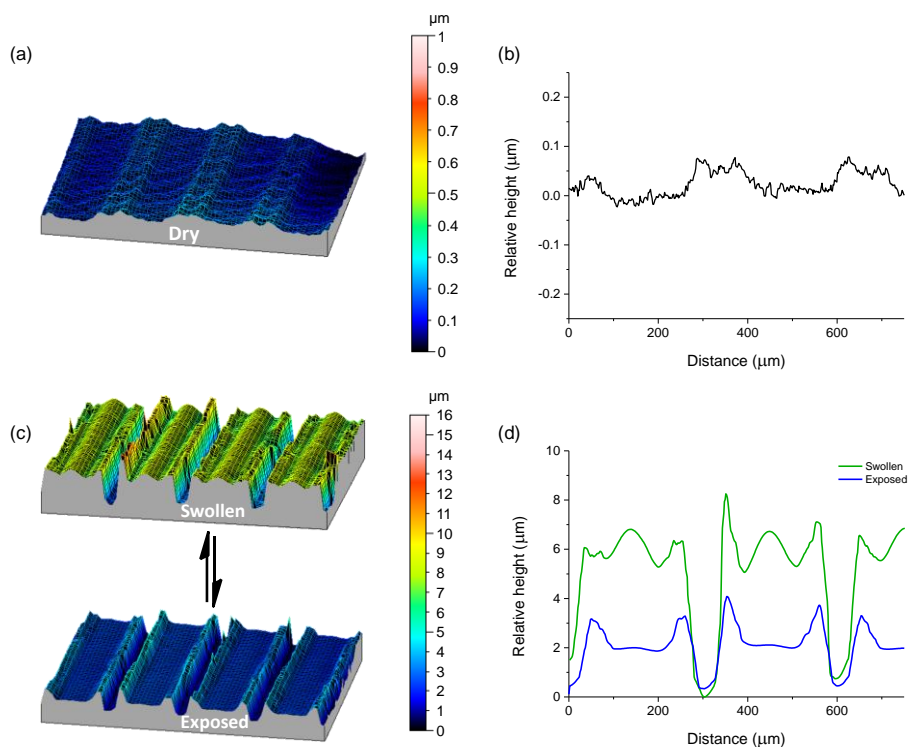


Figure 2.5 (a) Surface topography of a film obtained by photopolymerisation-induced diffusion (100 μm open, 200 μm dark line mask) before swelling and (b) the corresponding cross-section of the surface topography. (c) The surface topographies swollen in 2 mM HCl solution, before and after light exposure and (d) averaged cross-sections of the surface topographies, as observed by interferometry.

After the swollen hydrogel films were exposed to light, the height difference between the centres of the two regions with different crosslink densities was reduced from ~ 6 μm to ~ 2 μm in a reversible fashion. The thickness of the entire film decreased from 100 to 90 μm. In the **S200** regions, the decrease in thickness was 10%; in the **D100** regions this decrease was only 6% due to the higher crosslink density in the double exposed areas. On the basis of the data for the freestanding films (Table 2.1), a rough estimate of the TPGDA concentration in the different areas could be made, yielding values of 1-2 mol% in **D100** and 0.5-1 mol% in **S200**. However, since the films were constrained and surface-confined, shrinkage was observed in the z-direction only and overall shrinkage was therefore less than in the case of freestanding films.³ Contact angle measurements showed that the

changes in the patterned films were similar to those in the flat films (86° - 93°) since the structures are not small enough to induce Wenzel wetting.^{15,19,40,41}

2.3 Conclusion

A novel photochromic spiropyran acrylate was prepared and its characteristics established. After random copolymerisation with NIPAAm, the resulting polymer exhibited relative fast switching behaviour. The incorporation of a crosslinking diacrylate monomer resulted in photoresponsive hydrogels which change in size upon exposure to visible light. Photoswitchable hydrogel surface topographies were induced with a straightforward method based on polymerisation-induced diffusion. Two subsequent UV-polymerisation steps were introduced, resulting in patterned hydrogel films in which the spatial crosslink density can be controlled. When the polymer coating was swelled in 2 mM HCl solution, a surface topography formed. The height difference in the surface relief was reduced from $\sim 6 \mu\text{m}$ to $\sim 2 \mu\text{m}$ after light exposure, leading to a reversible alteration in the roughness of the surface topography. Photoresponsive patterned hydrogels of this kind have considerable potential benefits for the field of microfluidic devices or for the development of coatings which can change their smoothness or hydrophilicity by light.

Experimental section

Characterisation of compounds and materials: $^1\text{H-NMR}$ (400 MHz) and $^{13}\text{C-NMR}$ (100 MHz) spectra were recorded on a Varian spectrometer (Varian Mercury Vx 400). Splitting patterns are designated as s, singlet; d, doublet; dd, double doublet; t, triplet; quin, quintet; m, multiplet. MALDI measurements were carried out on a PerSeptive Biosystems Voyager DE-PRO spectrometer using α -cyano-4-hydroxycinnamic acid as a matrix. GPC was performed on a Varian PL-GPC50 Plus, with DMF as eluent. IR spectroscopy was recorded on a 3100 FT-IR Excalibur Series from Varian. UV/Vis spectroscopy was performed on a Shimadzu UV-3102 PC spectrometer using 1 cm quartz cuvettes (Hellma Analytics) for polymer solutions. For UV/Vis spectroscopy of the films, an HR2000+ high-resolution spectrometer from Ocean Optics mounted on a DM6000 M microscope from Leica microsystems was used. The corresponding light source emits between 400 and 800 nm. The dimensions of the hydrogel films were determined by flattening the films on a glass substrate before measuring with a ruler. Height profiles and 3D-images of patterned films were recorded using a 3D interferometer (Fogale Nanotech Zoomsurf). The UV light

intensities produced by the collimated EXFO Omnicure S2000 lamp were determined using a UV Power Puck II by EIT Instrument Markets Group. Static water contact angle measurements were performed on a Dataphysics OCA 30 at room temperature using deionised water as a probe liquid. Spin coating was performed on a Karl Suss RC6 spin coater.

Materials: Unless stated otherwise, all reagents and chemicals - UV-photoinitiator 2-hydroxy-1-[4-(2-hydroxyethoxy) phenyl]-2-methyl-1-propanone-1-one (Irgacure 2959, Ciba Specialty Chemicals), *N*-isopropylacrylamide (NIPAAM, Sigma-Aldrich), tripropylene glycol diacrylate (TPGDA, Sigma Aldrich), 1*H*,1*H*,2*H*,2*H*-perfluorodecyltriethoxysilane (Sigma Aldrich), 3-(trimethoxysilyl)propyl methacrylate (Sigma Aldrich), dye K160 (Risk Reactor) - were obtained from commercial sources and used without further purification. Deuterated solvents for recording NMR spectra were obtained from Cambridge Isotope Laboratories, Inc. (United States).

Synthesis of 6-bromohexan-1-ol (1)³³: A heterogeneous mixture of 1,6-hexanediol (5.0 g, 42.3 mmol), concentrated HBr solution (8.5 mL of a 48% aqueous solution, 50.4 mmol) and toluene (100 mL) was stirred and heated at reflux for 18 h under an argon atmosphere. Diethyl ether was added to the mixture and the aqueous layer was removed. The organic layer was subsequently washed with 1 M KOH solution, brine and water. The organic layer was dried with MgSO₄ and concentrated by rotary evaporation. The remaining oil was purified by column chromatography over a short plug of silica (10-15 vol% EtOAc in heptane), yielding 6.65 g (36.7 mmol, 86.8%) of **1** as a colourless oil. ¹H-NMR (400 MHz, CDCl₃, 25 °C, TMS): δ = 3.65 (t, *J* (H,H) = 6.52 Hz, 2H, HOCH₂), 3.41 (t, *J* (H,H) = 6.79 Hz, 2H, BrCH₂), 1.92-1.83 (m, 2H, BrCH₂CH₂), 1.63-1.54 (m, 2H, HOCH₂CH₂), 1.52-1.34 (m, 4H, CH₂ alkane), 1.30 ppm (s, 1H, OH).

Synthesis of 6-bromohexyl acrylate (2): 6-Bromohexan-1-ol (**1**, 5.0 g, 27.6 mmol) and triethylamine (4.7 mL, 33.7 mmol) were dissolved in dichloromethane under an argon atmosphere and cooled to 0 °C whilst stirring. Acryloyl chloride (2.7 mL, 33.2 mmol) was added slowly at this temperature. After stirring at 0 °C for 1 h, the mixture was allowed to warm up to room temperature. After 17 h, the mixture was concentrated and the white solid was filtered off. Column chromatography (10 vol% EtOAc in heptane) yielded 2.9 g (12.3 mmol, 44.7%) of **2** as a colourless oil (*NMR experiments revealed that a small portion of the bromide had been substituted by chloride*). In order to avoid premature polymerisation of the compound, a small amount of *tert*-butylhydroquinone (TBHQ) was added. ¹H-NMR (400 MHz, CDCl₃, 25 °C, TMS): δ = 6.40 (d, *J* (H,H) = 17.36 Hz, 1H, *trans*-HC=C), 6.12 (dd, *J* (H,H) = 17.33, 10.46 Hz, 1H, H₂C=CH), 5.82 (d, *J* (H,H) = 10.39 Hz, 1H, *cis*-HC=C), 4.16 (t, *J*

(H,H) = 6.51 Hz, 2H, ROCH₂), 3.41 (t, J (H,H) = 6.71 Hz, 2H, BrCH₂), 1.93-1.83 (m, 2H, BrCH₂CH₂), 1.69 (quin, J (H,H) = 6.63 Hz, 2H, ROCH₂CH₂), 1.54-1.36 ppm (m, 4H, CH₂ alkane); ¹³C-NMR (100 MHz, CDCl₃, 25 °C, TMS): δ = 166.28 (C=O), 130.55 (CH=CH₂), 128.54 (CH=CH₂), 64.39 (OCH₂), 33.68 (BrC), 32.60 (BrCH₂C), 28.45 (OCH₂C), 25.29 (CH₂ alkane), 25.17 ppm (CH₂ alkane).

Synthesis of 1',3',3'-trimethylspiro[chromene-2,2'-indolin]-6-ol (3)³⁴: A mixture of 1,3,3-trimethyl-2-methyleneindoline (0.50 g, 2.90 mmol) and 2,5-dihydroxybenzaldehyde (0.40 g, 2.90 mmol) in ethanol (10 mL) was heated at reflux temperature under an argon atmosphere for 2 h. The solvent was removed by rotary evaporation and the resulting mixture was subjected to column chromatography (8 vol% EtOAc in heptane) to yield 0.72 g (2.45 mmol, 84.8%) of **3** as an off-white solid. (Note: impure fractions were successfully purified using sublimation; 110 °C, 10⁻³ bar, cooling water at 20 °C) ¹H-NMR (400 MHz, CDCl₃, 25 °C, TMS): δ = 7.17 (t, J (H,H) = 7.64 Hz, 1H, CH Ar), 7.07 (d, J (H,H) = 6.72 Hz, 1H, CH Ar), 6.83 (t, J (H,H) = 7.21 Hz, 1H, CH Ar), 6.77 (d, J (H,H) = 10.20 Hz, 1H, NCCH=CH), 6.62-6.49 (m, 4H, CH Ar), 5.70 (d, J (H,H) = 10.19 Hz, 1H, NCCH=CH), 4.32 (s, 1H, OH), 2.71 (s, 3H, NCH₃), 1.29 (s, 3H, CCH₃), 1.15 ppm (s, 3H, CCH₃); ¹³C-NMR (100 MHz, CDCl₃, 25 °C, TMS): δ = 148.63, 148.20, 136.80, 128.98, 127.54, 121.46, 120.48, 119.27, 119.00, 116.33, 115.59, 112.8, 106.73, 103.81, 51.63, 28.94, 25.84, 20.23 ppm; MALDI TOF MS: *m/z* calcd for C₁₉H₁₉NO₂ (M+H)⁺: 294.15, found: 294.09.

Synthesis of 6-((1',3',3'-trimethylspiro[chromene-2,2'-indolin]-6-yl)oxy)hexyl acrylate (SPA)³⁵: Compound **2** (0.40 g, 1.70 mmol), compound **3** (0.50 g, 1.70 mmol), K₂CO₃ (0.95 g, 6.87 mmol) and a grain of KI were suspended in butanone under an argon atmosphere before the mixture was heated to reflux temperature for 15 h, after which the mixture was cooled down and filtered, and solvent was removed by rotary evaporation. The crude mixture was subjected to column chromatography (8 vol% EtOAc in heptane). The organic layer was dried with MgSO₄ and concentrated by rotary evaporation. A small amount of TBHQ was added to the mixture before it was dissolved in a minimum amount of dichloromethane and precipitated in hexane to yield target compound **SPA** as white crystals (0.44 g, 0.98 mmol, 57.4%). ¹H-NMR (400 MHz, CDCl₃, 25 °C, TMS): δ = 7.17 (t, J (H,H) = 7.60 Hz, 1H, CH Ar), 7.06 (d, J (H,H) = 7.03 Hz, 1H, CH Ar), 6.83 (t, J (H,H) = 7.45 Hz, 1H, CH Ar), 6.79 (d, J (H,H) = 10.26 Hz, 1H, NCCH=CH), 6.68-6.58 (m, 3H, CH Ar), 6.51 (d, J (H,H) = 7.84 Hz, 1H, CH Ar), 6.40 (d, J (H,H) = 17.34 Hz, 1H, *trans*-HC=C), 6.12 (dd, J (H,H) = 17.30, 10.70 Hz, 1H, H₂C=CH), 5.82 (d, J (H,H) = 10.41 Hz, 1H, *cis*-HC=C), 5.69 (d, J (H,H) = 10.08 Hz, 1H, NCCH=CH), 4.17 (t, J (H,H) = 6.58 Hz, 2H, OCH₂), 3.89 (t, J (H,H) = 6.38 Hz, 2H, ArOCH₂), 2.72 (s, 3H, NCH₃), 1.81-1.66 (m, 4H, ROCH₂CH₂), 1.53-1.39 (m, 4H, CH₂ alkane), 1.30 (s, 3H, CCH₃), 1.16 ppm (s, 3H, CCH₃); ¹³C-NMR (100 MHz, CDCl₃, 25 °C, TMS): δ =

166.31, 152.54, 148.51, 148.23, 136.83, 130.50, 129.28, 128.58, 127.53, 121.45, 120.19, 119.05, 118.97, 115.90, 115.45, 112.23, 106.71, 103.80, 68.44, 64.53, 51.60, 29.27, 28.93, 28.57, 25.84, 25.77, 25.75, 20.24 ppm; MALDI TOF MS: m/z calcd for $C_{28}H_{33}NO_4$ (M)⁺: 447.24, found: 447.31.

Copolymerisation of SPA and NIPAAM (PNS): SPA (11.9 mg, 0.027 mmol), NIPAAM (98.6 mg, 0.87 mmol) and AIBN (3.0 mg, 0.018 mmol) were dissolved in THF (0.5 mL) and the mixture was degassed using 5 freeze-pump-thaw cycles. The mixture was heated at reflux temperature under an argon atmosphere for 19 h before it was cooled down to room temperature. Viscosity was reduced by adding additional THF and the polymer was precipitated in diethyl ether, resulting in 84 mg (76.0%) of PNS as a white compound. ¹H-NMR (400 MHz, [D₇]DMF, 25 °C): δ = 7.50 (br, 34H, NH), 7.14 (dd, J (H,H) = 7.40 Hz, 3H), 7.05 (d, J (H,H) = 10.26 Hz, 1H) 6.88-6.84 (br, 1H), 6.80 (t, J (H,H) = 7.36 Hz, 1H), 6.75 (d, J (H,H) = 8.64 Hz, 1H), 6.59 (dd, J (H,H) = 12.59, 8.21 Hz, 2H), 5.83 (d, J (H,H) = 10.12 Hz, 1H), 3.96 (s, 45H, (CH₃)₂CH), 2.27-2.16 (m, 40H, backbone), 1.81-1.38 (m, 80H, backbone), 1.13 ppm (s, 242H, CH(CH₃)₂).); $M_w \approx 15,000$, PDI ≈ 2.4 .

Glass functionalisation: Glass substrates were cleaned by sonication (ethanol, 15 minutes), followed by treatment in a UV-ozone photoreactor (Ultra Violet Products, PR-100, 20 minutes). The surface of the glass substrates was modified by spin coating 3-(trimethoxysilyl)propyl methacrylate solution (1 vol% solution in a 1:1 water-isopropanol mixture) or 1H,1H,2H,2H-perfluorodecyltriethoxysilane solution (1 vol% solution in ethanol) onto the activated glass substrate for 45 seconds at 3000 rpm. The substrates were ready to use after curing for 10 minutes at 100 °C.

Preparation of photoresponsive coatings: A cell consisting of two (perfluorodecyl-triethoxysilane functionalised) glass substrates with a spacing of $\sim 55 \mu\text{m}$ was prepared for the freestanding films. At 110 °C, these cells were capillary filled with mixtures of NIPAAM, SPA, TPGDA and Irgacure 2959 in the molten state. Illumination for 300 seconds at the same temperature (unfiltered spectrum of a collimated EXFO Omnicure S2000 lamp, 48 mW/cm² intensity in the range 320-390 nm) resulted in fully polymerised films. In the case of the substrate-attached patterned films, the cell consisted of one upper perfluorodecyl-triethoxysilane functionalised glass slide and a lower propyl methacrylate functionalised glass slide with a spacing of $\sim 55 \mu\text{m}$. The cells were placed on a black surface in order to minimise polymerisation in non-exposed areas as a result of additional optical effects caused by reflection of the light that had already passed through the sample. A mask was placed on top of the sample and the sample was exposed (50 sec, 13.5 mW/cm² intensity in

the range 320-390 nm). The mask was then removed and the cell was fully exposed for another 300 seconds (48 mW/cm² intensity in the range 320-390 nm).

Photoactivation of the films and solutions: An EXFO Omnicure S2000 lamp was used for the light irradiation of the films and solutions and the desired wavelengths were selected using a 400 nm cut-on filter (Newport FSQGG400, 100 mW/cm² in the range 395-445 nm).

References

- 1 R. Byrne, F. Benito-Lopez and D. Diamond, *Mater. Today*, 2010, **13**, 16-23.
- 2 J. M. Spruell and C. J. Hawker, *Chem. Sci.*, 2011, **2**, 18-26.
- 3 D. Liu, C. W. M. Bastiaansen, J. M. J. den Toonder and D. J. Broer, *Soft Matter*, 2013, **9**, 588-596.
- 4 D. Liu, C. W. M. Bastiaansen, J. M. J. den Toonder and D. J. Broer, *Angew. Chem., Int. Ed.*, 2012, **51**, 892-896.
- 5 J. Wei and Y. Yu, *Soft Matter*, 2012, **8**, 8050-8059.
- 6 L. Florea, D. Diamond and F. Benito-Lopez, *Macromol. Mater. Eng.*, 2012, **297**, 1148-1159.
- 7 C. Ohm, M. Brehmer and R. Zentel, *Adv. Mater.*, 2010, **22**, 3366-3387.
- 8 S. Pedron, S. van Lierop, P. Horstman, R. Penterman, D. J. Broer and E. Peeters, *Adv. Funct. Mater.*, 2011, **21**, 1624-1630.
- 9 S. Sortino, *J. Mater. Chem.*, 2012, **22**, 301-318.
- 10 F. Benito-Lopez, R. Byrne, A. M. Raduta, N. E. Vrana, G. McGuinness and D. Diamond, *Lab Chip*, 2010, **10**, 195-201.
- 11 S.-W. Fu, H.-W. Chien and W.-B. Tsai, *Langmuir*, 2013, **29**, 14351-14355.
- 12 D. J. Beebe, J. S. Moore, J. M. Bauer, Q. Yu, R. H. Liu, C. Devadoss and B.-H. Jo, *Nature*, 2000, **404**, 588-590.
- 13 V. I. Minkin, *Chem. Rev.*, 2004, **104**, 2751-2776.
- 14 R. Klajn, *Chem. Soc. Rev.*, 2014, **43**, 148-184.
- 15 A. Athanassiou, M. I. Lygeraki, D. Pisignano, K. Lakiotaki, M. Varda, E. Mele, C. Fotakis, R. Cingolani and S. H. Anastasiadis, *Langmuir*, 2006, **22**, 2329-2333.
- 16 R. Byrne and D. Diamond, *Nat. Mater.*, 2006, **5**, 421-424.
- 17 F. Ercole, T. P. Davis and R. A. Evans, *Polym. Chem.*, 2010, **1**, 37-54.
- 18 A. Garcia, M. Marquez, T. Cai, R. Rosario, Z. Hu, D. Gust, M. Hayes, S. A. Vail and C.-D. Park, *Langmuir*, 2007, **23**, 224-229.
- 19 W. Jiang, G. Wang, Y. He, X. Wang, Y. An, Y. Song and L. Jiang, *Chem. Commun.*, 2005, **0**, 3550-3552.
- 20 G. Joseph, J. Pichardo and G. Chen, *Analyst*, 2010, **135**, 2303-2308.
- 21 A. Szilágyi, K. Sumaru, S. Sugiura, T. Takagi, T. Shinbo, M. Zrínyi and T. Kanamori, *Chem. Mater.*, 2007, **19**, 2730-2732.
- 22 T. Satoh, K. Sumaru, T. Takagi, K. Takai and T. Kanamori, *Phys. Chem. Chem. Phys.*, 2011, **13**, 7322-7329.
- 23 K. Sumaru, M. Kameda, T. Kanamori and T. Shinbo, *Macromolecules*, 2004, **37**, 7854-7856.

- 24 K. Sumaru, M. Kameda, T. Kanamori and T. Shinbo, *Macromolecules*, 2004, **37**, 4949-4955.
- 25 T. Satoh, K. Sumaru, T. Takagi and T. Kanamori, *Soft Matter*, 2011, **7**, 8030-8034.
- 26 J. Kim, J. A. Hanna, M. Byun, C. D. Santangelo and R. C. Hayward, *Science*, 2012, **335**, 1201-1205.
- 27 S. Sugiura, K. Sumaru, K. Ohi, K. Hiroki, T. Takagi and T. Kanamori, *Sens. Actuators, A*, 2007, **140**, 176-184.
- 28 T. Sun and G. Qing, *Adv. Mater.*, 2011, **23**, H57-H77.
- 29 D. Liu, C. W. M. Bastiaansen, J. M. J. den Toonder and D. J. Broer, *Macromolecules*, 2012, **45**, 8008-8012.
- 30 C. M. Leewis, A. M. de Jong, L. J. van Ijzendoorn and D. J. Broer, *J. Appl. Phys.*, 2004, **95**, 8352-8356.
- 31 J. Madsen and S. P. Armes, *Soft Matter*, 2012, **8**, 592-605.
- 32 H. G. Schild, *Prog. Polym. Sci.*, 1992, **17**, 163-249.
- 33 J. M. Chong, M. A. Heuft and P. Rabbat, *J. Org. Chem.*, 2000, **65**, 5837-5838.
- 34 R. Kießwetter, N. Pustet, F. Brandl and A. Mannschreck, *Tetrahedron: Asymmetry*, 1999, **10**, 4677-4687.
- 35 D. A. Davis, A. Hamilton, J. Yang, L. D. Cremar, D. Van Gough, S. L. Potisek, M. T. Ong, P. V. Braun, T. J. Martinez, S. R. White, J. S. Moore and N. R. Sottos, *Nature*, 2009, **459**, 68-72.
- 36 J. T. C. Wojtyk, A. Wasey, N.-N. Xiao, P. M. Kazmaier, S. Hoz, C. Yu, R. P. Lemieux and E. Buncel, *J. Phys. Chem. A*, 2007, **111**, 2511-2516.
- 37 K. Sumaru, K. Ohi, T. Takagi, T. Kanamori and T. Shinbo, *Langmuir*, 2006, **22**, 4353-4356.
- 38 S. Tsoi, D. J. Broer, C. W. Bastiaansen and M. G. Debije, *Opt. Express*, 2010, **18**, A536-A543.
- 39 B.-J. de Gans, C. Sánchez, D. Kozodaev, D. Wouters, A. Alexeev, M. J. Escuti, C. W. M. Bastiaansen, D. J. Broer and U. S. Schubert, *J. Comb. Chem.*, 2006, **8**, 228-236.
- 40 F. Xia, H. Ge, Y. Hou, T. Sun, L. Chen, G. Zhang and L. Jiang, *Adv. Mater.*, 2007, **19**, 2520-2524.
- 41 G. Qing and T. Sun, *Adv. Mater.*, 2011, **23**, 1615-1620.

Chapter 3

Photoresponsive hydrogel ratchet topographies in a neutral environment

Abstract

This chapter describes the preparation of self-protonating spiropyran-based poly(*N*-isopropylacrylamide) polymer networks. These photoresponsive hydrogel coatings can change their surface topography upon exposure to visible light in a neutral environment. Photoresponsive surface-constrained films were produced in which the swelling behaviour could be controlled in a reversible manner. In a first step, symmetrical, switchable surface topologies with varying crosslink densities were obtained by polymerisation-induced diffusion. Upon exposure to light, the areas with a low crosslink density swell more than the areas with a high crosslink density, with a corrugated surface as a result. Asymmetric ratchet-like photoresponsive surfaces were prepared on pre-structured asymmetric substrates. Variation in the thickness of the surface-confined hydrogel layer resulted in asymmetric swelling behaviour. Depending on the crosslink density of the hydrogel, it is possible to use light to switch between a ratchet and flat surface topography or even an inverse ratchet surface.

This chapter is partially reproduced from: J. E. Stumpel, B. Ziółkowski, L. Florea, D. Diamond, D. J. Broer and A. P. H. J. Schenning, *ACS Applied Materials & Interfaces*, 2014, **6**, 7268-7274.

3.1 Introduction

Responsive surface topographies manufactured from materials that change their properties in a reversible fashion attract increasing attention in recent years.^{1,2} Chapter 2 describes the development of such photoresponsive N-isopropylacrylamide(NIPAAm)-based hydrogels containing spiropyran which operate in a slightly acidic environment.³⁻⁷ So far, most of the related research has focused on symmetrical, responsive surface topographies, and there have been few studies of asymmetrically responsive topologies.⁸ Such types of coatings can be interesting for transport or fluidic control. Ratchet-like structures in particular have considerable promise in terms of the induction of the unidirectional transport of liquids and particles.⁹⁻¹² A new kind of hydrogel containing spiropyran was reported recently.¹³ In this system, the incorporation of a small amount of acrylic acid into the polymer backbone, which acts as an internal proton source, leads to freestanding photoresponsive polymer gels that operate in a neutral environment. This chapter describes the fabrication of asymmetrical, light-responsive topographies based on self-protonating spiropyran-PNIPAAm hydrogels, which operate at neutral pH (Scheme 2.1 depicts the switch between protonated merocyanine and spiropyran induced by isomerisation). Initially, surface-constrained films were prepared to study the photoresponsive behaviour of the coating at neutral pH. It was found that the response time is similar to that of hydrogels operating at pH = 2.7. The degree of swelling can be controlled by the amount of crosslinker. Subsequently, symmetrical, switchable surface topologies with varying crosslink densities in the polymer network were obtained by polymerisation-induced diffusion. Novel asymmetric surface topographies were prepared in a single photopolymerisation step on a pre-structured surface with a ratchet-like topography.⁸ Because of the variable thickness of the hydrogel in different areas, the surface topography changes upon exposure to visible light. A thicker layer will result in a larger degree of swelling of the confined pattern. Depending on the crosslink density in the polymer film, asymmetric, responsive surfaces can be produced that switch between a ratchet and flat surface or a mirror-image ratchet topography.

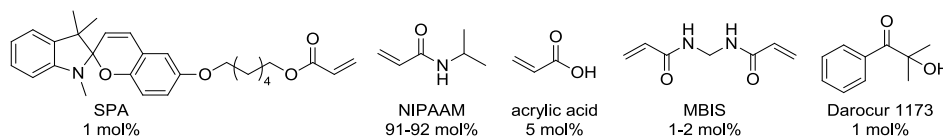
3.2 Results and discussion

3.2.1 Preparation and photoresponse of surface-constrained hydrogel films

Initially, the photoresponsive behaviour of self-protonating spiropyran hydrogels covalently attached to a surface was investigated. A chemical composition similar to that previously reported was used for these hydrogels (Scheme 3.1).¹³ *N*-Isopropylacrylamide (NIPAAM) was used as main component (92% and 91% in mixtures **1** and **2**, respectively). The spiropyran derivative **SPA** was incorporated as the photochromic unit (1%) and acrylic acid (5%) was added to obtain the self-protonated merocyanine form.^{4,13} For the chemical crosslinking of the network, 1 or 2 mol% of *N,N'*-methylenebisacrylamide (MBIS) was used (mixture **1** or **2**, Table 3.1). Darocur 1173 was used as the photoinitiator. The monomer mixture was dissolved in anhydrous dioxane prior to use. Unless stated otherwise, mixture **1** was used in all experiments.

Table 3.1 Variation in the composition of the studied mixtures; all mixtures contained 1 mol% of the photoinitiator Irgacure 2959

Mixture	NIPAAM (mol%)	MBIS (mol%)	SPA (mol%)	Acrylic acid (mol%)
1	92	1	1	5
2	91	2	1	5



Scheme 3.1 Materials used for the preparation of the polymer coatings

A glass cell (spacing = 55 μm) with a lower methacrylate functionalised surface and an upper fluorinated surface was used. This cell was filled with the monomer mixture, which was then photopolymerised to full conversion to result in a surface-constrained polymer coating firmly adhering to the lower glass plate. The upper glass plate was then removed and the dioxane was evaporated, resulting in a film (approximately 25 μm thick) which was covalently attached to its substrate. The polymer coating was then placed in demineralised water, allowing the film to swell. After swelling for at least 1 hour to reach equilibrium, the thickness of the film had increased to roughly 140 μm . This high degree of swelling (5.6 times) was

probably caused by the fact that the polymer network was prepared in solution, resulting in a non-rigid porous network. Polymer coatings prepared from mixture 2 swell slightly less because there are twice as many the crosslinks. Here, a thickness of 120 μm (4.8 times) was obtained. As the hydrogel cannot swell in a unidirectional fashion, swelling occurs mostly in the z-direction, and swelling behaviour is therefore different than for freestanding films.¹⁴

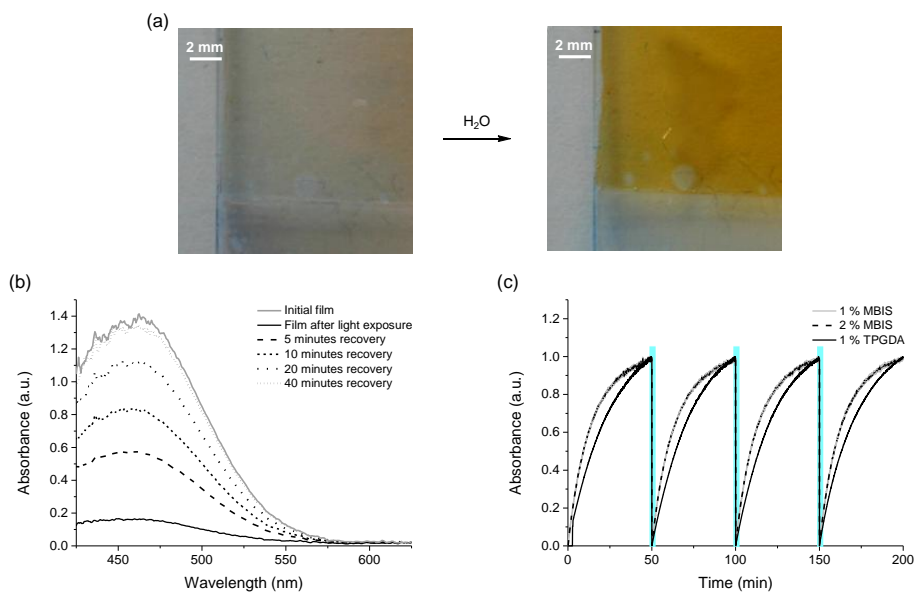


Figure 3.1 (a) Optical images of a surface-constrained hydrogel before and after swelling in demineralised water, showing its self-protonating behaviour. (b) UV/Vis spectrum showing a spontaneous recovery of spiropyran into protonated merocyanine after exposure to light (455 nm) for 5 minutes. (c) Reversible photoresponsive behaviour of hydrogel films with 1 or 2% MBIS and 1% TPGDA as crosslinker. The change in absorption at 470 nm is depicted after 5 minutes of photo-exposure for four successive cycles.

During the swelling of the hydrogels, the slightly off-colour hydrogel film changed to a more intense orange colour (Figure 3.1a), which indicates that the protonated merocyanine isomer formed spontaneously in water because of the carboxylic acid that is incorporated in the polymer backbone. Absorption measurements of the film showed an absorption maximum of $\lambda = 470$ nm, which is consistent with the formation of the self-protonated merocyanine hydrogel.^{4,15} When the sample was exposed to visible light ($\lambda = 455$ nm) for 5 minutes, the protonated merocyanine absorbance at 470 nm almost completely disappeared (Figure 3.1b), demonstrating

complete isomerisation of the protonated merocyanine into the spiroopyran form (Scheme 2.1).

The back-isomerisation of spiroopyran to protonated merocyanine was monitored with UV/Vis spectroscopy. After 50 minutes at room temperature, the absorption band at $\lambda = 470$ nm returned to its initial intensity (Figure 3.1b, c), demonstrating complete recovery. Four successive exposure cycles show that this recovery is fully reversible and can be repeated multiple times.¹⁶ The $t_{1/2}$ value of the recovery is ~ 10 minutes, which is slightly faster than the hydrogels without acrylic acid immersed in an acidic environment which were discussed in Chapter 2.⁴ The faster recovery is most likely related to the use of MBIS instead of tripropylene glycol diacrylate (TPGDA) rather than to the difference between internal or external protonation. When the amount of crosslinker was increased from 1 to 2 mol%, the same recovery time scale was observed despite the difference in the crosslink density (Figure 3.1c). Furthermore, the spiroopyran moiety modified with hexyl acrylate leads to faster recovery than its directly acrylated spiroopyran analogue (Figure 3.2). This behaviour can be explained by the fact that an ether group on the benzene ring has a stronger electron-donating character than an ester group.¹⁵

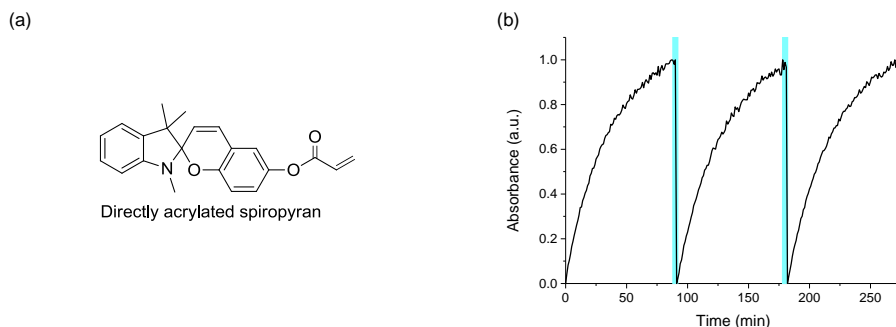


Figure 3.2 (a) Chemical structure of directly acrylated spiroopyran. (b) The reversible photoresponsive behaviour of a hydrogel based on this photochromic moiety. The absorption intensity at 430 nm is depicted during three successive exposure steps.

To measure the swelling behaviour of the initially flat hydrogel coating, masked exposure ($\lambda = 455$ nm) was performed using a line mask with dark lines of 1 mm and a pitch of 2 mm (schematic representation in Figure 3.3a). After this masked exposure step, the exposed areas lost their colour and the non-exposed areas remained unchanged (Figure 3.3b). It can therefore be concluded that isomerisation

was confined to the exposed parts of the film. As with the experiments performed without a photomask, spiropyran isomerised back into the protonated merocyanine isomer in approximately 50 minutes.

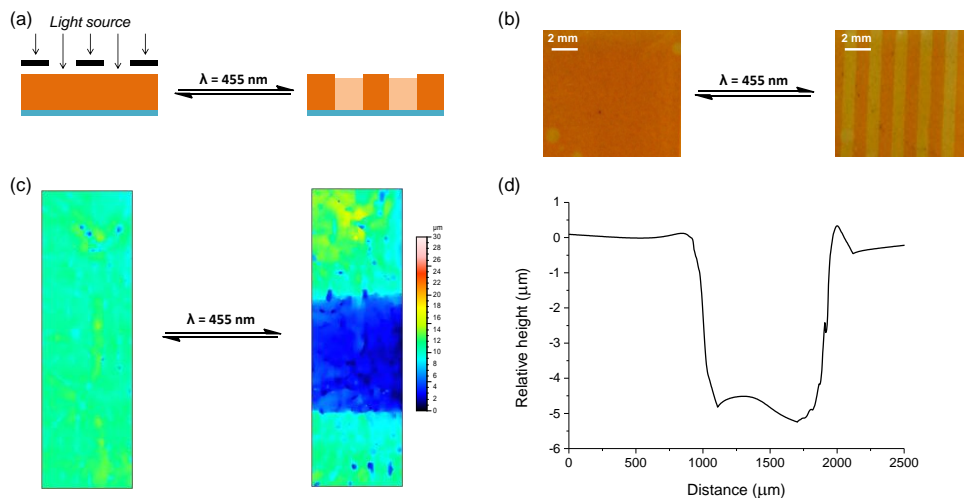


Figure 3.3 (a) Schematic representation of masked illumination of the initially flat hydrogel coating, (b) photographs of a hydrogel (mixture 1) before (left) and after (right) masked illumination (455 nm), (c) corresponding height profile (dimensions $2.5 \times 0.75 \text{ mm}^2$) and (d) cross-section of the surface topography as observed by interferometry. The average height of the unexposed area has been set as zero.

After mask exposure, the change in surface topography was investigated. Interferometry measurements revealed (Figure 3.3c, d) that the exposed areas shrank after masked exposure, leading to a symmetrically structured surface topography.¹⁷ In the exposed areas, the thickness of the film decreased by approximately $5 \mu\text{m}$; in other words, the swollen film shrank by 3.6%. To investigate the influence of the amount of crosslinker, similar experiments were performed in which the amount of MBIS was doubled (mixture 2, gel thickness is $120 \mu\text{m}$). The thickness of the structures obtained using these hydrogels fell by only $3.2 \mu\text{m}$ after the masked exposure step, which is much less than with the lesser amount of MBIS. This lower shrinkage of 2.7% is attributable to the higher crosslink density, which results in less swelling and shrinkage. The results show that photoresponsive surface topography changes can be fine-tuned by varying the crosslink density of the hydrogel.

3.2.2 *Symmetric, photoresponsive surface topographies by polymerisation-induced diffusion*

We first created symmetrical, photoresponsive surface topography hydrogels that operate at neutral pH. These films were produced using a controlled spatial distribution of the crosslink density, leading to patterned swelling.^{18,19} Hydrogels were therefore prepared by polymerisation-induced diffusion in the presence of a solvent (see Scheme 2.4 for the preparation method).^{4,20} Polymerisation-induced diffusion occurs during the patterned UV-light exposure of a monomer mixture because of the different diffusion and polymerisation rates of the monomers. This leads to a patterned crosslink density following the pattern of the mask used during the photopolymerisation step. In previous solvent-free experiments at elevated temperature, polymerisation was faster than diffusion, resulting in the accumulation of the diacrylate monomers near the edges of the photomask.^{4,21,22}

The same types of cells as those used in the preparation of surface-constrained hydrogel films were used. However, in case of the production of patterned hydrogels, the photopolymerisation process consisted of two sequential photo-exposure steps at room temperature. The first step was masked UV illumination, after which the mask was removed and flood UV exposure was used to ensure the formation of a polymer film over the entire surface area. These polymerisations were performed in solution and so there was a high degree of monomer mobility. Diffusion of the monomers during the first exposure step was therefore faster than in the solvent-free experiments, resulting in smooth structures instead of the accumulation of monomers at the edges of the exposed areas (Figure 3.4b).

The initial thickness of the coatings prepared by polymerisation-induced diffusion was approximately 30 μm . After swelling, the thickness of areas with a low crosslink density increased to 200 μm (6.6 times swollen). The height of the relief structure was 28 μm , with the areas exposed twice swelling less (5.6 times, Figure 3.4b). This behaviour indicates that these areas contain more crosslinker since the more reactive diacrylate crosslinker diffuses to the exposed areas during the first exposure step.

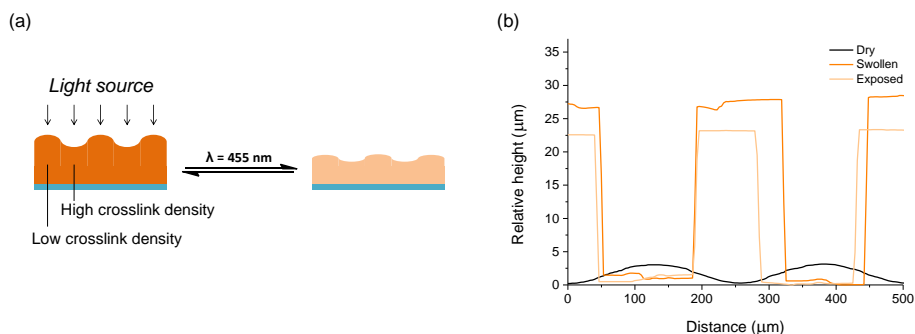


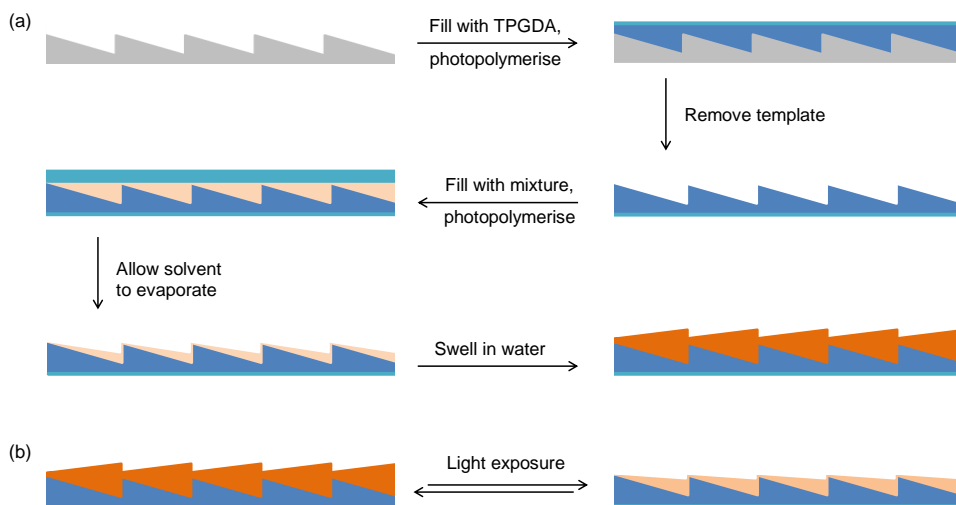
Figure 3.4 (a) Schematic representation of the hydrogel prepared by polymerisation-induced diffusion and (b) height profiles of the surface topography of a hydrogel prepared by polymerisation-induced diffusion before and after exposure, as observed by interferometry. The lowest heights were set as zero (note: due to smoothing software, the topographies are presented as more block-like than their actual shape; however, the minimum and maximum values are accurate).

After exposure to visible light ($\lambda = 455 \text{ nm}$), the total thickness of areas with a low crosslink density decreased to $180 \mu\text{m}$ (-10%) and the thickness of the relief structure fell to $23 \mu\text{m}$ (-18%, Figure 3.4b). It can therefore be concluded that a crosslink density difference throughout the film can be obtained using polymerisation-induced diffusion for solubilised systems as well. The polymer film is surface-constrained and it can therefore only swell in the direction perpendicular to the surface. It should be noted that the swelling and photoresponsive behaviour of the coating are larger than is the case of the constrained homogeneous polymer coatings (see above). This behaviour indicates that the areas with low or high crosslink density do not behave independently; in other words, they are affected by each other.

3.2.3 Asymmetric, photoresponsive surface topographies on pre-structured substrates

An asymmetric ratchet substrate was used to produce asymmetric, photoresponsive surface topographies. This approach is based on the fact that a thicker surface-constrained hydrogel film swells more and because the asymmetry in the substrate results in asymmetric swelling.⁸ A copy of a ratchet template (a Fresnel lens) was made using TPGDA, which was partly photopolymerised so that pendant acrylate groups were still present at this point. Subsequently, the structure was filled with the hydrogel mixture and photopolymerised, resulting in a hydrogel that was covalently linked to the asymmetric substrate. Following

evaporation of dioxane after polymerisation, the dried film had a topography that was similar to, but less steep than, the topography of the TPGDA substrate (Scheme 3.2a).



Scheme 3.2 (a) Preparation method and (b) working mechanism of the photoresponsive hydrogel with ratchet-like topography

In its dry state, the maximum height of the polymer network is $10.7\ \mu\text{m}$. The surface, after the film was swollen in demineralised water, had a ratchet topography (Figure 3.5) that was the inverse of that of the dry film. This behaviour shows that, as expected, the thicker surface parts swell more, where swelling here is defined as the absolute increase of local volume (Scheme 3.2b). The maximum height difference was around $6\ \mu\text{m}$ (the total height of the swollen hydrogel $26\ \mu\text{m}$). Upon light exposure, the ratchet slope decreased. The maximum change that could be obtained was a reduction of $3\ \mu\text{m}$ in height. Subsequent illumination and reswelling cycles resulted in similar shrinkage and swelling behaviour, showing that the hydrogel coating can be reversibly switched between a ratchet and a more flat surface topography.

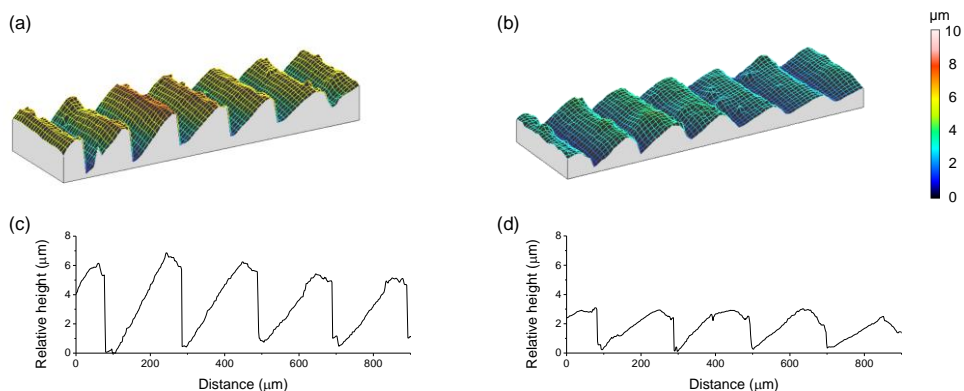


Figure 3.5 3D height profiles of a ratchet prepared from mixture 1 before (a) and after (b) light exposure and (c, d) corresponding cross-sections of the surface topography, as observed by interferometry (dimensions of the surface are $379 \times 1262 \mu\text{m}^2$)

In order to show that the surface topography can be controlled by varying the amount of crosslinker, similar ratchet films were prepared from mixture 2 containing 2 wt% crosslinker (Figure 3.6). Because of the higher crosslink density, the hydrogel obtained swelled less than the hydrogel discussed previously (the initial height is $10.8 \mu\text{m}$, and the height of the swollen hydrogel is $21.3 \mu\text{m}$). This results in an asymmetric structure with a difference in height of only $1.8 \mu\text{m}$ after being swollen in demineralised water, which is comparable with the difference in the case of surface-constrained films (see above). Upon exposure to visible light, the surface went from ratchet-structured to flat and even formed an inverse ratchet structure with a $1 \mu\text{m}$ height difference. Furthermore, the alteration of the protrusions was easy to control by varying the intensity of the illumination and the exposure time. It was possible to photoswitch both ratchet structures many times. After several months of storage in demineralised water, the response of the coating to light was still present (in other words, there was no decrease in the response by comparison with fresh samples), showing that it is possible to produce durable photoresponsive topographies.

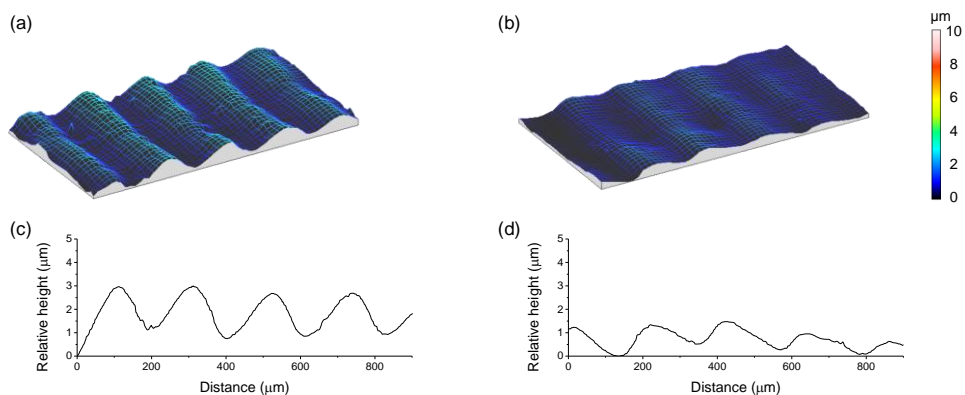


Figure 3.6 3D height profiles of a ratchet prepared from mixture 2 before (a) and after (b) light exposure and (c, d) corresponding cross-sections of the surface topography, as observed by interferometry (dimensions of the surface are $505 \times 946 \mu\text{m}^2$)

3.3 Conclusion

Hydrogels based on polymer networks of NIPAAm, spiropyran and acrylic acid have been used to produce photoresponsive symmetric and asymmetric surface topographies that can operate in a neutral aqueous environment. By using pre-structured ratchet substrates, the light-responsive asymmetric surface topography can, in principle, be fully controlled by the chemical composition of the mixture. Furthermore, one can expect that even more complex surface topographies are possible by combining the approaches reported here, in other words local light exposure, polymerisation-induced diffusion and pre-structured substrate approaches. The results show that dynamic robust asymmetric hydrogel surfaces can be obtained that can be useful in, for instance, microfluidic and biological applications.²³⁻²⁷

Experimental section

Characterisation of materials: UV/Vis experiments were performed on an HR2000+ high resolution spectrometer from Ocean Optics mounted on a DM6000 M microscope from Leica microsystems. The corresponding light source produces reliable emissions between 400 and 800 nm. Height profiles and 3D images of the patterned films were recorded using a 3D interferometer (Fogale Nanotech Zoomsurf with a vertical resolution of 0.1 nm). Spin coating was performed on a Karl Suss RC6 spin coater.

Materials: Unless stated otherwise, all reagents and chemicals - UV-photoinitiators 2-hydroxy-2-methyl-1-phenyl-1-propan-1-one (Darocur 1173, Ciba Specialty Chemicals), 2-hydroxy-1-[4-(2-hydroxyethoxy) phenyl]-2-methyl-1-propanone-1-one (Irgacure 2959, Ciba Specialty Chemicals), acrylic acid, *N*-isopropylacrylamide (NIPAAM), *N,N'*-methylenebisacrylamide (MBIS), tripropylene glycol diacrylate (TPGDA), 1*H*,1*H*,2*H*,2*H*-perfluorodecyl triethoxysilane and 3-(trimethoxysilyl)propyl methacrylate - were obtained from commercial sources (Sigma Aldrich unless stated otherwise) and used without further purification. 6-((1',3',3'-Trimethylspiro[chromene-2,2'-indolin]-6-yl)oxy)hexyl acrylate (**SPA**) was prepared as described in Chapter 2.⁴ Bartosz Ziółkowski kindly synthesised and provided 1',3',3'-Trimethylspiro[chromene-2,2'-indolin]-6-yl acrylate.¹³ Four monomer mixtures were used. Mixture **1** consists of 92, 1, 5, 1 and 1 mol% of NIPAAM, **SPA**, acrylic acid, MBIS and Darocur 1173 respectively. The amounts in mixture **2** were 91, 1, 5, 2 and 1 mol%. Mixture **3** contained 1% of TPGDA instead of MBIS as crosslinker and mixture **4** was based on the directly acrylated spiropyran. Both mixtures were dissolved in anhydrous dioxane (445 mg mixture was dissolved in 1 mL dioxane).

Substrate preparation: Glass substrates were cleaned by means of sonication (ethanol, 15 minutes), followed by treatment in a UV-ozone photoreactor (Ultra Violet Products, PR-100, 20 minutes). The surface of the glass substrates was modified by spin coating 3-(trimethoxysilyl)propyl methacrylate solution (1 vol% solution in a 1:1 water-isopropanol mixture) or 1*H*,1*H*,2*H*,2*H*-perfluorodecyltriethoxysilane solution (1 vol% solution in ethanol) onto the activated glass substrate for 45 seconds at 3000 rpm. The substrates were ready for use after curing for 10 minutes at 100 °C.

Preparation of surface-constrained coatings: Substrate-attached patterned films were prepared in a home-made cell which consisted of one upper 1*H*,1*H*,2*H*,2*H*-perfluorodecyltriethoxysilane functionalised glass slide and a lower propyl methacrylate functionalised glass slide with a spacing of ~55 µm. The cells were capillary filled with the monomer solution and subsequently exposed to UV light (unfiltered spectrum of a collimated EXFO Omnicure S2000 lamp, 300 sec, 48 mW/cm² intensity in the range 320-390 nm). This dose of UV exposure leads to full polymerisation, as confirmed by FT-IR spectroscopy (characteristic signals at 986, 956 and 808 cm⁻¹ related to the polymerisable acrylamide disappeared after the photopolymerisation procedure).

Preparation of symmetrically patterned hydrogels coatings by polymerisation-induced diffusion: Similar cells as those used for surface-constrained coatings were capillary filled before being placed on a black surface. A mask was placed on top of the sample and the sample exposed to UV light (unfiltered spectrum of a collimated EXFO Omnicure S2000

lamp, 45 sec, 13.5 mW/cm² intensity in the range 320-390 nm). The mask was then removed and the cell was fully exposed for another 300 seconds (48 mW/cm² intensity in the range 320-390 nm).

Preparation of asymmetric ratchet-like hydrogel coatings using pre-structured substrates:

An inverse copy of a Fresnel lens was prepared as follows. A droplet of TPGDA containing 2 wt% photoinitiator Irgacure 2959 was placed on a propyl methacrylate functionalised glass slide. The Fresnel lens was placed firmly on top and the sample was subjected to mild UV light exposure (60 sec, 13.5 mW/cm² intensity in the range 320-390 nm) in order to have unreacted acrylates left for covalent bonding between the template and the hydrogel in the next processing step. The Fresnel lens was carefully removed using a razor blade. A droplet of the monomer mixture was placed on the copy and a 1*H*,1*H*,2*H*,2*H*-perfluorodecyl-triethoxysilane functionalised glass slide was pressed firmly on top prior to photopolymerisation for 300 seconds (48 mW/cm² intensity in the range 320-390 nm).

Photoresponse of the films: In all samples, the upper glass slide of the hydrogel films was removed and the dioxane was allowed to evaporate before the hydrogel was swollen in deionised water. During water uptake, the films become coloured because of the protonation of merocyanine. Furthermore, the increase in size was more than twice that of the film in dioxane. After being immersed in water for 1 hour, the film was stable (i.e. both the colour of the film and its dimensions were in equilibrium). The rather long swelling time of 1 hour was used to ensure that both hydration and isomerisation had equilibrated. Due to the pre-treatment of the substrate, the film was covalently attached to the surface. This was confirmed by the fact that there was no detachment of the coating during the swelling procedure. The photoresponse of the material was determined while it was immersed in deionised water. A DC4100 4-Channel LED driver fitted with a M455L3-C2 collimated LED (455 nm, full width at half-maximum = 18 nm, 0-1000 mA) from Thorlabs, Inc. was used for the light irradiation of the films. The photoresponsiveness of surface-constrained films was analysed after exposure at 700 mA for 5 minutes, and masked exposures were performed at 700 mA for 1 minute (in the case of mixtures **1**, **2** and **3**) or 10 seconds (in the case of mixture **4**, Figure 3.2).¹³ Surface topographies obtained by polymerisation-induced diffusion or by pre-structured substrates were exposed at 700 mA for 15 minutes.

References

- 1 J. M. Spruell and C. J. Hawker, *Chem. Sci.*, 2011, **2**, 18-26.
- 2 R. Byrne, F. Benito-Lopez and D. Diamond, *Mater. Today*, 2010, **13**, 16-23.
- 3 T. Satoh, K. Sumaru, T. Takagi and T. Kanamori, *Soft Matter*, 2011, **7**, 8030-8034.
- 4 J. E. Stumpel, D. Liu, D. J. Broer and A. P. H. J. Schenning, *Chem. - Eur. J.*, 2013, **19**, 10922-10927.
- 5 A. Szilágyi, K. Sumaru, S. Sugiura, T. Takagi, T. Shinbo, M. Zrínyi and T. Kanamori, *Chem. Mater.*, 2007, **19**, 2730-2732.
- 6 K. Sumaru, K. Ohi, T. Takagi, T. Kanamori and T. Shinbo, *Langmuir*, 2006, **22**, 4353-4356.
- 7 H. G. Schild, *Prog. Polym. Sci.*, 1992, **17**, 163-249.
- 8 D. Liu, C. W. M. Bastiaansen, J. M. J. den Toonder and D. J. Broer, *Langmuir*, 2013, **29**, 5622-5629.
- 9 T. A. Duncombe, E. Y. Erdem, A. Shastry, R. Baskaran and K. F. Böhringer, *Adv. Mater.*, 2012, **24**, 1545-1550.
- 10 T. A. Duncombe, J. F. Parsons and K. F. Böhringer, *Langmuir*, 2012, **28**, 13765-13770.
- 11 K. Sekeroglu, U. A. Gurkan, U. Demirci and M. C. Demirel, *Appl. Phys. Lett.*, 2011, **99**, 063703.
- 12 N. A. Malvadkar, M. J. Hancock, K. Sekeroglu, W. J. Dressick and M. C. Demirel, *Nat. Mater.*, 2010, **9**, 1023-1028.
- 13 B. Ziólkowski, L. Florea, J. Theobald, F. Benito-Lopez and D. Diamond, *Soft Matter*, 2013, **9**, 8754-8760.
- 14 Y. Li and T. Tanaka, *J. Chem. Phys.*, 1990, **92**, 1365-1371.
- 15 T. Satoh, K. Sumaru, T. Takagi, K. Takai and T. Kanamori, *Phys. Chem. Chem. Phys.*, 2011, **13**, 7322-7329.
- 16 W. Wang, E. Metwalli, J. Perlich, C. M. Papadakis, R. Cubitt and P. Müller-Buschbaum, *Macromolecules*, 2009, **42**, 9041-9051.
- 17 S. Zhou and C. Wu, *Macromolecules*, 1996, **29**, 4998-5001.
- 18 S. M. Hashmi and E. R. Dufresne, *Soft Matter*, 2009, **5**, 3682-3688.
- 19 S. Radji, H. Alem, S. Demoustier-Champagne, A. M. Jonas and S. p. Cuenot, *J. Phys. Chem. B*, 2010, **114**, 4939-4944.
- 20 D. Liu, C. W. M. Bastiaansen, J. M. J. den Toonder and D. J. Broer, *Soft Matter*, 2013, **9**, 588-596.
- 21 B.-J. de Gans, C. Sánchez, D. Kozodaev, D. Wouters, A. Alexeev, M. J. Escuti, C. W. M. Bastiaansen, D. J. Broer and U. S. Schubert, *J. Comb. Chem.*, 2006, **8**, 228-236.

- 22 C. M. Leewis, A. M. de Jong, L. J. van Ijzendoorn and D. J. Broer, *J. Appl. Phys.*, 2004, **95**, 8352-8356.
- 23 L. Florea, D. Diamond and F. Benito-Lopez, *Macromol. Mater. Eng.*, 2012, **297**, 1148-1159.
- 24 M. Czugala, C. O'Connell, C. Blin, P. Fischer, K. J. Fraser, F. Benito-Lopez and D. Diamond, *Sensors and Actuators B-Chemical*, 2014, **194**, 105-113.
- 25 M. A. Cole, N. H. Voelcker, H. Thissen and H. J. Griesser, *Biomaterials*, 2009, **30**, 1827-1850.
- 26 R. M. P. da Silva, J. F. Mano and R. L. Reis, *Trends in Biotechnology*, 2007, **25**, 577-583.
- 27 S. Schmidt, M. Zeiser, T. Hellweg, C. Duschl, A. Fery and H. Möhwald, *Adv. Funct. Mater.*, 2010, **20**, 3235-3243.

Chapter 4

Water-responsive optical surface topographies based on cholesteric liquid crystals

Abstract

This chapter describes patterned water-responsive coatings which upon activation alter both their topological and optical properties. The polymer coatings are based on a hydrogen-bonded cholesteric liquid crystalline polymer network. A two-step photopolymerisation procedure leads to a patterned coating with repeating liquid crystalline and isotropic areas. The cholesteric liquid crystalline areas reflect green light, whilst the isotropic areas are fully transparent. Treatment with alkaline solution results in a hygroscopic polymer salt coating. When placed in demineralised water, the polymer film swells, leading to an enhancement of the protrusions due to the fact that the liquid crystalline areas swell more uniaxially than the isotropic regions. Moreover, the pitch of the helical organisation in the cholesteric areas increases due to this swelling, leading to a colour change from green to red. Various kinds of patterns were made, which become visible or fade away when placed in water. Furthermore, multi-coloured patterns were easily produced with this material by using patterned cholesteric liquid crystalline areas with different pitches. All effects are reversible and can be repeated on the same sample.

This chapter is partially reproduced from: J. E. Stumpel, D. J. Broer, C. W. M. Bastiaansen and A. P. H. J. Schenning, *Proceedings of SPIE 9137*, 2014, 91370U.

4.1 Introduction

Materials which can reversibly change their properties are a focus in present-day research.^{1,2} The previous two chapters described the development of photoswitchable hydrogel surface topographies. Similar systems, such as thermo-, pH- and photoresponsive hydrogel coatings which change their surface topography, have been reported in literature.³⁻⁶ Furthermore, multi-stimulus-responsive coatings have been described which can undergo a change between superhydrophilicity and superhydrophobicity in response to three different stimuli (pH, temperature and glucose concentration).⁷ In most of these responsive coatings, there is an emphasis on the change in a single property of the coating. Research looking at a single stimulus leading to multiple property changes has rarely been investigated. Moreover, light-, pH- and temperature-responsive materials have often been reported but there has been less exploration of the fabrication of humidity-responsive materials.^{2,8} This chapter reports on water-responsive patterned coatings based on cholesteric liquid crystals (CLCs), which alter both their topological and optical properties.

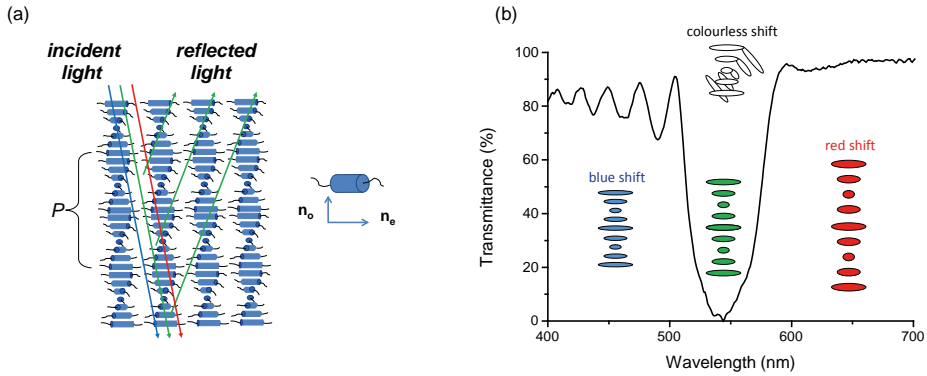
4.1.1 Cholesteric liquid crystals

A CLC is a special case of a nematic liquid crystalline phase.⁹ In nematic liquid crystals the rod-like mesogens do not have a positional order but a directional order in which the mesogens align parallel to their long axis (the director). Nematic mesogens have anisotropic properties, which are different depending on whether they are positioned longitudinally or perpendicularly with respect to the director. The anisotropy in the refractive index is presented as the birefringence (Δn), which is the difference between the ordinary and the extraordinary refractive indices (n_o and n_e), which are the refractive indices of the material when positioned longitudinally or perpendicularly with respect to the director, respectively.

$$\Delta n = n_e - n_o \quad (1)$$

In CLCs, the chirality present in the phase leads to a twist of the director axis, forming a helix, as shown in Scheme 4.1a. This results in a helical structure with a given helical periodicity, the pitch (P). The chirality in the system is either present in the LC molecules or it can be induced by the addition of a chiral dopant, a chiral

additive which forces the nematic phase to adopt the cholesteric liquid crystalline phase. The materials described in this thesis were obtained using a chiral dopant of this kind. The combination of the rotating director axis and the birefringence of the LC leads to an alternating refractive index throughout the material, which induces partial reflection of the incident light. Like Bragg reflectors, CLCs can reflect incident light.^{10,11} The reflection band of a CLC (Scheme 4.1b) shifts when the thickness is increased (red shift) or decreased (blue shift). The loss of organisational order in the CLC leads to a decrease in the intensity of the reflection band (colourless shift).



Scheme 4.1 (a) Schematic molecular organisation of a CLC and its (green) selective reflection band. An enlarged rod-like mesogen displays the direction of n_o and n_e . (b) The selective reflection band of a CLC material, measured with polarised light.

The reflected wavelength (λ_{refl}) depends on the average refractive index (n_{av}) and the helical pitch of the cholesteric material:

$$\lambda_{refl} = n_{av} \cdot P \quad (2)$$

Furthermore, the spectral bandwidth ($\Delta\lambda_{refl}$) of the selective reflection band (SRB) relies on the birefringence (Δn) of the liquid crystalline material:

$$\Delta\lambda_{refl} = \Delta n \cdot P \quad (3)$$

In the case of cholesteric materials produced using a chiral dopant, the pitch is proportionally dependent on the concentration $[c]$ of chiral dopant and its helical twisting power (HTP):

$$P \cong \frac{1}{HTP \cdot [c]} \quad (4)$$

The value for the *HTP* of a chiral dopant depends the off-set in the director of the layers in the LC material (Scheme 4.1a). A chiral dopant with a positive *HTP* gives a right-handed helix; a negative *HTP* creates a left-handed helix. A maximum of 50% of the incident light can be reflected because of the polarisation dependence of the selective reflection band, reflecting circular polarised light of handedness equal to the handedness of the helix while the opposite handedness is being transmitted. In the special case of the helical pitch multiplied by the refractive index being in the order of the wavelength of visible light, coloured CLCs are obtained (Eq. 2). The helical pitch in a CLC is temperature-responsive. However, upon the incorporation of polymerisable groups (that is to say, acrylate groups) onto the LC molecules, the helical arrangement can be imprinted at a set temperature by polymerisation.¹²⁻¹⁴ Such polymer CLCs can be used as stimuli-responsive coatings.¹⁵

The literature reports on temperature-responsive patterned CLC polymer films and dynamic and permanent light-responsive surface topographies.¹⁶⁻¹⁸ These systems used the difference in expansion behaviour between the CLC and other phases. Those studies focused exclusively on topological alterations in the polymer coating. Recently, hygroscopic CLC polymer salt films have also been reported which could be used as humidity responsive sensors with a visible colour change.¹⁹ This response is caused by an increase or decrease in the pitch of the helix due to the absorption or desorption of water. Only the optical differences in this material were investigated and topological alterations or variations in the thickness of the coatings were not examined.

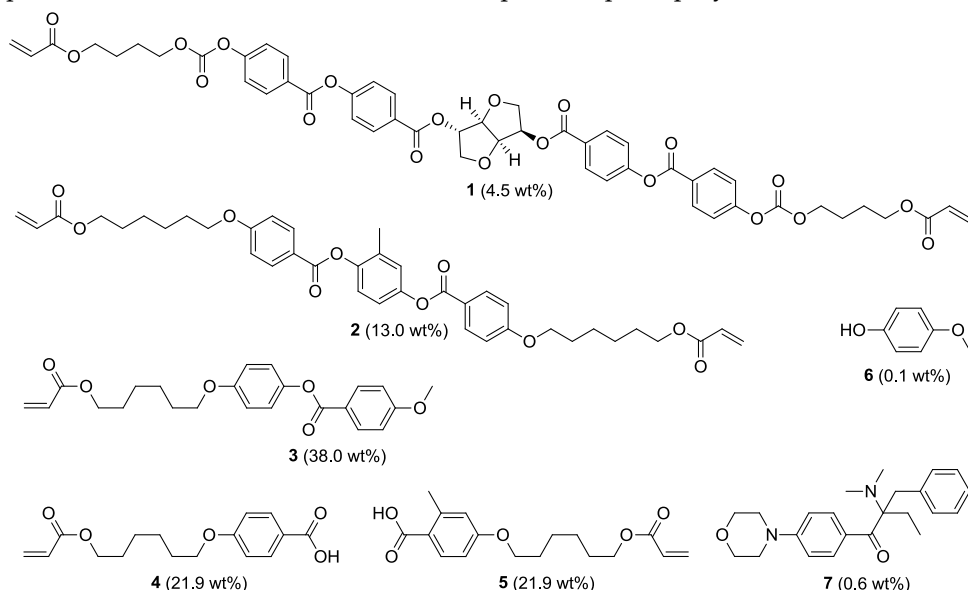
This chapter describes a combination of the systems described above to obtain water-responsive surface topographies which also change their colour.^{16,18} The coatings were prepared by using a hydrogen-bonded cholesteric liquid crystal monomer mixture.¹⁹ Mask photopolymerisation at two different temperatures led to a patterned coating with green-reflecting CLC and transparent isotropic areas. The subsequent treatment of the coatings with alkaline solution induces the disruption of hydrogen bonds and the formation of a hygroscopic polymer salt. The placement of the polymer film in water induces a change in the surface topography as the cholesteric areas expand predominantly in the direction

perpendicular to the substrate. In addition, as a result of the swelling, the reflection band shifts from green to red. In other words, exposure of the film to water leads to both a topological and an optical change in the coating.

4.2 Results and discussion

4.2.1 Preparation and characterisation of water-responsive CLC polymer salt coatings

A CLC mixture similar to the one discussed before (Scheme 4.2) was used to prepare water-responsive cholesteric coatings.¹⁹ The mono- and diacrylate LCs (**2** and **3**) induce nematic behaviour in the mixture and compound **2** also forms a chemical network after photopolymerisation. Polymerisable hydrogen-bonded benzoic acid derivatives **4** and **5** were added to make the coating water-responsive. The cholesteric molecular order and corresponding reflection band of the mixture was induced using the non-liquid crystalline chiral dopant **1**. Thermal inhibitor **6** was used to establish the thermal stability in the monomer mixture to prevent premature polymerisation at elevated temperatures. The addition of photoinitiator **7** renders the mixture susceptible to photopolymerisation.



Scheme 4.2 The chemicals used for the preparation of the cholesteric liquid crystal polymer. The mixture consisted of chiral dopant **1**, nematic mesogens **2** and **3**, benzoic acid derivatives **4** and **5**, thermal inhibitor **6** and photoinitiator **7**. Homogeneity of the mixture was ensured by the preparation of a solution (20 wt% in THF) prior to use.

Initially, non-patterned polymer coatings were prepared to study the water-responsive behaviour of the CLC films. The CLC mixture (Scheme 4.2) was therefore aligned by shear force between two glass plates after evaporation of the solvent. The lower glass substrate was functionalised with methacrylate groups, leading to covalent linkages after photopolymerisation between the polymer coating and the glass substrate. The upper substrate was functionalised with a fluorinated alkylsilane in order to become more hydrophobic and to ensure effortless opening of the cell after photopolymerisation was completed. The monomer mixture was photopolymerised at room temperature (up to roughly 60 °C, the mixture is in its cholesteric phase). After the removal of the upper glass plate, a green-reflecting polymer coating was obtained. The absorption spectrum of the polymer film showed a green reflection band of $\lambda = 525$ nm (Figure 4.1a). As the CLC polymer film reflects only left-handed polarised light, a maximum of 50% of the incident light is reflected. No change in reflection colour was observed after placing the polymer film in demineralised water, revealing that the film is not sensitive to water in this state.

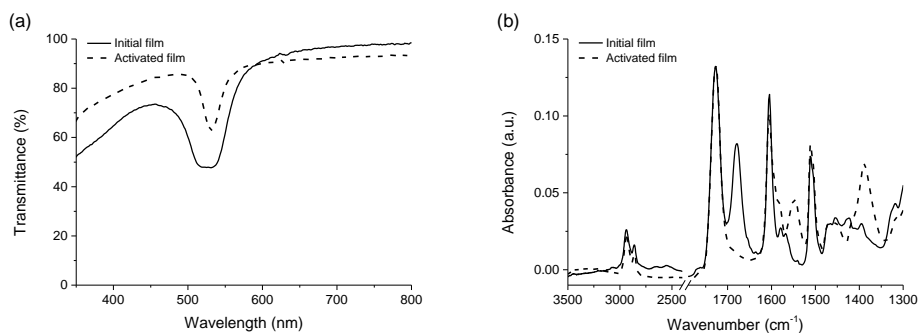


Figure 4.1 (a) UV/Vis spectra (with unpolared light) of the CLC coating before and after treatment with an alkaline solution. (b) FT-IR spectra of the polymer coating before and after activation by alkaline treatment.

The polymer coating was made water-responsive by treatment with an alkaline (0.1 M KOH, 10 h) solution, leading to the disruption of the hydrogen-bonded physical network and the formation of a polymer salt. The FT-IR spectrum of the initial film displays broad signals between 2700 and 2450 cm^{-1} and a strong signal at 1680 cm^{-1} that can be attributed to the OH-stretching (Figure 4.1b). This indicates the presence of hydrogen-bonded carboxylic acids. After alkaline treatment, these signals clearly disappeared. Furthermore, two additional signals appeared at 1547

and 1388 cm^{-1} that are related to ν_s and ν_{as} of the carboxylate salt. A slight increase in absorption between 3500 and 3000 cm^{-1} was observed which could be the result of water uptake from air of the hygroscopic polymer film. After base treatment and subsequent drying, a CLC coating was obtained that maintained its green reflection. The helical organisation of the polymer network remained due to the chemical crosslinking in the material. However UV-Vis absorption measurements in ambient conditions showed that the reflection band became more narrow and underwent a marginal red shift to $\lambda = 530\text{ nm}$ (Figure 4.1a).¹⁹ A slight decline in molecular order resulted in a loss in the intensity of the reflection band. These observations are in accordance with previous results for optical humidity sensors based on hydrogen-bonded cholesteric liquid crystal networks.¹⁹

The film was placed in water to investigate the water-response of the polymer salt coating. When the CLC polymer salt coating was swollen, the reflected colour changed from green to red ($\lambda = 720\text{ nm}$) due to an increase in the helical pitch (Figure 4.2). When the sample was allowed to dry, the initial green reflection band was recovered. This process was fully reversible and could be repeated many times. UV/Vis measurements of the drying process showed that, after 4 minutes in ambient conditions, the initial reflection band of the polymer salt film was obtained, revealing that the water absorbed by the coating had evaporated (Figure 4.2). Interferometry experiments found a thickness for the dry film of $9\text{ }\mu\text{m}$ and $12\text{ }\mu\text{m}$ for the swollen film. The thickness of the film increased by a factor 1.33, which is a good match with the UV/Vis measurements, in which the observed red shift in the reflection band was a factor 1.38. As the coating is fully polymerised, the molecular orientation at the boundaries of the film are fixed and the number of pitches present in the film remains unchanged upon swelling or drying. As a result the reflection band is dependent on the thickness of the film only.

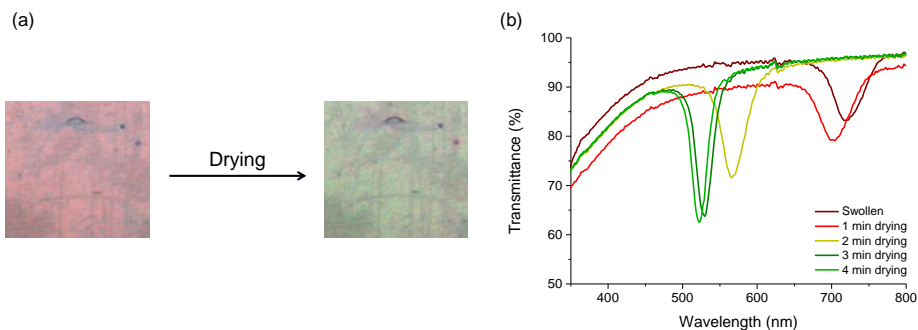
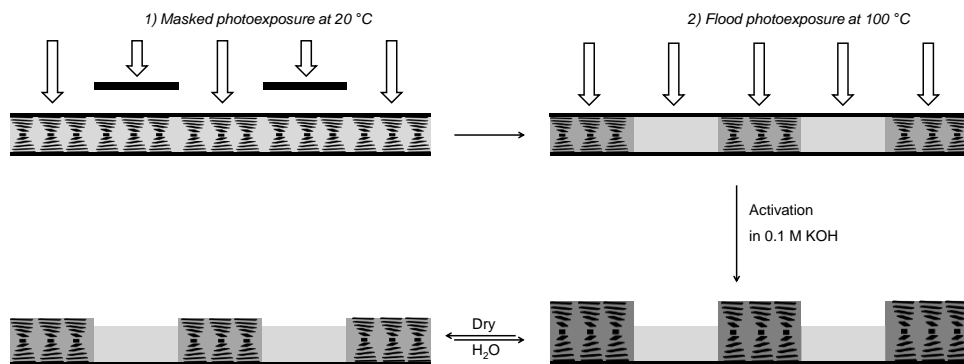


Figure 4.2 (a) Optical images of the hygroscopic CLC coating turning from red to green upon drying in ambient conditions (RH = 40, T = 20 °C). (b) UV/Vis spectra showing the changes in the reflection band upon drying of a water-saturated CLC polymer coating.

4.2.2 Preparation and characterisation of patterned isotropic-CLC polymer coatings

In order to prepare water-responsive surface topographies, the polymer film needs to contain regions with different phases (cholesteric/isotropic, Figure 4.3a). The helical alignment of the CLC area results in predominantly uniaxial swelling; the isotropic area swells in a more isotropic fashion.^{17,18} The uptake of water by a patterned coating of this kind will therefore result in different swelling behaviour. Furthermore, the CLC areas will reveal a colour shift towards red, while the isotropic parts remain colourless due to the lack of molecular organisation. Patterned polymer coatings can be prepared using a mask and two subsequent photopolymerisation steps.⁴ During the first step at room temperature, a mask ensures polymerisation in the exposed CLC areas. The cholesteric order is fixed in these areas. Afterwards, a flood exposure at 100 °C, a temperature above the clearing point of the CLC mixtures, results in a fully polymerised patterned film (Figure 4.3a). Both cholesteric and isotropic areas are present in the coating (Figure 4.3a). As with the non-patterned coating, these patterned coatings were treated with an alkaline solution, resulting in hygroscopic films which can absorb water (Scheme 4.3b).



Scheme 4.3 (a) Schematic representation of the manufacturing method for a patterned CLC coating. The mixture was partially polymerised in the CLC phase during the masked photo-exposure step. Subsequent flood exposure at 100 °C polymerises the isotropic areas and ensures full polymerisation. (b) Activation with an alkaline solution leads to a patterned hygroscopic CLC polymer coating.

In the first polymerisation step, a mask with dark lines of 200 μm and a pitch of 300 μm was used. After the flood exposure the dry film was already unequal in height, most likely due to diffusion processes during this photopolymerisation step (Figure 4.3b).¹⁸ During polymerisation, the monomers cannot reach the centre of the mask, leading to accumulation and subsequent polymerisation at the edges of the mask.²⁰ The CLC areas are thicker than the isotropic areas, showing that the reactive mesogens diffused to the double exposed areas. Furthermore, the cholesteric areas have a greenish reflection band, while the isotropic areas are colourless. After alkaline treatment of the coating, it was fully swollen and the cholesteric regions reflected light outside the visual spectrum and so both areas appeared to be colourless. Upon evaporation of the water, the reflection band in the cholesteric region shifted to within the visible spectrum (Figure 4.3a, after 40 seconds the coating is similar to its initial state). The changes in the thickness and colour of the cholesteric areas were the same as those observed in the non-patterned CLC films. The swollen topography had protrusions with a thickness of 600 nm; after drying the height difference was reduced to 300 nm (the height was measured at the centre of the corresponding area). Again, the behaviour of the film was fully reversible: different drying cycles resulted in similar changes in both surface topography and reflected colour. It should be noted that the reflection bands were slightly different than those of the non-patterned films, probably due

to expansion of the monomer mixture at elevated temperature during the second photopolymerisation step.

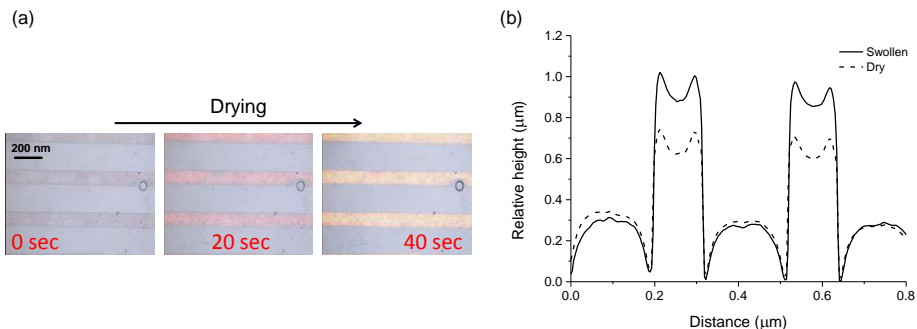


Figure 4.3 (a) Optical images of the water-saturated patterned CLC coating upon drying, showing the changes in appearance of the CLC structures from near infrared to orange ($100\ \mu\text{m}$ cholesteric, $200\ \mu\text{m}$ isotropic, $\text{RH} = 40$, $T = 20\ ^\circ\text{C}$) and (b) height profiles of the surface topography of the swollen and dried CLC polymer salt film, as observed by interferometry.

Figure 4.3b shows the difference in swelling behaviour between the cholesteric and the isotropic parts. Uniaxial swelling was observed in the cholesteric regions only. However, as the coating is surface-confined and crosslinked, even the isotropic areas have a tendency to swell in the z -direction. In order to confirm that the discrepancy in the swelling behaviour of the two regions is a result of the different phases, a patterned film was prepared in which both areas were in the isotropic phase (Figure 4.4). A slightly different surface topography was obtained than with the cholesteric-isotropic coating, which can be explained by the fact that both polymerisation steps were performed at elevated temperature. The protrusion was $300\ \text{nm}$ in the swollen state. Upon drying it was reduced to $250\ \text{nm}$, which is a result of the slightly higher thickness in the double exposed areas (both areas swell and shrink by the same degree). This experiment indicates that the major change observed in the patterned CLC coating is related to differences in molecular organisation within the polymer network.

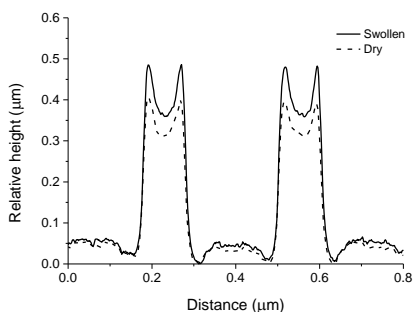


Figure 4.4 Change in the surface topography of an isotropic patterned polymer salt coating before and after drying in ambient conditions (RH = 40, T = 20 °C), as observed by interferometry. The thickness of the lower areas in the dry coating is 10.4 μm .

4.2.3 Preparation and characterisation of bicoloured CLC polymer coatings

In the coatings presented above, exposure to water leads to a single colour change. However, the toolbox that we have available with these materials can be used to prepare multiple colour-changing coatings as well.^{21,22} The combination of multiple polymerisation steps at different temperatures and the variation of the amount of chiral dopant results in multicoloured polymer coatings. In addition to patterned coatings with cholesteric and isotropic regions, it is possible to prepare patterned coatings with different cholesteric areas that have a distinct reflected colour. As the reflection band of a cholesteric material is temperature-dependent, the polymerisation temperature determines the SRB. Using the same method as for the isotropic-CLC coatings, with a flood exposure at a temperature below the CLC clearing point, results in a patterned CLC-CLC coating, as depicted in Figure 4.5a. Since both areas are cholesteric, the topological changes of the film in the dry and wet state are rather small, as with the fully isotropic patterned coating. Figure 4.5b shows the surface profile of the coating in the wet and dry states. When the coating was treated with demineralised water, the thickness increased by approximately 1 μm over the entire coating. In both cases, the height difference of the entire protrusion was ~ 500 nm. The shift in the reflection band of the swollen coating corresponded to the change in thickness (from 548 to 657 and 616 to 702 nm for the initially green and red areas respectively).

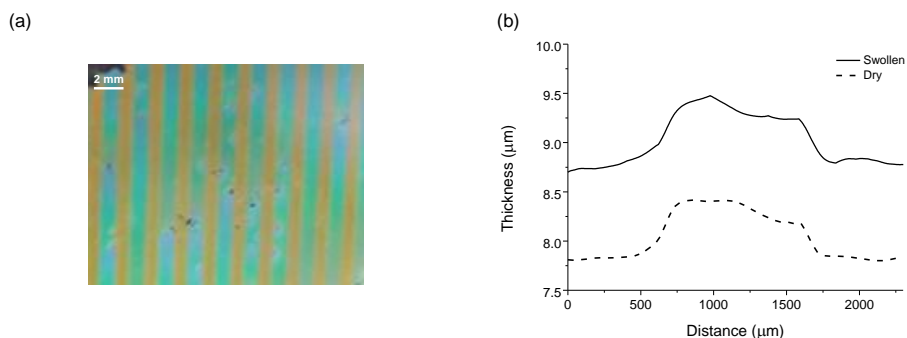


Figure 4.5 (a) Optical image showing a patterned CLC-CLC coating after mask exposure at 20 °C (red areas) and flood exposure at 40 °C (green regions), resulting in a patterned bicoloured material. (b) The corresponding activated coating in the fully swollen and dry (RH = 37%, 20 °C) state.

In order to prepare materials with an initial green reflection band in the centre of the visible spectrum, 4.5 wt% of chiral dopant **1** was used. However, the use of a different concentration of **1** leads to materials which, as explained above (in section 4.1.1, Eq. 4), reflect light with another wavelength. For instance, a reduction (4.0 wt%) in the concentration of chiral dopant results in the reflection of a longer wavelength; an increase (5.5 wt%) initially results in UV-reflecting materials (Table 4.1). These materials are of interest because the SRB of both changes dramatically when they are placed in water. The initially red CLC turns colourless, while the originally colourless UV-reflecting film turns purple.

Table 4.1 Variation in the amount of chiral dopant **1** leads to the reflection of different wavelengths.

Mixture	Amount of chiral dopant 1 (wt%)	$\lambda_{\text{refl dry}}^{\text{[a]}}$ (nm)	$\lambda_{\text{refl swollen}}$ (nm)
1	4.5	584	793
2	4.0	655	850
3	5.5	480	632
4	8.0	350	421

[a] The samples were photopolymerised at 20 °C

To prove the principle, three coatings containing a logo (the letter "F"), and different colour-reflecting regions, were prepared. Mask photopolymerisation of mixture **3** at 20 °C, followed by flood exposure at 50 °C, resulted in a coating with two responsive colours in both the wet and dry states (Figure 4.6a). Another coating was prepared with mixture **1** using the same procedure. This initially red-

green bicoloured sample reflected infrared and red light respectively when the coating was swollen; the visible colour of the logo vanished (Figure 4.6b). Finally, a sample was prepared from mixture 4, with mask exposure at 20 °C followed by flood illumination at 100 °C. In the resulting optically colourless coating, the character “F” appeared in purple when the coating was in contact with water (Figure 4.6c). The time scale for the change in the optical properties of these three coatings was ~30 seconds when they were moved from a dry to a wet environment and slightly longer (1-2 minutes) when the sample was drying in ambient conditions. After several months of storage in open air where relative humidity fluctuated slightly, the response was still as fully reversible as in the fresh samples.

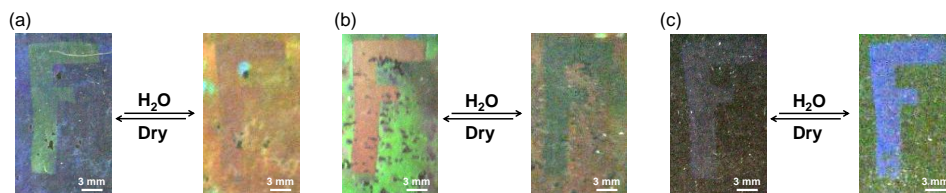


Figure 4.6 Optical images showing three different polymer salt coatings with the letter “F” in ambient conditions (RH = 40, T = 20 °C) and in the wet state. The coatings were made as follows: (a) mixture 3, 20 °C mask; 50 °C flood exposure, (b) mixture 1, 20 °C mask; 50 °C flood exposure and (c) mixture 4, 20 °C mask; 100 °C flood exposure. Note: the colours in the photographs have been enhanced to provide additional contrast.

4.3 Conclusion

Hydrogen-bonded cholesteric liquid crystals can be used to create coatings which change both their colour and their surface topography reversibly upon exposure to water. With the use of a masked and subsequent flood exposure at two different temperatures, structured surface topographies in which the two areas react differently can be prepared. Swelling and shrinkage are unidirectional due to the helical organisation of the cholesteric areas. The difference between the thickness of the swollen and dry cholesteric areas corresponds to the difference in reflected wavelength as the reflection band is dependent on the length of the pitch. When dried, the protrusions are half the height of those in the fully swollen state. Various kinds of multi-coloured patterned coatings were prepared by fine-tuning the amount of chiral dopant and the polymerisation temperature. Furthermore, coatings were produced that changed from optically transparent to visible-colour-reflecting when placed in water. The preparation method for these kinds of

structures can, in principle, be optimised to obtain larger changes and ultimately to produce humidity-responsive surface topographies and optical coatings. Moreover, the introduction of photochromic moieties in the polymer backbone could lead to materials with properties that can be changed by humidity, photo-exposure or a combination of both stimuli. Further research focusing on coatings of these kinds could give rise to a new class of responsive materials which can change their optical transparency and topological roughness in response to several environmental changes.

Experimental section

Characterisation of materials: For UV/Vis spectroscopy of the films, an HR2000+ high-resolution spectrometer from Ocean Optics mounted on a DM6000 M microscope from Leica microsystems was used. The corresponding light source emits between 400 and 800 nm. A Varian 670 FT-IR spectrometer with slide-on ATR (Ge) and a Varian-3100 FT-IR spectrometer were used to measure IR spectra. Height profiles and 3D images of patterned films were recorded using a 3D interferometer (Fogale Nanotech Zoomsurf). The UV light intensities produced by the collimated EXFO Omnicure S2000 lamp were determined using a UV Power Puck II by EIT Instrument Markets Group. Spin coating was performed on a Karl Suss RC6 spin coater.

Materials: Unless stated otherwise, all reagents and chemicals were obtained from commercial sources. Chiral dopant **1** was purchased from BASF. Compound **2** was obtained from Merck and monomer **3** was custom-made by Synthron. Benzoic acid derivatives **4** and **5** were prepared by Philips and Synthron respectively. Photoinitiator **6** and inhibitor **7** were obtained from CIBA and Fluka respectively. All solvents were obtained from Biosolve. The silanes for substrate modification were obtained from Sigma-Aldrich.

Glass functionalisation: Glass substrates were cleaned by sonication (ethanol, 15 minutes), followed by treatment in a UV-ozone photoreactor (Ultra Violet Products, PR-100, 20 minutes). The surface of the glass substrates was modified by spin coating 3-(trimethoxysilyl)propyl methacrylate solution (1 vol% solution in a 1:1 water-isopropanol mixture) or 1*H*,1*H*,2*H*,2*H*-perfluorodecyltriethoxysilane solution (1 vol% solution in ethanol) onto the activated glass substrate for 45 seconds at 3000 rpm. The substrates were ready to use after curing for 10 minutes at 100 °C.

Preparation of a the CLC mixture: A typical green-reflecting CLC-mixture was prepared by dissolving compounds 1-7, respectively 4.5, 13.0, 38.0, 21.9, 21.9, 0.1 and 0.6 wt%, in four weight equivalents of THF. In the case of the mixtures with a different amount of chiral dopant, the amount of compound 1 was increased or decreased, while the ratio between the other compounds was kept constant.

Preparation of water-responsive coatings: Water-responsive topographies with a typical thickness of between 8 and 10 μm were prepared as follows: 20 μl of the CLC mixture was placed on a methacrylate functionalised glass substrate at 70 $^{\circ}\text{C}$ and the solvent was allowed to evaporate. After complete evaporation of THF, a perfluorodecyl-triethoxysilane functionalised glass substrate was placed on top and pressed firmly. At lower temperatures, the chiral nematic liquid crystals were aligned by shear forces. The contents of the cells of the homogenous films were photopolymerised at room temperature for 300 seconds (48 mW/cm^2 intensity in the range 320-390 nm). In case of the patterned coatings, the cells were placed on a black surface. A mask was placed on top of the sample and the sample was exposed to UV light (0.2 sec, 48 mW/cm^2 intensity in the range 320-390 nm) at a set temperature. Afterwards, the mask was removed, the cell was equilibrated at the second set temperature and the mixture was exposed for an additional 300 seconds (48 mW/cm^2 intensity in the range 320-390 nm) to ensure complete polymerisation. The upper perfluorodecyl functionalised glass substrates could be easily removed with a razor blade.

Formation of the hygroscopic polymer salt coatings: Coatings were activated by placing them in 0.1 M KOH-solution for 10 hours to ensure complete deprotonation of the hydrogen-bonded benzoic acid derivatives. The samples were used after drying at room temperature (RH = 40%, T = 20 $^{\circ}\text{C}$).

References

- 1 C. Alexander and K. M. Shakesheff, *Adv. Mater.*, 2006, **18**, 3321-3328.
- 2 H. Meng and Jinlian Hu, *J. Intell. Mater. Syst. Struct.*, 2010, **21**, 859-885.
- 3 J. Kim, J. A. Hanna, M. Byun, C. D. Santangelo and R. C. Hayward, *Science*, 2012, **335**, 1201-1205.
- 4 D. Liu, C. W. M. Bastiaansen, J. M. J. den Toonder and D. J. Broer, *Soft Matter*, 2013, **9**, 588-596.
- 5 D. Liu, C. W. M. Bastiaansen, J. M. J. den Toonder and D. J. Broer, *Langmuir*, 2013, **29**, 5622-5629.
- 6 B. Ziólkowski, L. Florea, J. Theobald, F. Benito-Lopez and D. Diamond, *Soft Matter*, 2013, **9**, 8754-8760.
- 7 F. Xia, H. Ge, Y. Hou, T. Sun, L. Chen, G. Zhang and L. Jiang, *Adv. Mater.*, 2007, **19**, 2520-2524.
- 8 E. Kim, S. Y. Kim, G. Jo, S. Kim and M. J. Park, *ACS Appl. Mater. Interfaces*, 2012, **4**, 5179-5187.
- 9 T. Geelhaar, K. Griesar and B. Reckmann, *Angew. Chem., Int. Ed.*, 2013, **52**, 8798-8809.
- 10 C. W. Oseen, *Trans. Faraday Soc.*, 1933, **29**, 883-899.
- 11 G. Chilaya, in *Chirality in Liquid Crystals*, eds. H.-S. Kitzerow and C. Bahr, Springer New York, 2001, pp. 159-185.
- 12 V. Shibaev, *Polym. Sci., Ser. A*, 2009, **51**, 1131-1193.
- 13 D. Liu and D. J. Broer, *Langmuir*, 2014, Article ASAP.
- 14 D. J. Broer, C. M. W. Bastiaansen, M. G. Debije and A. P. H. J. Schenning, *Angew. Chem., Int. Ed.*, 2012, **51**, 7102-7109.
- 15 D.-J. Mulder, A. P. H. J. Schenning and C. W. M. Bastiaansen, *J. Mater. Chem. C*, 2014, Accepted Manuscript.
- 16 D. Liu, C. W. M. Bastiaansen, J. M. J. den Toonder and D. J. Broer, *Macromolecules*, 2012, **45**, 8008-8012.
- 17 D. Liu, C. W. M. Bastiaansen, J. M. J. den Toonder and D. J. Broer, *Angew. Chem., Int. Ed.*, 2012, **51**, 892-896.
- 18 M. E. Sousa, D. J. Broer, C. W. M. Bastiaansen, L. B. Freund and G. P. Crawford, *Adv. Mater.*, 2006, **18**, 1842-1845.
- 19 N. Herzer, H. Guneysoy, D. J. D. Davies, D. Yildirim, A. R. Vaccaro, D. J. Broer, C. W. M. Bastiaansen and A. P. H. J. Schenning, *J. Am. Chem. Soc.*, 2012, **134**, 7608-7611.
- 20 C. M. Lewis, A. M. de Jong, L. J. van Ijzendoorn and D. J. Broer, *J. Appl. Phys.*, 2004, **95**, 8352-8356.

- 21 R. J. Carlton, J. T. Hunter, D. S. Miller, R. Abbasi, P. C. Mushenheim, L. N. Tan and N. L. Abbott, *Liq. Cryst. Rev.*, 2013, **1**, 29-51.
- 22 J. Ge and Y. Yin, *Angew. Chem., Int. Ed.*, 2011, **50**, 1492-1522.

Chapter 5

Humidity-responsive optical surface topographies based on interpenetrating polymer networks

Abstract

This chapter describes the production of humidity-responsive optical polymer coatings based on interpenetrating polymer networks (IPNs). These coatings combine the advantage of the molecular order of a liquid crystal with the strong response of a hydrogel: the material consists of a cholesteric liquid crystalline network that reflects colour and a hygroscopic potassium polyacrylate network that provides a humidity-dependent volume response. As the two networks are tightly interwoven, the volume change in the crosslinked polymer salt results in a volume change in the cholesteric network as well, which in turn leads to a colour change. The coating reflects light with wavelengths of 497 nm and 650 nm at low and high relative humidity respectively and there is an almost linear relationship between the relative humidity and the reflected colour. The same method was used to prepare patterned coatings based on an IPN in which one of the networks is non-responsive. Humidity-responsive surface topographies were created by preparing alternating regions containing polystyrene or potassium polyacrylate networks only.

5.1 Introduction

Optical materials which autonomously detect differences in relative humidity (RH) have attracted considerable attention for numerous applications in areas such as the medical and food industries. Various kinds of polymer-based photonic humidity sensors have been proposed with different measuring ranges, optical detection principles and response times (see Chapter 1 for more details).^{1,2} A typical photonic sensor has a periodical structure of alternating refractive indices, leading to Bragg reflection. The majority of these materials are based on hydrogels, which can easily undergo high volumetric alterations under the influence of water, leading to a change in the reflection band.^{3,4} However, a common drawback of hydrogels is that they are rather fragile.

Following on from Chapter 4, this chapter investigates the use of CLCs for the development of humidity sensors, an application that has already been discussed in the literature.⁵ For instance, a CLC-based system based on a chemical reaction between the chiral dopant and water has been produced.⁶ The presence of water results in a large colour shift, but the system cannot be used as a coating since the mixture is not polymer-based. Another study reported on the use of a hygroscopic CLC coating for optically observable humidity sensors.⁷ A shift of only 40 nm in the reflection band was observed in these materials when the RH changed from 3 to 83%. This chapter describes the preparation of an interpenetrating polymer network (IPN) that combines the large response of a hydrogel and the rigidity of a highly crosslinked CLC polymer network to produce responsive durable sensors.

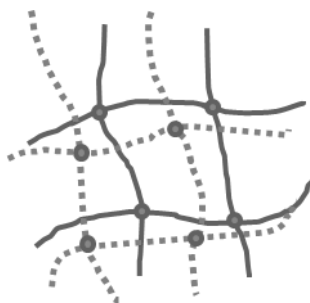


Figure 5.1 Schematic drawing of an IPN with two perfectly separated polymer networks

An IPN is defined as a combination of two polymers in network form, at least one of which is synthesised and/or crosslinked in the immediate presence of the other.⁸

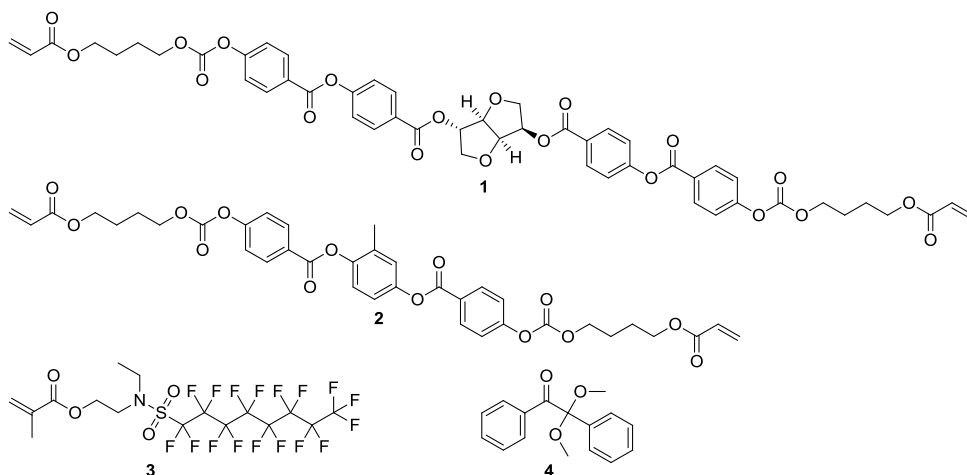
Basically, they consist of two separate but interwoven polymer networks (Figure 5.1).⁸⁻¹³ Most commonly, a mixture of monomers is absorbed by a polymer network and subsequently polymerised, resulting in a sequential IPN. Recently, there has been a rise in interest in these IPNs. However, little is known about IPNs containing liquid crystalline polymer networks. The swelling behaviour of common nematic liquid crystals (5CB and E7) in an IPN of poly(*n*-butyl acrylate) and poly(2-ethylhexyl acrylate) has been investigated.^{14,15} However, IPNs based on liquid crystalline networks have not been reported, although they could give rise to a unique class of materials. In these materials, the monolithic molecular order of LC materials can be combined with the functional properties of another polymeric system. For instance, IPNs based on nematic liquid crystalline networks combined with elastomers could increase the response and durability of elastomeric actuators.^{16,17}

This chapter describes the development of novel humidity-responsive photonic coatings based on an IPN combining CLC polymer networks and hydrogels. The optical properties are provided by the cholesteric network and the swelling behaviour by the potassium polyacrylate hydrogel network. The sodium and potassium salts of poly(acrylic acid) have super-absorbent properties. These crosslinked acrylic polymers are known as "super absorbents" and used in, for example, incontinency materials. An IPN coating was prepared by the photopolymerisation of a cholesteric mixture containing a non-reactive mesogenic unit.^{18,19} The subsequent removal of this moiety makes the network permeable. The polymer network was swollen using a second monomer mixture based on acrylic acid. Another photopolymerisation procedure leads to the formation of an IPN. Subsequent treatment with an alkaline solution leads to the deprotonation of the carboxylic acid groups present in the system. The cholesteric liquid crystal network leads to colour reflection by the coating and the potassium polyacrylate network to the humidity responsiveness. Since the two networks are tightly interwoven, swelling of the hygroscopic polymer salt results in swelling of the entire coating. The method was used to prepare humidity-responsive surface topographies. Mask exposure steps were used to produce a material consisting of two different IPNs, namely responsive and static IPN regions.

5.2 Results and discussion

5.2.1 Prerequisites for the preparation of a sequential cholesteric IPN

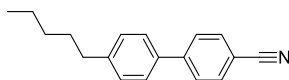
To create a cholesteric IPN, the cholesteric polymer network was prepared first as the alignment of this network is crucial for the optical properties. As the helical organisation is fixed after polymerisation, diffusion of a second monomer mixture into the cholesteric network can lead to swelling of the material. This can then be followed by polymerisation to produce the IPN. Commercially available mesogenic molecules were used for the preparation of the CLC polymer network (Scheme 5.1). Compound **2** is a polymerisable diacrylate nematic mesogen which was used to enhance the rigidity of the coating. The cholesteric liquid crystalline phase was induced with chiral dopant **1**. Surfactant **3** was added to induce the planar alignment of the mixture at the air-liquid interface and **4** was used as the photoinitiator for photopolymerisation.



Scheme 5.1 Structures of the compounds used for the preparation of cholesteric coatings: chiral dopant **1**, nematic monomer **2**, surfactant **3** and photoinitiator **4**. The mixture was dissolved in xylene, 1 : 1, prior to being used.

The CLC mixture consists of 4, 94, 1 and 1 wt% of **1**, **2**, **3** and **4** respectively. The mixture was subsequently dissolved in a 1 : 1 ratio in xylene and spin coated onto a pre-rubbed polyimide-coated glass substrate. The solvent was evaporated and the mixture was photopolymerised in a nitrogen atmosphere, resulting in a green-yellow-reflecting polymer network (**PN1**, Figure 5.2a, solid line, $\lambda_{Rmax} = 576$ nm).

However, the addition of acrylic acid resulted only in the marginal swelling of the coating. This may be attributable to the fully crosslinked network, which does not allow for additional swelling. In order to prepare a sequential IPN, a polymer film is required that can swell after the addition of a second monomer. A less rigid polymer network is required to prepare a cholesteric polymer network that can absorb another monomer mixture. In the monomer mixture, therefore, 30 wt% of compound **2** was replaced by a non-polymerisable mesogen 5CB (Scheme 5.2) that was washed out in a second step.^{18,19} 5CB was selected as it exhibits nematic phase behaviour at room temperature and its optical properties were similar to those of monomer **2**. The removal of 5CB can lead to the creation of porosity in the polymer network. This mixture was prepared and photopolymerised in the same fashion as the mixture without 5CB, resulting in **PN2** with a yellow reflection band at $\lambda_{Rmax} = 588$ nm (Figure 5.2a, grey line,). **PN2** was less transparent than **PN1**, which can be explained by the fact that some phase separation takes place after polymerisation, as observed by optical microscopy (Figure 5.2b). Small droplets of 5CB on the surface of the coating led to light scattering, which resulted in a lower transmission of light.



Scheme 5.2 Structure of nematic mesogen 5CB

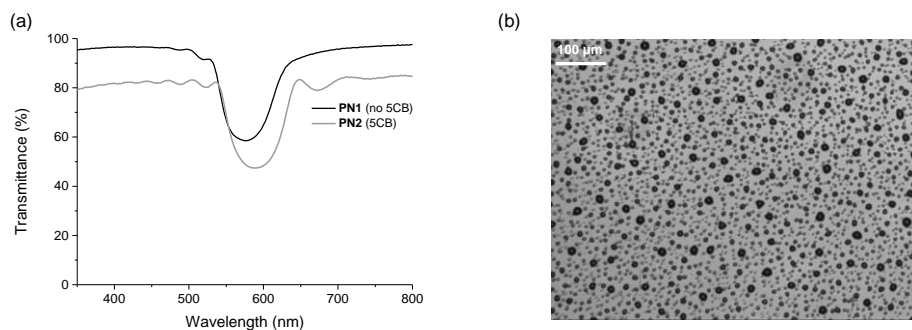


Figure 5.2 (a) UV/Vis spectra of **PN1** and **PN2** on a rubbed polyimide substrate and (b) optical microscopy image of **PN2** showing small droplets of 5CB on top

In order to create free volume in the polymer network, 5CB needs to be extracted from the coating. Thermogravimetric analysis (TGA) showed that **PN2** undergoes

a weight loss of 30% between 140 and 200 °C before it starts to degrade at around 300 °C (Figure 5.3a). This weight loss corresponds to the initial amount of 5CB in the polymer network. As a reference measurement, **PN1** was subjected to TGA and degradation was observed at 300 °C only. The removal of 5CB from **PN2** was achieved by heating the sample at 140 °C for 15 minutes, leading to **PN2H**. After this procedure, the initially yellow-orange film was purple and the reflection band reduced by 30.6% to $\lambda_{Rmax} = 408$ nm, which means that the helical pitch had dropped (Figure 5.3b, c). Furthermore, there was less scattering in the sample. As the helical structure is fixed after polymerisation, the decrease in pitch length can only be related to a decrease in the thickness of the sample. Interferometry measurements of **PN2** and **PN2H** found a decrease of 30% in the thickness of the sample (from 3.0 to 2.1 μm). Furthermore, FT-IR analysis revealed that the signal disappeared at 2220 cm^{-1} (Figure 5.3d). This signal is attributable to the cyano group present in 5CB. Combining the results obtained with these techniques indicates that all the 5CB was successfully removed, resulting in the collapse of the polymer coating. **PN1** was subjected to a similar heating experiment. A change in the reflection band of only 1.5% was observed, which can be ascribed to the relaxation of polymerisation-induced stresses within the polymer network above its T_g . No decrease in the thickness of the film was observed after the heating procedure.

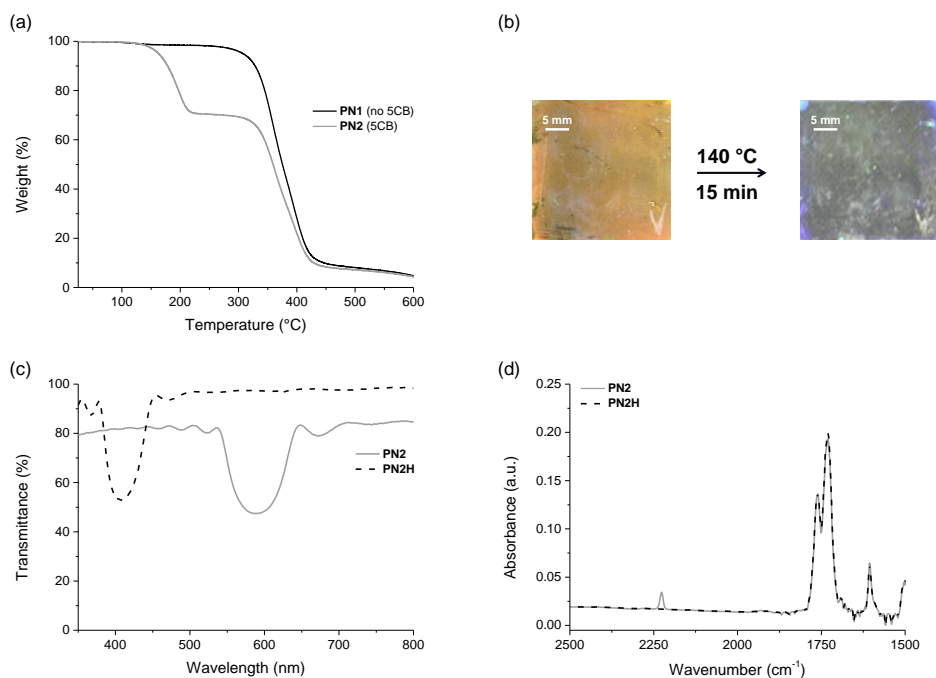


Figure 5.3 (a) TGA of **PN1** and **PN2**, (b) optical images of **PN2** and **PN2H**, (c) UV/Vis spectra of **PN2** and **PN2H** on a rubbed polyimide substrate and (d) FT-IR spectra of **PN2** and **PN2H**

5.2.2 Formation and activation of a cholesteric IPN

The previous section looked at polymer films on top of a rubbed polyimide layer, showing that CLC films with good reflective properties can be prepared with spin coating. However, the aim here was to prepare humidity-responsive coatings and so a polyimide substrate is not ideal. As there is no covalent bonding between this type of substrate and the polymer film, the films will most probably separate from the substrate when they start to deform. The materials described from this point on were therefore prepared on methacrylate-functionalised glass substrates using a procedure analogous to the one described in Chapter 4. The reflection bands of these surface-attached coatings were similar to the spin coated samples in position and intensity, although the coating was less transparent at shorter wavelengths, as shown in Figure 5.4a.

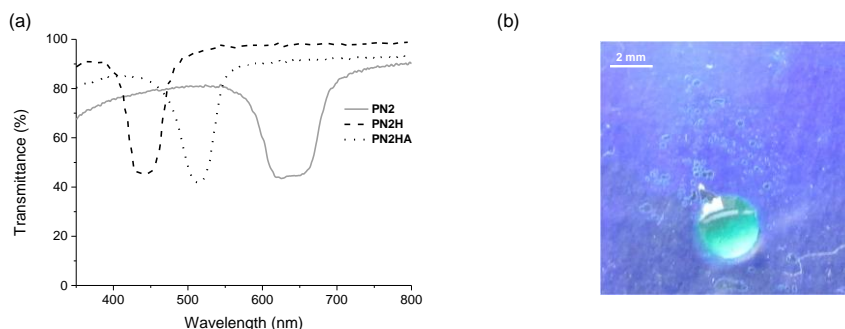
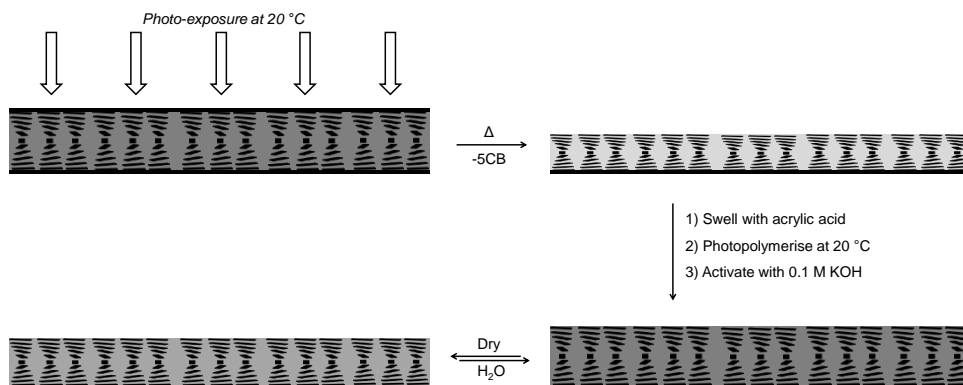


Figure 5.4 (a) UV/Vis spectra of **PN2**, **PN2H** and **PN2HA**, covalently bound to their substrate. (b) Optical image of purple **PN2H**: after a drop of acrylic acid was placed on top, the colour difference (which is induced by local swelling of the cholesteric network) could be clearly observed.

As mentioned above, a polymer scaffold needs to be swollen with a second monomer mixture to prepare a sequential IPN. As the cholesteric material reflects colour, the visual detection of the swelling of the material was straightforward. While no swelling – or the corresponding colour change – was observed in the case of **PN1**, the addition of a drop of acrylic acid on top of the **PN2H** coating resulted in a colour change from purple to green (Figure 5.4b shows the absorption of acrylic acid in the film). Due to the removal of the non-reactive mesogen 5CB, **PN2H** is a less rigid network that can swell. **PN2H** is therefore considered to be a good template material for the preparation of cholesteric IPNs.



Scheme 3 Schematic representation of the preparation procedure of a humidity-responsive cholesteric-based IPN

PN2H was swollen with acrylic acid containing 1 wt% of both crosslinker tripropylene glycol diacrylate (TPGDA) and photoinitiator **4**. After 15 minutes, no additional swelling was observed. The excess monomers were removed, a perfluorodecyltriethoxysilane functionalised glass slide was placed on top and the mixture was photopolymerised, resulting in **PN2HA** (Scheme 5.3). Figure 5.4a shows its reflection band, with $\lambda_{Rmax} = 520$ nm, which had a shorter wavelength than the reflection band of **PN2**. This might be a result of polymerisation shrinkage. Another explanation is that the volume created by the removal of 5CB was not entirely filled with the second monomer mixture. It should be noted that the processing steps led to small variations in the refilling ratio between different samples.

The IPNs were activated by placing **PN2HA** in a 0.1 M KOH solution for 16 hours, resulting in **PN2HAK**, in which the poly(acrylic acid) network was successively converted to the corresponding potassium polyacrylate salt. Initially, cross-sections were analysed using scanning electron microscopy (SEM). More representative observations were obtained with transmission electron microscopy (TEM) (Figure 5.5a). TEM is a well-known method for the examination of cholesteric liquid crystals.²⁰ The periodic anisotropy of the orientation of the molecules results in the observation of alternating dark and bright bands in which the centre-to-centre distance corresponds to half the pitch of the cholesteric helix. This contrast difference arises due to different atom densities depending on whether when the director axis is parallel or perpendicular to the electron beam, since intramolecular distances are shorter than intermolecular ones. Since the samples for TEM were microtomed, rather than fractured as for SEM preparations, the surface is smoother and the pitch can be determined more reliably. The formation of an IPN was further confirmed by transmission FT-IR spectroscopy measurements (Figure 5.5b). After the formation of **PN2HA**, the signal was saturated between 1800 and 1650 cm^{-1} due to the large amount of carboxylic acids in the IPN. When **PN2HAK** was created, the appearance of a signal at 1573 cm^{-1} indicated the formation of carboxylate ions. Furthermore, the signals typical of the CLC polymer network's ester bonds at 1764 and 1735 cm^{-1} reappeared.

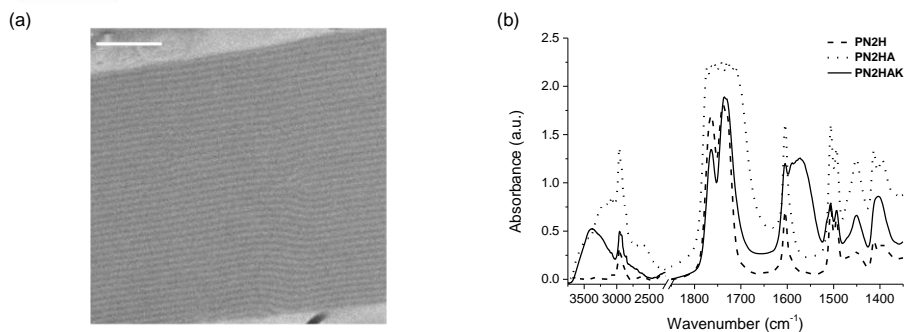


Figure 5.5 (a) Typical TEM image of **PN2HA**. The sample reveals bright and dark areas that are related to the anisotropy of the cholesteric orientation. The scale bar represents 2 μm . (b) Transmission FT-IR spectra of **PN2H**, **PN2HA** and **PN2HAK**.

Table 5.1 lists the thicknesses, selective reflection bands and pitches of the cholesteric IPN in the different production steps. After removal of non-reactive mesogen 5CB, the thickness and SRB fell by approximately 31%, as mentioned above. The formation of **PN2HA** leads to an increase in thickness, SRB and pitch that is approximately 1.25 times larger than with **PN2H**. Subsequent activation of the coating led to marginal changes. The thickness and the SRB were determined using exactly the same sample at the same position, resulting in similar observations. However, different samples were required for TEM analysis and so a discrepancy between the data was seen. As stated earlier, the available volume present in the CLC scaffold was not completely filled with the acrylic acid mixture, resulting in small variations between the measured samples.

Table 5.1 Summary of the properties of a typical polymer coating at different points in the manufacturing procedure

Material	Thickness (μm)	SRB ($\lambda_{R\text{max}}$)	Pitch (nm) ^[a]
PN2	4.5	620 nm	— ^[b]
PN2H	3.1 (69%)	420 nm (68%)	300
PN2HA	4.0 (89%)	520 nm (84%)	375
PN2HAK	4.0 (89%)	530 nm (85%)	350

[a] Different samples were used for the TEM studies as the samples were embedded in epoxy resin prior to the measurement. The average pitch sizes for several measurements are shown. [b] No contrast was observed with TEM.

5.2.3 Response of the activated cholesteric IPN to humidity

After the successful preparation and characterisation of the IPN based on a cholesteric scaffold and hygroscopic potassium polyacrylate, its response to water was explored. When **PN2HAK** was placed in demineralised water, its colour changes from green (530 nm) to the near infrared (750 nm). More interestingly, the coating even reacts to changes in the RH. For instance, when the RH was lowered to 6%, the reflection band fell to 497 nm whereas a reflection band of 650 nm was observed at high humidity (85%). Relative-humidity-dependent UV/Vis spectra were recorded for **PN2HAK** to clarify the relationship between RH and reflection band (Figure 5.6a, b). At low RH, only a slight increase in the reflection band was seen. Between 25 and 70% RH, there was an almost linear increase, which flattens after reaching a high relative humidity. At higher RH, the overall transparency of the coating decreases, probably as a result of water condensing on top of the coating.

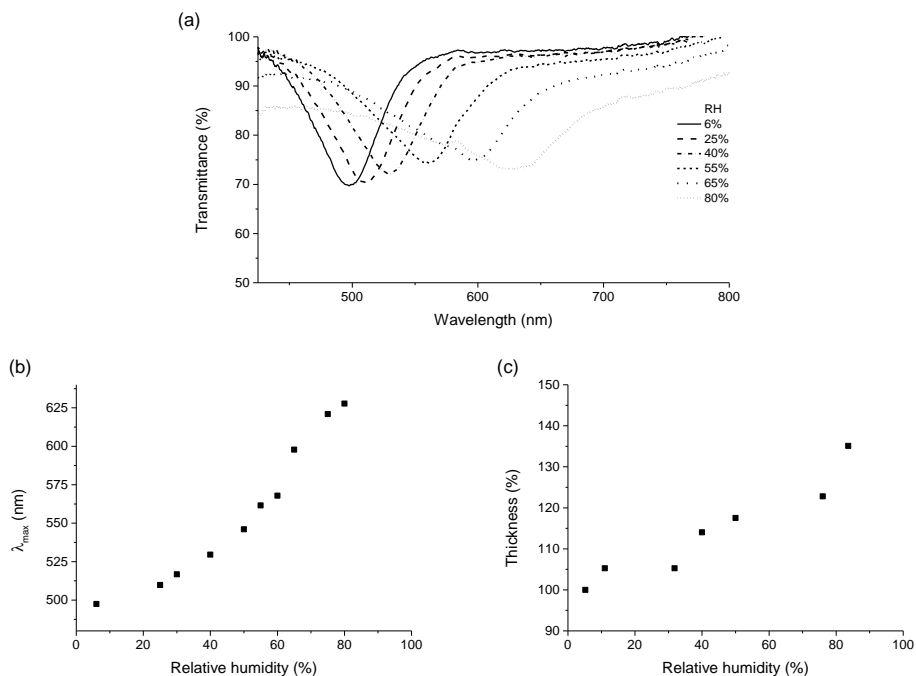
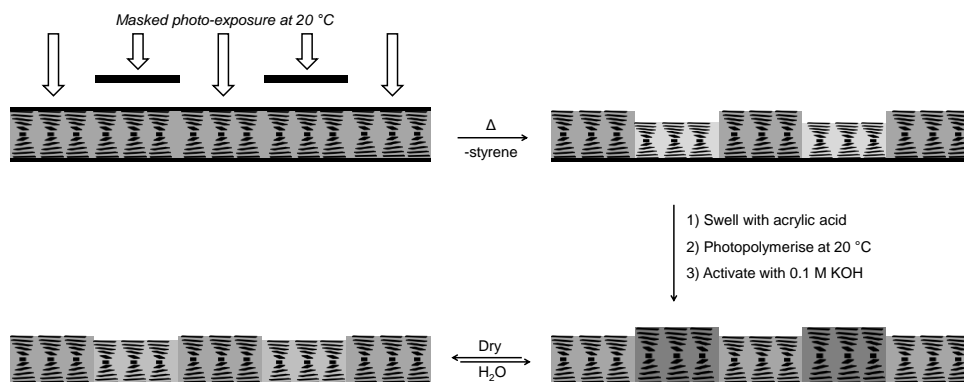


Figure 5.6 (a) UV/Vis spectra for the humidity dependence of **PN2AK**, (b) retrieved λ_{Rmax} plotted against RH and (c) the thickness of the coating against RH

Moreover, a similar humidity experiment was performed while measuring the height of the sample with an interferometer. The thickness at a RH of 84% is 1.35 times higher than at a RH of 5% (Figure 5.6c). These changes are comparable with the changes in the reflection band ($650/497 \text{ nm} = 1.31$). Reversible swelling and shrinkage of the film, which corresponds to the change in the wavelength being reflected, are indirect indicators that an IPN has indeed been produced. Volumetric alterations in the potassium poly(acrylate) network were translated to changes in the cholesteric network as well, leading to a colour change. Furthermore, with two entangled networks present, the response remains present after multiple switching cycles as the two polymer networks cannot separate from each other. By comparison with the humidity-responsive CLC-based materials discussed elsewhere, the change in reflection band was higher by a factor of 3.75 ($\Delta\lambda = 150 \text{ nm}$).⁷ This response is in the same range as seen in materials in which the highest humidity-dependent colour changes has been reported.¹

5.2.4 *Patterned cholesteric IPN coatings*

Previous chapters discussed several kinds of responsive surface topographies. In those systems, the entire coating swells or shrinks when a stimulus is applied, even though only a local change is required for some applications. The preparation of patterned IPNs can lead to surface topographies with both static and responsive regions. As with the IPN discussed in the previous section, the response depends on potassium poly(acrylate). However, the IPN was not made solely from this material. The incorporation of a second, non-responsive, monomer leads to changes in the potassium poly(acrylate) regions exclusively. A **PN2H** coating was swollen with styrene containing 1 wt% of both crosslinker TPGDA and photoinitiator **4**. Masked exposure results in partially polymerised networks **PN2HS**. Excess monomer was evaporated at elevated temperature. Afterwards, the remaining areas were filled with acrylic acid containing 1 wt% of both crosslinker TPGDA and photoinitiator **4** and subsequently flood exposed with UV light. After the activation of the coating with alkaline solution, an IPN was obtained in which only the **PN2HAK** regions were humidity-responsive (Scheme 5.4).



Scheme 5.4 Schematic representation of the fabrication of a patterned humidity-responsive IPN

Table 5.2 Summary of the properties of a typical polymer coating at different points in the production procedure

Material	Thickness (μm)		$\lambda_{R\text{max}}$ (nm)	
	PS area	PAA area	PS area	PAA area
PN2	10.5	10.5	620	620
PN2H	6.9 (66%)	6.9 (66)	420 (68%)	420 (68%)
PN2HS	9.0 (86%)	8.2 (78%)	[a]	[a]
PN2HSA	9.3 (89%)	8.8 (84%)	[a]	[a]
PN2HSAK (RH = 15%)	9.0 (86%)	8.7 (83%)	532 (86%)	518 (84%)
PN2HSAK (RH = 50%)	9.0 (86%)	9.1 (87%)	528 (85%)	531 (86%)
PN2HSAK (RH = 80%)	9.0 (86%)	9.4 (90%)	527 (85%)	573 (92%)

[a] Selective reflection bands were not determined in the intermediate processing steps for the IPN

It should be noted that it is challenging to prepare small responsive structures which respond independently of each other because of the rigidity of the materials used. A mask with a rather large pitch of 2 mm (1 mm dark areas) was therefore used for the mask photopolymerisation. The thickness and SRB of the sample during the different preparation steps for a patterned humidity-responsive IPN are presented in Table 5.2. As with the coatings described previously, removing 5CB led to a fall in thickness. After the formation of a patterned polystyrene IPN, the thickness of the exposed areas increased. However, the unexposed regions were also slightly thicker, as styrene polymerised partially in those areas as well. Afterwards, an alternating polystyrene-poly(acrylic acid) IPN was prepared. The thickness in the polystyrene areas also increased slightly during this step. The

coating was activated in alkaline solution to result in a humidity-responsive surface topography.

In ambient conditions, the surface topography was homogeneously coloured and almost flat (Figure 5.7). The thickness of the **PN2HAK** regions fell at low RH and increased at higher RH. The **PN2HS** areas did not alter when RH changed and so, when RH increased, distinct alternating green and red regions could be clearly observed with the naked eye. It should be noted that the response in the patterned IPN is smaller than in homogeneous IPNs. This can be explained by the fact that the overall structure is more rigid due to the incorporation of the polystyrene network. The polystyrene regions affect the maximum swelling capacity of the polyacrylate regions. The preparation of this patterned IPN shows that a surface topography which has both humidity-responsive and static regions is possible. In the approach presented for IPNs, only relatively small monomers were used for the second polymer network. Fine-tuning of the cholesteric network's composition (such as a higher amount of 5CB in the initial mixture) could result in a material which can be swollen by more complex monomer mixtures. For instance, a cholesteric IPN with the photoresponsive hydrogel described in Chapter 3 as the second network will result in a photoresponsive material that changes colour.

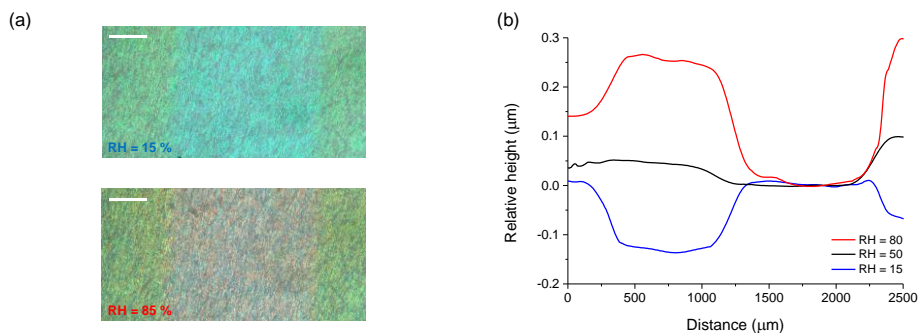


Figure 5.7 (a) Optical micrographs of a patterned IPN at a RH of 15 and 85%. The colour change in the **PN2HAK** areas is clear to see. The scale bar represents 250 μm . (b) Surface topography of the patterned humidity-responsive IPN coating at RH = 15, 50 and 80% ($T = 20\text{ }^\circ\text{C}$), as observed by interferometry (smoothing software was used). The mask used has dark areas of 1 mm and a pitch of 2 mm.

5.3 Conclusion

A new type of optical humidity sensor based on an IPN was prepared. In the first step, a cholesteric polymeric template coating was swollen with a mixture of acrylic acid and a crosslinking agent, and subsequently polymerised. Treatment with an alkaline solution led to the conversion of the poly(acrylic acid) network into a hygroscopic carboxylate network. As the two networks are tightly interwoven, humidity-dependent volume changes in the polyacrylate network are translated to the cholesteric polymer network, causing the reflected colour to change. The resulting optical sensor has an operational range of 150 nm (~500 nm at low humidity and ~650 at high humidity), which is an increase of a factor 3.75 compared to previously reported humidity-responsive cholesteric polymer networks. In addition, as a proof of principle, patterned IPN coatings were prepared. These coatings consist of similar carboxylate regions but they also have polystyrene areas, resulting in a coating which has both static and humidity-responsive areas. This method can be used to prepare materials with multiple regions that respond to different stimuli. Various kinds of analytes can be detected simultaneously with an optical sensor of this kind. Overall, the results show that an IPN can be produced in which the monolithic molecular order of LC materials can be combined with the functional properties of another polymeric system. This opens up numerous avenues for the preparation of stimuli-responsive polymer systems with tuneable functional properties.

Experimental section

Characterisation of materials: Spin coating was performed on a Karl Suss RC6 spin coater. The UV-light intensities produced by the collimated EXFO Omnicure S2000 lamp were determined using a UV Power Puck II by EIT Instrument Markets Group. A Shimadzu UV-3102 PC spectrometer was used for UV/Vis spectroscopy of the films. An HR2000+ high-resolution spectrometer from Ocean Optics mounted on a DM6000 M microscope from Leica microsystems was used for time-dependent UV/Vis spectroscopy of the films. The corresponding light source emits between 400 and 800 nm. A Varian 670 FT-IR spectrometer was used to record transmission IR spectra. The same device with a slide-on ATR crystal (Ge) and a Varian-3100 FT-IR spectrometer were used to measure reflection IR-spectra. Height profiles and 3D images of patterned films were recorded using a 3D interferometer (Fogale Nanotech Zoomsurf). Differential scanning calorimetry was performed on a DSC

Q1000 from TA instruments and a TGA Q500 from TA instruments was used for thermogravimetric analysis. Scanning electron microscopy was done on a SEM-Quanta 3D, FEI, cross-sections were prepared by fracturing the films in liquid nitrogen. The thin films were embedded in an epoxy resin (Epofix) at 70 °C. Ultrathin sections were obtained at room temperature using a Leica Reichert Ultracut S microtome equipped with a Diatome 45° knife (cutting direction not parallel to the CLC director). The sections were transferred to a 200 mesh copper grid with a carbon support layer. Transmission Electron Microscopy was performed using a Tecnai 20 microscope, operated at 200 kV.

Materials: Unless stated otherwise, all reagents and chemicals were obtained from commercial sources. Compounds **1** and **2** were purchased from BASF. Photoinitiator **4** (Irgacure 651) and surfactant **3** were obtained from Ciba Specialty Chemicals and Acros Chemicals respectively. 5CB was obtained from Merck. All solvents were obtained from Biosolve. The silanes for substrate modification were obtained from Sigma-Aldrich. Polyimide OPTMER AL 1051 was purchased at JSR Corporation.

Polyimide substrate preparation: Glass substrates were cleaned by sonication (ethanol, 15 minutes) followed by treatment in a UV-ozone photoreactor (Ultra Violet Products, PR-100, 20 minutes). The substrates were spin coated (two-step cycle: 1000 rpm for 5 sec and 5000 rpm for 40 sec) and then cured (pre-baked on a hot plate at 90 °C for 10 min and baked on an oven for 1 hour at 180 °C). Prior to being used, the substrates were rubbed with a velvet cloth.

Glass functionalisation: Glass substrates were cleaned by sonication (ethanol, 15 minutes) followed by treatment in a UV-ozone photoreactor (Ultra Violet Products, PR-100, 20 minutes). The surface of the glass substrates was modified by spin coating 3-(trimethoxysilyl)propyl methacrylate solution (1 vol% solution in a 1:1 water-isopropanol mixture) or 1*H*,1*H*,2*H*,2*H*-perfluorodecyltriethoxysilane solution (1 vol% solution in ethanol) onto the activated glass substrate for 45 seconds at 3000 rpm. After curing for 10 minutes at 100 °C, the substrates were ready to use.

Preparation of the CLC films by spin coating: The monomer mixture (mixtures **1** and **2** contain **4**, 94, 1, 1, 0 and 4, 64, 1, 1, 30 wt% of **1**, **2**, **3**, **4** and 5CB respectively) in xylene (1 : 1) was spin coated onto the rubbed polyimide glass slides at 1000 rpm for 30 seconds. The solvent was then fully evaporated at 95 °C. The samples were photopolymerised in a nitrogen box for 150 seconds (48 mW/cm² intensity in the range 320-390 nm).

Preparation of the CLC coatings: Cholesteric coatings with a typical thickness of between 8 and 10 μm were prepared as follows: 10 μl of the CLC mixture (dissolved 1 : 1 in xylene) was placed on a methacrylate functionalised substrate at 95 $^{\circ}\text{C}$ and the solvent was allowed to evaporate. After the complete evaporation of xylene, a perfluorodecyl-triethoxysilane functionalised glass substrate was placed on top and pressed firmly. At lower temperatures, the chiral nematic liquid crystals were aligned by shear forces. The contents of the cells were photopolymerised at room temperature for 300 seconds (48 mW/cm^2 intensity in the range 320-390 nm).

Removal of the non-reactive mesogen 5CB: In order to remove 5CB from the polymer film, the sample was heated at 140 $^{\circ}\text{C}$ for 10 minutes. During this process, the initially yellow-orange reflecting film turned blue. Various techniques confirmed that 5CB was fully removed from the coating.

Preparation of the cholesteric – acrylic acid IPN: A drop of acrylic acid with 1 wt% crosslinker TPGDA and 1 wt% of photoinitiator **4** was placed on the polymer coating. In order to prevent evaporation, a glass sheet was placed on top. The monomer mixture was allowed to swell for 15 minutes, after which no additional visible colour change was observed. The upper glass plate was removed and excess of monomer mixture was removed before a perfluorodecyl-triethoxysilane functionalised glass slide was placed on top and the mixture was photopolymerised for 300 seconds (48 mW/cm^2 intensity in the range 320-390 nm).

Preparation of patterned IPNs: A drop of styrene containing 1 wt% crosslinker TPGDA and 1 wt% of photoinitiator **4** was placed on the polymer coating. The swelling procedure was similar to the one described for the cholesteric – acrylic acid IPN. After being fully swollen, the cells were placed on a black surface and a mask was placed on top. The sample was photopolymerised for 350 seconds (13.5 mW/cm^2 intensity in the range 320-390 nm). The sample was then placed on a hot plate to evaporate the remaining unpolymerised styrene. The procedure for the preparation of the cholesteric – acrylic acid IPN was then used, resulting in an IPN coating with alternating regions of polystyrene and poly(acrylic acid).

Activation of the IPNs: The films containing poly(acrylic acid) were placed in a 0.1 M KOH solution for 16 hours to ensure full formation of the corresponding carboxylate salt.

References

- 1 E. Kim, S. Y. Kim, G. Jo, S. Kim and M. J. Park, *ACS Appl. Mater. Interfaces*, 2012, **4**, 5179-5187.
- 2 J. Ge and Y. Yin, *Angew. Chem., Int. Ed.*, 2011, **50**, 1492-1522.
- 3 C. Fenzl, T. Hirsch and O. S. Wolfbeis, *Angew. Chem., Int. Ed.*, 2014, **53**, 3318-3335.
- 4 R. Byrne, F. Benito-Lopez and D. Diamond, *Mater. Today*, 2010, **13**, 16-23.
- 5 D.-J. Mulder, A. P. H. J. Schenning and C. W. M. Bastiaansen, *J. Mater. Chem. C*, 2014, Accepted Manuscript.
- 6 A. Saha, Y. Tanaka, Y. Han, C. M. W. Bastiaansen, D. J. Broer and R. P. Sijbesma, *Chem. Commun.*, 2012, **48**, 4579-4581.
- 7 N. Herzer, H. Guneyasu, D. J. D. Davies, D. Yildirim, A. R. Vaccaro, D. J. Broer, C. W. M. Bastiaansen and A. P. H. J. Schenning, *J. Am. Chem. Soc.*, 2012, **134**, 7608-7611.
- 8 L. H. Sperling, in *Encyclopedia of Polymer Science and Technology*, John Wiley & Sons, Inc., 2002.
- 9 E. S. Dragan, *Chem. Eng. J.*, 2014, **243**, 572-590.
- 10 Y. S. Lipatov and T. T. Alekseeva, in *Phase-Separated Interpenetrating Polymer Networks*, Springer-Verlag Berlin, Berlin, 2007, vol. 208, pp. 1-227.
- 11 D. Myung, D. Waters, M. Wiseman, P.-E. Duhamel, J. Noolandi, C. N. Ta and C. W. Frank, *Polym. Adv. Technol.*, 2008, **19**, 647-657.
- 12 L. H. Sperling, *J. Polym. Sci., Part D: Macromol. Rev.*, 1977, **12**, 141-180.
- 13 L. H. Sperling and V. Mishra, *Polym. Adv. Technol.*, 1996, **7**, 197-208.
- 14 K. Boudraa, T. Bouchaour and U. Maschke, *Macromol. Symp.*, 2011, **303**, 95-99.
- 15 K. Boudraa, T. Bouchaour and U. Maschke, *Mol. Cryst. Liq. Cryst.*, 2011, **545**, 1444-1453.
- 16 L. T. de Haan, C. Sánchez-Somolinos, C. M. W. Bastiaansen, A. P. H. J. Schenning and D. J. Broer, *Angew. Chem., Int. Ed.*, 2012, **51**, 12469-12472.
- 17 H. Yu and T. Ikeda, *Adv Mater*, 2011, **23**, 2149-2180.
- 18 C.-K. Chang, C. M. W. Bastiaansen, D. J. Broer and H.-L. Kuo, *Adv. Funct. Mater.*, 2012, **22**, 2855-2859.
- 19 C.-K. Chang, C. W. M. Bastiaansen, D. J. Broer and H.-L. Kuo, *Macromolecules*, 2012, **45**, 4550-4555.
- 20 T. J. Bunning, D. L. Vezie, P. F. Lloyd, P. D. Haaland, E. L. Thomas and W. W. Adams, *Liq. Cryst.*, 1994, **16**, 769-781.

Simplicity is the ultimate sophistication
- Leonardo da Vinci -

Chapter 6

Amine-responsive hydrogen-bonded cholesteric liquid crystal coatings as a sensor

Abstract

This chapter describes an inkjet-printed hydrogen-bonded cholesteric liquid crystal (CLC) polymer film that can be used as a sensor for the detection of gaseous trimethylamine (TMA). The virgin CLC polymer network in this optical sensor reflected green light. When anhydrous TMA gas penetrated into the film, the hydrogen bonds were disrupted and carboxylate salts were formed at the same time. The resulting reduction of the molecular order caused the green-reflecting CLC film to become colourless. However, exposure to TMA in water-saturated nitrogen gas resulted in a red-reflecting film. Due to the hygroscopic nature of the polymer salt formed by TMA, water vapour present in the environment was absorbed by the films. This led to the swelling of the film, resulting in an increase in pitch size and therefore a red shift in the reflection band. Interestingly, when subsequently exposed to ambient conditions, the initial green colour was restored, showing that the sensor can be used multiple times. In a proof of principle experiment, it was shown that these CLC films can be used as optical sensors to detect volatile amines, which are produced by decaying fish.

This chapter is partially reproduced from: J. E. Stumpel, C. Wouters, N. Herzer, J. Ziegler, D. J. Broer, C. W. M. Bastiaansen and A. P. H. J. Schenning, *Advanced Optical Materials*, 2014, **2**, 459-464.

6.1 Introduction

Materials which respond to the presence of gases or vapours are of interest for sensing applications and the detection of amines is important in environmental, industrial and food quality monitoring.¹⁻³ Furthermore, sell-by dates may be inadequate, resulting in the waste of food. Food poisoning as a result of fish decay is a major problem for the food industry and its customers. One of the components of the total volatile basic nitrogen content produced by decaying fish is trimethylamine (TMA).⁴ An easy-to-use, battery-free sensor for amine detection is therefore desirable. Several kinds of amine sensors have been developed in the past based on a variety of different working principles.⁵⁻⁷ For example, optical sensors based on indicator dyes have been reported.⁸⁻¹¹ However, these systems are susceptible to photobleaching and often require advanced processing and readout procedures.

Cholesteric liquid crystalline polymers are proven, printable, optical sensors¹²⁻¹⁴ that do not require batteries.¹⁵⁻¹⁷ Cholesteric liquid crystals (CLC) reflect circularly polarised light at a wavelength that corresponds to the pitch of the molecular helices corrected for the refractive index (see Chapter 4 for a more detailed explanation). When used for sensor applications, a molecular trigger changes the molecular order in the CLC, resulting in a change in the reflection band. For example, Shibaev and co-workers have produced hydrogen-bonded CLC polymer films which change their selective reflection band (SRB) after exposure to different aqueous amino acid solutions.¹⁸⁻²⁰ To date, most of the CLC polymer sensors have been designed to detect analytes in solution, while sensors detecting vapours or gases are rare.^{18,21-23}

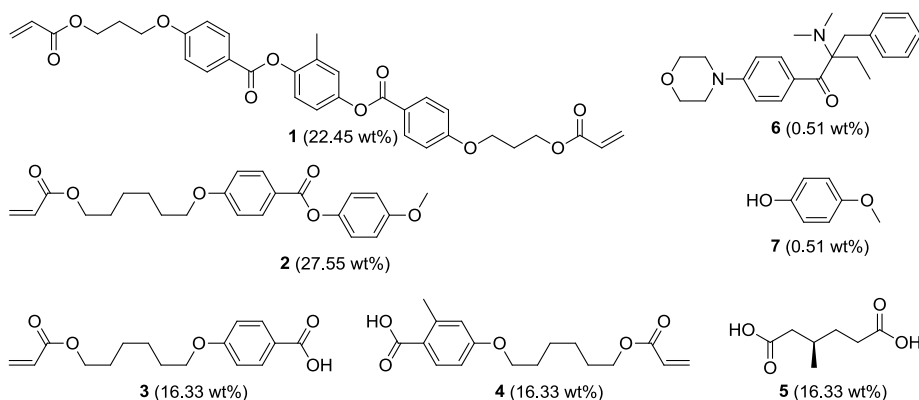
Recently, there have been reports of fast-responding humidity sensors in which the reflection colour changes in response to variations in relative humidity.²⁴ A hygroscopic CLC polymer salt film was used for the preparation of this sensor. Absorption and desorption of water in the film results in the swelling or shrinkage of the material, leading to changes in the reflection band as a result of a change in the helical pitch. This chapter describes a similar material which is amine-responsive. An initially green-reflecting hydrogen-bonded CLC-based sensor which responds to TMA vapour was made. When the liquid crystalline mixture was exposed to TMA in water-saturated nitrogen gas, the hydrogen-bonded

polymer network was disrupted, resulting in a colour change from green to red. The amine-responsive material can be printed on foil and could be used as an optical sensor to monitor the freshness of fish.

6.2 Results and discussion

6.2.1 Preparation and characterisation of inkjet-printed CLC coatings

The CLC mixture used in this study is similar to the hydrogen-bonded liquid crystalline polymer mixture reported by Shibaev et al.¹⁸ A slightly different monomer composition was used which creates an initial green-reflecting polymer film (Scheme 6.1). The mono- and diacrylate LCs without carboxylic acid groups (**1** and **2**) induce nematic behaviour in the mixture and form a chemical network after photopolymerisation. To allow the film to respond to amine vapour, polymerisable benzoic acid derivatives (**3** and **4**) and (*R*)-(+)-3-methyladipic acid (MAA, **5**) were added.²⁴ In addition, the non-polymerisable dicarboxylic acid MAA was used as chiral dopant to introduce a chiral nematic phase to the mixture. Additionally, a photoinitiator (**6**, Irgacure 369) was added to the system. To prevent premature polymerisation, *p*-methoxyphenol (**7**) was added as an inhibitor. The mixture was photopolymerised in the cholesteric liquid crystalline phase.



Scheme 6.1 The chemicals that were used for the cholesteric liquid crystalline film: diacrylate crosslinker **1** and nematic mesogen **2**, polymerisable benzoic acid derivatives **3** and **4**, benzoic acid-based chiral dopant **5**, photoinitiator **6** and inhibitor **7**. The mixture was dissolved in THF in a 1 : 1 ratio (weight) prior to the printing process.

Thin, well-ordered homogeneous films were inkjet-printed using THF as a solvent.²⁴ Triacetyl cellulose (TAC) foil, which was rubbed beforehand with a velvet cloth, was used as the substrate. After printing, the solvent was evaporated to obtain a cholesteric phase that was planarly aligned on the rubbed TAC substrate. The printed cholesteric film was photopolymerised at room temperature in a nitrogen atmosphere. The green reflectance of the CLC film was visible (Figure 6.1a). UV/Vis spectroscopy (Figure 6.1b) shows a polarisation-selective reflection band (SRB) at approximately 550 nm.

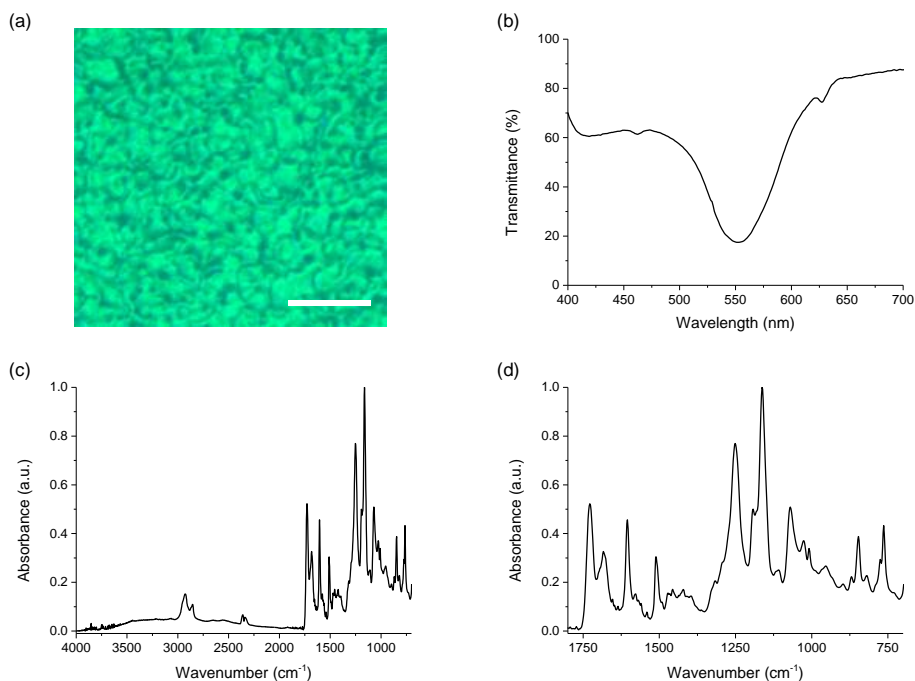


Figure 6.1 Characterisation of the inkjet-printed CLC polymer film. (a) Optical micrograph of the inkjet printed film (scale bar represents 125 μm), (b) UV/Vis transmission spectrum measured with circularly polarised light and (c, d) an FT-IR spectrum of the corresponding film.

The FT-IR spectrum of the printed film displays small signals between 2700 and 2450 cm^{-1} , which can be assigned to the OH stretching. A strong signal at 1680 cm^{-1} indicates the presence of hydrogen bonds between carboxylic acid moieties (Figure 6.1c, d).^{24,25} The presence of hydrogen-bonding between benzoic and aliphatic acids was not clearly visible as these signals overlap. Given the molar ratio of **3**, **4** and **5** (1:1:2), it could be concluded that there was an excess of chiral dopant **5** (which is

required for obtaining a green coloured film). Not all **5** can therefore be hydrogen-bonded with benzoic acid moieties **3** and **4**. The characteristic signals of the C=C double bond of the acrylate located at 809 and 985 cm^{-1} were significantly less intense than in the initial monomer mixture, indicating a high degree of polymerisation. Additional characterisation using optical interferometry showed that a homogeneous film with a thickness of approximately 6 μm was produced with the inkjet printing method.

6.2.2 Control experiment: response of the CLC sensor to pure water vapour

In order to check the cross-sensitivity of the coating to water vapour, the CLC hydrogen-bonded polymer film was exposed to water-saturated nitrogen gas. UV/Vis transmission spectroscopy revealed no changes in the position of the SRB, indicating no interaction of the CLC film with water vapour in the hydrogen-bonded state (Figure 6.2).

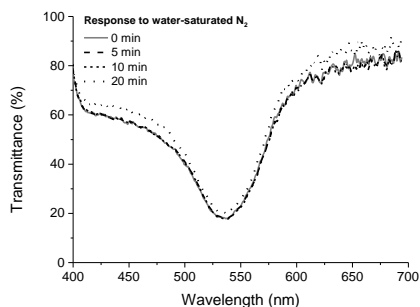


Figure 6.2 UV/Vis transmission spectra using circularly polarised light of the hydrogen-bonded CLC polymer film exposed to water-saturated nitrogen gas over time

6.2.3 Response of the CLC sensor to pure TMA

The response of these films to gaseous TMA was investigated with a UV/Vis spectrophotometer equipped with a gas chamber. In the first set of experiments, the gas chamber of the UV/Vis spectrophotometer was flooded with anhydrous TMA and the UV/Vis spectra were recorded over time. Treatment of the films with 100% TMA gas leads to a fast reduction in the intensity of the reflection band (Figure 6.3a). After an induction period of 3 minutes, the reflection band vanished completely within 5 minutes of total exposure time (Figure 6.3b). The S-shaped

responsive behaviour (Figure 6.3c) was probably caused by the time required for TMA to diffuse into the film in a non-Fickian fashion (see below).¹⁸ The polymer network is close to its glass transition temperature (T_g), which leads to a diffusion front rather than a diffusion gradient. When amine vapour penetrates into the film, the first 1-2 affected pitches will not dramatically change the intensity of the SRB as light is still being reflected by the underlying layers.

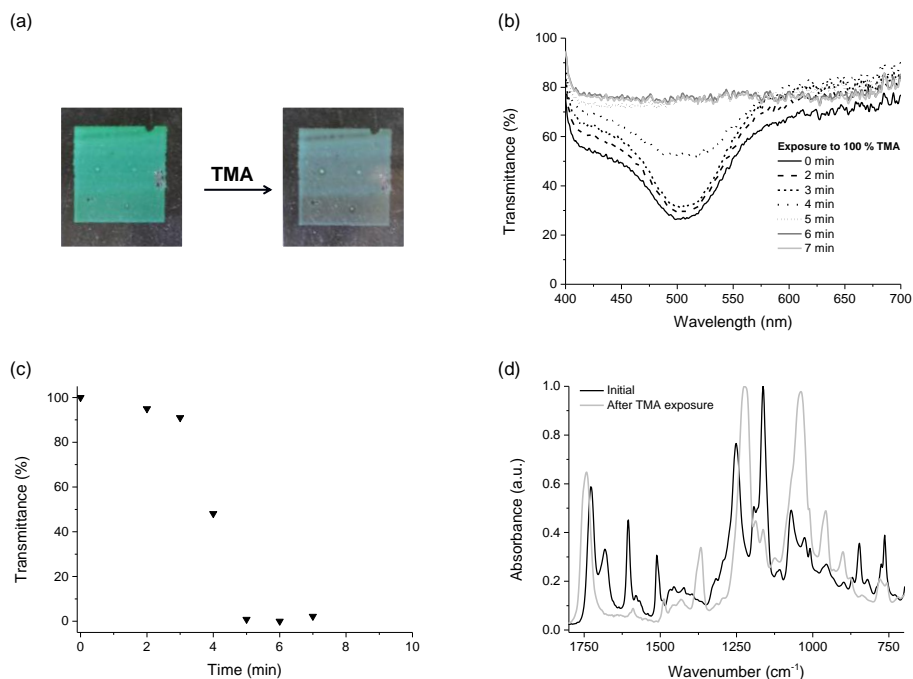


Figure 6.3 (a) Optical images of the films ($1 \times 1 \text{ cm}^2$) before and after TMA exposure. (b) UV/Vis transmission spectra with circularly polarised light of the CLC film taken after different exposure times to 100% TMA. (c) A plot of the transmission intensity change at maximum SRB (507 nm) of the CLC film exposed to 100% TMA and (d) FT-IR spectra of the CLC polymer film before and after being exposed to 100% TMA.

The response of the films to lower concentrations of TMA was also explored. With anhydrous nitrogen as a second flowing gas, it was possible to control the TMA content in the gas chamber of the UV/Vis spectrometer. The UV/Vis transmission spectra of a CLC film treated with 13% TMA in nitrogen (a mixture of two parallel gas flows with a different flow rate) were measured, showing a decline in the intensity of the reflection band as well (Figure 6.4a). However, this decrease

required more time than pure TMA (Figure 6.4c). A decline of 60% in the initial intensity of the reflection band was observed after 100 minutes. The lowest amount of amine gas which could be reached with the present setup was 2% TMA. After 120 minutes of exposure at this concentration, a slight reduction was seen in the reflection band (about 7%, Figure 6.4b, c).

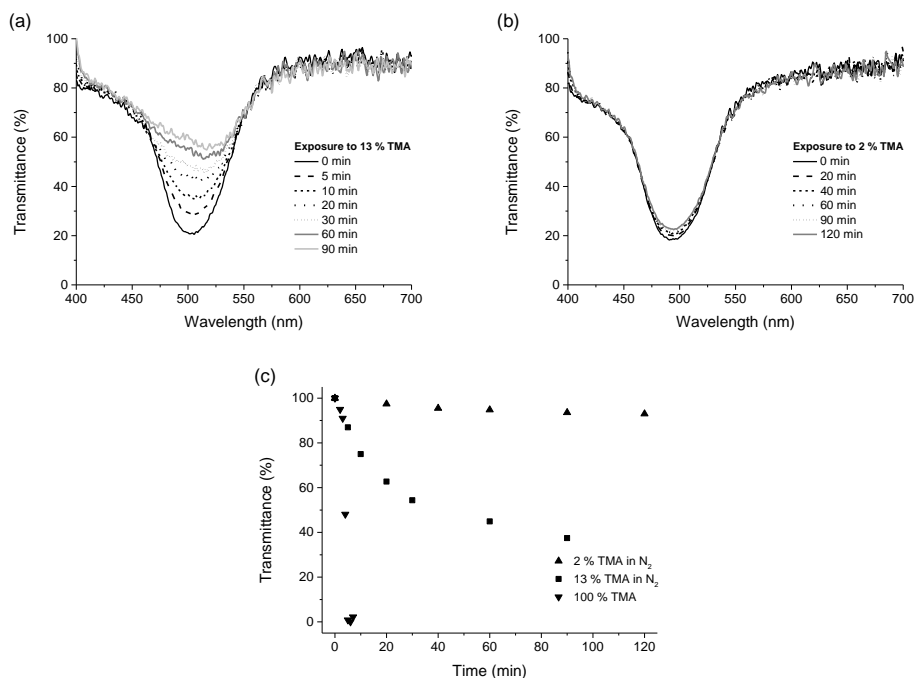


Figure 6.4 UV/Vis transmission spectra with circularly polarised light of the CLC film, taken after different exposure times to (a) 13% and (b) 2% TMA in nitrogen as carrier gas. (c) A plot of the transmission intensity change at the maximum SRB (λ_{Rmax}) of CLC films exposed to 2% (SRB = 495 nm), 13% (SRB = 507 nm) and 100% (SRB = 507 nm) TMA in nitrogen as carrier gas for different exposure times.

To investigate the response mechanism of the CLC films to TMA vapour, the samples were analysed by reflectance FT-IR spectroscopy before and after exposure to pure TMA (Figure 6.3d). The signal of the hydrogen-bonded carbonyl at 1680 cm^{-1} disappeared clearly after the treatment, while a signal related to the carboxylate salt appeared at 1365 cm^{-1} . Furthermore, the small signals between 2700 and 2450 cm^{-1} , which are attributable to the OH stretching, vanished after the TMA treatment. It can therefore be concluded that trimethylamine gas is acting as

a base that breaks up the carboxylic acid hydrogen-bonded network.²⁴ A polymer salt was formed, disrupting the cholesteric molecular order and resulting in the disappearance of the green reflection. Similar losses in molecular order have been found previously for smectic hydrogen-bonded polymer networks after treatment with an alkaline solution.²⁶

6.2.4 Response of the CLC sensor to TMA at high humidity

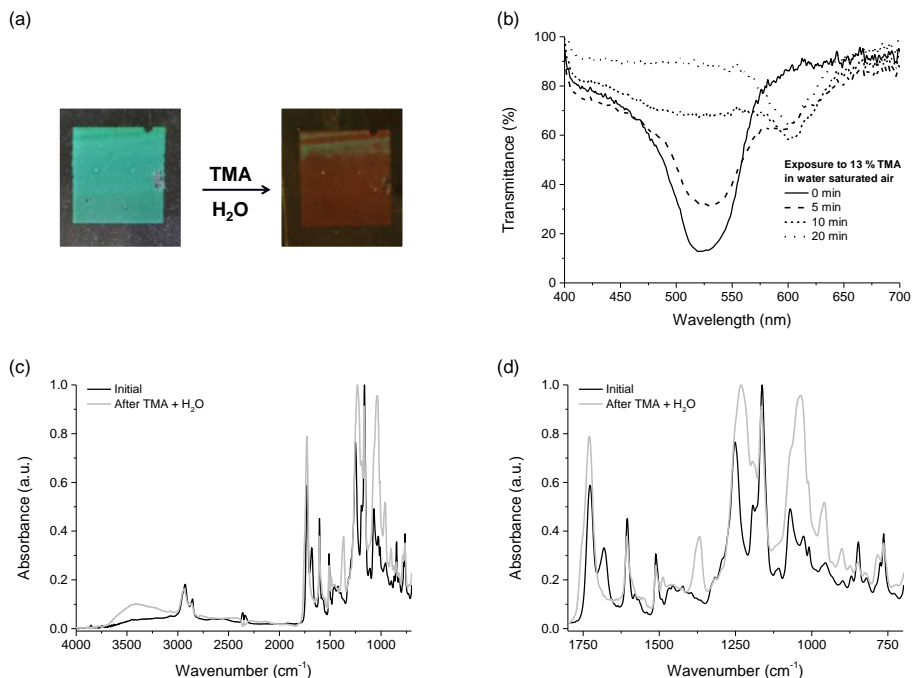


Figure 6.5 (a) Response of the CLC polymer film to a mixture of TMA and H₂O, (b) UV/Vis transmission spectra in circularly polarised light of the CLC film exposed to 13% TMA in water-saturated nitrogen as carrier gas taken after different exposure times (c, d) FT-IR data before and after TMA/H₂O exposure.

Sensing experiments were also performed using TMA mixed with water-saturated nitrogen gas (Figure 6.5 and Figure 6.6). Remarkably, when the green-reflecting films were exposed to TMA in the presence of water vapour, the colour changed from green to red (Figure 6.5a). Reflectance FT-IR spectroscopy (Figure 6.5c, d) revealed changes similar to those seen in the anhydrous TMA-exposed film (Figure 6.3d). However, in addition to the disrupted hydrogen-bonded network, water vibration signals were also observed, indicating the presence of water in the films

(Figure 6.5c). To investigate this behaviour in more detail, films were exposed to specific TMA/water vapour mixtures and analysed optically. With 13% TMA in water-saturated nitrogen gas, the intensity of the SRB at 524 nm decreased rapidly (Figure 6.5b). A red-shifted SRB around 600 nm appeared after only 5 minutes of exposure. After 20 minutes, the original SRB at 524 nm had disappeared completely and a new red-shifted SRB at 605 nm was observed. When exposed to 2% TMA in water-saturated nitrogen gas for 60 minutes, the intensity of the original SRB decreased and the band widened (Figure 6.6a). The disappearance of the green SRB over time at high humidity was faster than in the case of TMA mixed with dry nitrogen gas (Figure 6.4c). With 13% of TMA in nitrogen gas after 90 minutes the SRB was still visible; when humidity was high, the reflection band completely disappeared after 20 minutes and there was also a red shift.

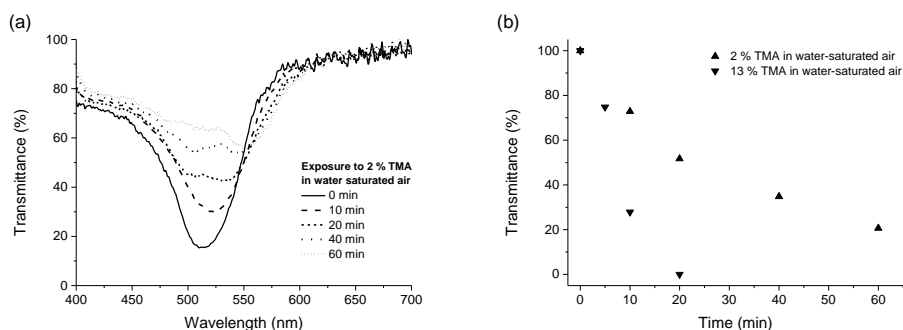


Figure 6.6 (a) UV/Vis transmission spectra with circularly polarised light of the CLC film taken after different exposure times after exposure to 2% TMA in water-saturated nitrogen as carrier gas. (b) A plot of the transmission intensity change at maximum SRB (λ_{Rmax}) of CLC films exposed to 2% (SRB = 513 nm) and 13% (SRB = 524 nm) TMA for different exposure times in water-saturated nitrogen as carrier gas.

On the basis of the data presented above, it is possible to propose the following responsive mechanism for the amine sensor. When the liquid crystalline mixture was exposed to TMA vapour, the hydrogen-bonded polymer network was disrupted by the amine base, resulting in a hygroscopic polymer salt. At high humidity, this polymer salt absorbs water,²⁴ leading to the swelling of the polymer film and an increase in the helical pitch in the film and a colour change from green to red. The fact that two reflection bands were observed simultaneously after a certain exposure time indicates non-Fickian diffusion behaviour by the TMA in the polymeric film.

6.2.5 Proof of principle: detecting fish decay

In order to test the inkjet-printed CLC films as a way of assessing food quality, the sensing of vaporous amine compounds released from decaying fish was investigated in a proof of principle experiment. A fresh piece of cod and the inkjet-printed CLC sensor foil were therefore placed in a glass vial in ambient conditions. Figure 6.7a shows the colour change of a CLC film exposed to cod. After 5 days, a clear colour change from green to red was seen that was most likely generated by the increasing amount of volatile amines due to spoilage of the cod in combination with the humid atmosphere. Moreover, after the CLC film was removed from the glass vial, the original green reflection was observed again after storage at ambient conditions for 30 minutes (Figure 6.7b). The UV/Vis spectrum of the CLC film showed the same SRB at 526 nm as in the initial film, suggesting that the total volatile basic nitrogen content and water had been evaporated from the coating.

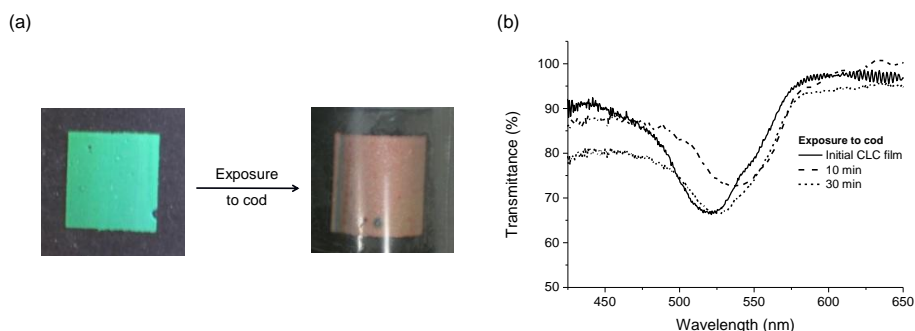


Figure 6.7 (a) Photographs of the green-reflecting CLC film before and after exposure to spoiling cod, (b) UV/Vis transmission spectra from the initial inkjet-printed CLC film and after different exposure times to ambient conditions after removal from the glass vial. The recovered film is also shown. Note: the reflections on the red film surface were caused by the vial in which the experiment was performed.

A few critical remarks about the results presented above are appropriate. First of all, sensitivity was evaluated to only a limited extent. The expectation is that sensitivity will have to be improved to produce a truly useful sensor for decaying seafood products.⁶ Secondly, the response time of the sensor is quite long, which may also limit actual practical usefulness. Furthermore, a systematic study will be needed to check for false positives. Even so, a proof of principle has now been established with respect to TMA-gas sensing using a CLC polymer film. The

expectation is that the threshold can be improved by changing the cholesteric liquid crystalline mixture, for instance by using an amine-responsive chiral dopant,^{15,16} while the response time can be enhanced by using porous CLC films.²¹

6.3 Conclusion

An optical gas sensor consisting of a hydrogen-bonded cholesteric liquid crystalline mixture was produced using inkjet printing. When the cholesteric films were exposed to TMA in water-saturated nitrogen gas, optical monitoring of the response was straightforward. The penetration of TMA gas into the hydrogen-bonded CLC film results in a hygroscopic polymer salt. Water adsorption results in the swelling of the film and an increase in the pitch that causes a colour change from green to red. To show that these reflective optical sensors can, in principle, be used in the food packaging industry, the detection of volatile amine compounds generated by spoiling fish was successfully demonstrated. These results indicate that cholesteric liquid crystalline polymers could be used as battery-free optical sensors for the detection of gases, an application of considerable interest for environmental, industrial and food quality monitoring.

Experimental section

Characterisation of the materials: The films were printed with a Dimatix Materials Printer DMP-2800 from Fujifilm. To photopolymerise the film, a collimated EXFO Omnicure S2000 mercury lamp (48 mW/cm² intensity in the range 320-390 nm) was used in a nitrogen atmosphere. The films were measured with a Shimadzu UV-3102 PC UV/Vis NIR scanning spectrophotometer. For the experiments with different gases, a UV/Vis spectrophotometer Ava-Spec-2048 Avantes, which contains a gas chamber, was utilised. The microscope images were taken using a CTR-6000 microscope from Leica. A Varian 670 FT-IR spectrometer with a slide-on ATR (Ge) and a Varian-3100 FT-IR spectrometer were used to measure IR spectra. Height profiles and 3D-images of patterned films were recorded using a 3D interferometer (Fogale Nanotech Zoomsurf).

Materials: Compounds **1** and **2** were manufactured by Merck. Benzoic acid derivative **3** was obtained from Philips and **4** was received from Synthon. *R*(+)-3-methyladipic acid (**5**) was purchased at Sigma Aldrich. The photoinitiator Irgacure 369 (**6**) was from CIBA and inhibitor hydroquinone monomethyl ether (**7**) was from Fluka. Tetrahydrofuran was obtained from Biosolve.

Preparation of the films: The film was fabricated from a mixture consisting of 22.45 wt% **1**, 27.55 wt% **2**, 16.33 wt% of each of **3**, **4** and **5**, 0.51 wt% **6** and 0.50 wt% **7**. The mixture was dissolved in tetrahydrofuran at elevated temperature in a weight ratio of 1:1. The films were printed on TAC foil (previously rubbed with a velvet cloth for planar alignment) with a Dimatix inkjet printer. The cartridge temperature was set to 50 °C and the substrate was heated to 55 °C. The films were printed with a drop spacing of 30 µm. After printing, the substrates were dried on a hot plate at 70 °C to evaporate the solvent. Before curing, the substrates were placed in a nitrogen atmosphere at room temperature for 10 minutes. During this time the mixture changed colour from red to green because a lower temperature leads to a lower CLC pitch. The films were photopolymerised in a nitrogen atmosphere for 5 minutes, during which time the colour did not alter.

Performance of UV/Vis transmission measurements: The films on the TAC foil were fixed on a cleaned glass substrate in order to place the films in the right position in the gas chamber. Background measurements for the UV/Vis transmission spectra were quantified with an empty piece of TAC foil on a similar glass substrate.

References

- 1 H. Xu, P. Wu, C. Zhu, A. Elbaz and Z. Z. Gu, *J. Mater. Chem. C*, 2013, **1**, 6087-6098.
- 2 C. Fenzl, T. Hirsch and O. S. Wolfbeis, *Angew. Chem., Int. Ed.*, 2014, **53**, 3318-3335.
- 3 J. H. J. Huis in't Veld, *Int. J. Food Microbiol.*, 1996, **33**, 1-18.
- 4 M. Sivertsvik, W. K. Jeksrud and J. T. Rosnes, *Int. J. Food Sci. Technol.*, 2002, **37**, 107-127.
- 5 J. K. Heising, M. Dekker, P. V. Bartels and M. A. J. S. van Boekel, *J. Food Eng.*, 2012, **110**, 254-261.
- 6 V. Venugopal, *Biosens. Bioelectron.*, 2002, **17**, 147-157.
- 7 S.-W. Lee, N. Takahara, S. Korposh, D.-H. Yang, K. Toko and T. Kunitake, *Anal. Chem.*, 2010, **82**, 2228-2236.
- 8 W. Qin, P. Parzuchowski, W. Zhang and M. E. Meyerhoff, *Anal. Chem.*, 2002, **75**, 332-340.
- 9 A. Pacquit, J. Frisby, D. Diamond, K. T. Lau, A. Farrell, B. Quilty and D. Diamond, *Food Chem.*, 2007, **102**, 466-470.
- 10 A. Pacquit, K. T. Lau, H. McLaughlin, J. Frisby, B. Quilty and D. Diamond, *Talanta*, 2006, **69**, 515-520.
- 11 K. I. Oberg, R. Hodyss and J. L. Beauchamp, *Sens. Actuators, B*, 2006, **115**, 79-85.
- 12 X. Ding and K.-L. Yang, *Sens. Actuators, B*, 2012, **173**, 607-613.
- 13 L. Sutarlie, J. Y. Lim and K.-L. Yang, *Anal. Chem.*, 2011, **83**, 5253-5258.
- 14 L. Sutarlie, H. Qin and K.-L. Yang, *Analyst*, 2010, **135**, 1691-1696.
- 15 Y. Han, K. Pacheco, C. W. M. Bastiaansen, D. J. Broer and R. P. Sijbesma, *J. Am. Chem. Soc.*, 2010, **132**, 2961-2967.
- 16 A. Saha, Y. Tanaka, Y. Han, C. M. W. Bastiaansen, D. J. Broer and R. P. Sijbesma, *Chem. Commun.*, 2012, **48**, 4579-4581.
- 17 D. J. Broer, C. M. W. Bastiaansen, M. G. Debije and A. P. H. J. Schenning, *Angew. Chem., Int. Ed.*, 2012, **51**, 7102-7109.
- 18 P. V. Shibaev, D. Chiappetta, R. L. Sanford, P. Palffy-Muhoray, M. Moreira, W. Cao and M. M. Green, *Macromolecules*, 2006, **39**, 3986-3992.
- 19 P. V. Shibaev, R. L. Sanford, D. Chiappetta and P. Rivera, *Mol. Cryst. Liq. Cryst.*, 2007, **479**, 161/[1199]-167/[1205].
- 20 P. V. Shibaev, K. Schaumburg and V. Plaksin, *Chem. Mater.*, 2002, **14**, 959-961.
- 21 C.-K. Chang, C. M. W. Bastiaansen, D. J. Broer and H.-L. Kuo, *Adv. Funct. Mater.*, 2012, **22**, 2855-2859.

- 22 A. Mujahid, H. Stathopoulos, P. A. Lieberzeit and F. L. Dickert, *Sensors*, 2010, **10**, 4887-4897.
- 23 N. Kirchner, L. Zedler, T. G. Mayerhofer and G. J. Mohr, *Chem. Commun.*, 2006, 1512-1514.
- 24 N. Herzer, H. Guneyusu, D. J. D. Davies, D. Yildirim, A. R. Vaccaro, D. J. Broer, C. W. M. Bastiaansen and A. P. H. J. Schenning, *J. Am. Chem. Soc.*, 2012, **134**, 7608-7611.
- 25 F. Chen, J. Guo, Z. Qu and J. Wei, *J. Mater. Chem.*, 2011, **21**, 8574-8582.
- 26 C. L. Luengo González, C. W. M. Bastiaansen, J. Lub, J. Loos, K. Lu, H. J. Wondergem and D. J. Broer, *Adv. Mater.*, 2008, **20**, 1246-1252.

In theory, theory and practice are the same. In practice, they are not
- Albert Einstein -

Chapter 7

Technology assessment

Abstract

This chapter describes the practical applications and improvements of the developed materials as described in this thesis. Photoresponsive surface topographies can be used for different kinds of applications. In the field of microfluidics or cell culturing, for example, these responsive structures have advantages compared to static materials. In addition, responsive photonic coatings are interesting as optical sensing materials and selectivity and sensitivity can be fine-tuned by changing the molecular design of these polymer networks. Spiropyran was used here in order to make materials photoresponsive. However, adding spiropyran derivatives to nematic liquid crystals could also result in photowritable optical materials or responsive luminescent solar concentrators.

7.1 Introduction

Various kinds of responsive polymer coatings have been described in this thesis. Photoresponsive hydrogel surface topographies were developed, as well as photonic coatings based on cholesteric liquid crystal polymers that change reflection colour when exposed to a stimulus. This chapter considers the extent to which the objectives have been achieved and proposes applications for these stimuli-responsive photonic coatings.

7.2 Photoresponsive hydrogel surface topographies

7.2.1 Microfluidics

Sensor platforms that measure different parameters simultaneously are used to monitor water quality. Most of the sensor platforms currently in use for these applications are costly and they use conventional pumps, valves and detectors (Figure 7.1a). The miniaturisation of these systems will therefore produce enormous cost savings. One approach is to use a microfluidic chip containing different chambers with multiple stimuli-responsive materials for sensing applications (Figure 7.1b and c show an example of a chip of this kind, and the dimensions). Replacing the current sensors with low-cost microfluidic systems in this way could lead to widely-applicable autonomous chemical sensors that can be used for the simultaneous detection of a range of analytes.

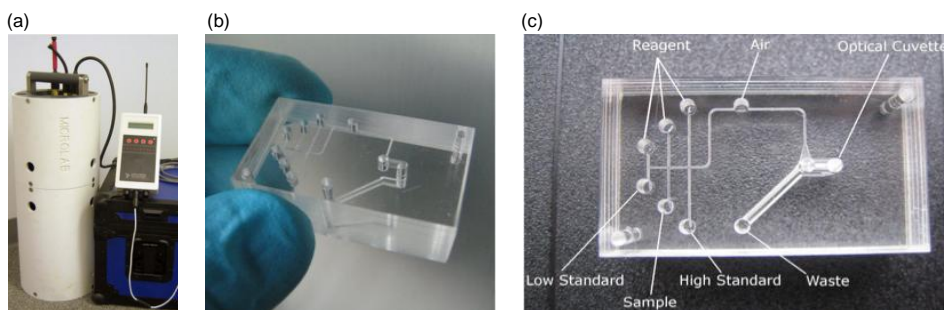


Figure 7.1 (a) A sensor platform currently in use. (b, c) Fluidic chips used in autonomous instruments showing fluidic inputs, optical cuvette and waste output. In these designs, all fluidic handling components (pumps, valves) are located off-chip, cutting costs and reducing dead volume. Reproduced with permission from references 1-3.

As discussed in greater detail in Chapter 1, photoresponsive materials can be used in microfluidic devices. The main advantage is the non-invasive character of light as a stimulus. In other words, the microfluidic device can be operated without physical contact. The preparation of photoresponsive valves has been a focus of particular interest, as well as flat surfaces locally exposed to light to obtain a certain topography.^{4,6} In Chapter 3, for example, masked light exposure leads to the formation of a surface relief structure. Flow and mixing behaviour in a microfluidic device is dependent on the structure in the channels of the surface. An alteration in the channel's interior can therefore lead to a change in the performance of the microfluidic system. In addition to photoresponsive coatings, responsive photonic coatings of the kind described in Chapters 4-6 can be employed for the optical detection of analytes. Both types of coating are appealing options in microfluidic devices.

7.2.2 *Cell culturing*

Photoresponsive coatings are potentially interesting for biomedical applications. These coatings could be used to control biological activity, and for the immobilisation of proteins and antibodies. They could also be used to modulate the growth of bacteria and cells and, indeed, photoresponsive hydrogel structures have been used for controlled cell culturing, which requires closely-controlled conditions as cells are highly sensitive to changes in their surroundings.⁷⁻⁹ The hydrophilicity and surface topography of substrates used for cell growth are therefore of crucial importance. A material which can reversibly switch its properties between cell-attractive and cell-repellent could be used to produce a functional substrate for tissue engineering.

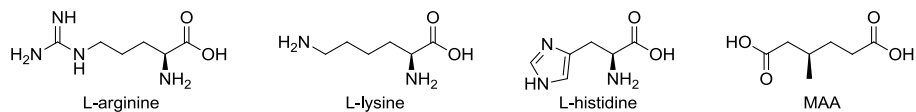
The photoresponsive materials described in this thesis could be useful in the field of cell culturing. The coatings that operate in a neutral aqueous environment, and which are described in Chapter 3, are of particular interest. In addition to the photo-induced change in hydrophilicity, there is also a change in the actual surface topography. Preliminary studies were performed on the ratchet-like structures and those experiments showed that it is indeed possible to grow cells on these substrates at 37 °C. Further development in this direction could result in systems for photo-induced cell harvesting.

7.3 Responsive cholesteric coatings

As described in the previous section, sensor platforms are rather costly. Responsive materials can be used for the miniaturisation of these devices. Optically responsive materials are a particularly attractive option for sensing because interpretation of the response is straightforward. Chapters 4, 5 and 6 presented responsive cholesteric polymer coatings. In some of these coatings, applying a stimulus alters the surface topography. The volume changes also result in changes in colour reflection. Chapter 5 described the development of a novel humidity-responsive visual sensor based on an interpenetrating polymer network. Chapter 6 looked at a coating that responds to gaseous amine. The drawback of these cholesteric liquid crystal-based sensors is their poor selectivity and sensitivity. Sections 7.3.1 and 7.3.2 discuss some possible avenues for the enhancement of the selectivity and sensitivity of these sensors.

7.3.1 *Enantioselective sensing*

Enantioselective sensing is an important topic in the pharmaceutical and agrochemical industry due to the increasing importance of enantiomerically pure compounds and drugs. There is therefore a demand for fast, sensitive, selective, and practical sensors for the stereochemical analysis of chiral building blocks. The amine-responsive material described in Chapter 6 is based on a hydrogen-bonded cholesteric material with a mobile chiral dopant of the kind presented by Shibaev and co-workers.¹⁰ Initially, they reported on the detection of aqueous solutions of naturally occurring amino acids (L-arginine, L-lysine and L-histidine, Scheme 7.1), focusing in particular on the response of the polymer coating to L-arginine. This amino acid gave the fastest response due to the high pK_a (12.48) of the guanidinium group, which leads to the rapid deprotonation of the carboxylic acids present in the polymer coating. As in the mechanism described in Chapters 4, 5 and 6, the coating becomes hygroscopic and takes up water. The volumetric increase of the coating leads to the reflection of light with longer wavelengths.



Scheme 7.1 Naturally-occurring amino acids L-arginine, L-lysine and L-histidine. The mobile chiral dopant (MAA) used for the preparation of the hydrogen-bonded cholesteric sensor is depicted on the right.

An interesting extension of this research is the development of an enantioselective optical sensor. Cholesteric liquid crystalline polymers have a preferred chiral helical organisation which could influence the penetration of chiral molecules. Depending on the chirality, molecules will diffuse faster or slower into the coating. Our initial experiments used the green-reflecting coating described in Chapter 6. When the coating was placed in a 10 wt% L-arginine solution, a red shift of the reflection band was observed (Figure 7.2a). As with the results set out in Chapter 6, there was a slight delay before the colour shift to red became visible. When the reflection band equilibrated, the sample was allowed to dry and the initial green reflection band returned. However, due to formation of the salt, the coating became water-responsive: when placed in water, the material instantly turned red. FT-IR spectroscopy showed the disappearance of the signal related to hydrogen-bonded carboxylic acids at 1698 cm^{-1} and the appearance of a signal related to the carboxylate salt at 1381 cm^{-1} , indicating that the mobile chiral dopant MAA had been replaced by L-arginine (Figure 7.2b). In a subsequent experiment, the same green-reflecting coating was treated with a D-arginine solution, resulting in a response with a comparable timescale. This preliminary result shows that enantioselective sensing is not possible with a coating prepared from this monomer mixture. The lack of enantioselectivity is probably a result of the high porosity of the system. An increase in the crosslink density or a reduction in the amount of the pore-creating component MAA in the monomer mixture may result in an enantioselective response from the sensor since these modifications would suppress the penetration of molecules into the coating. Nevertheless, it would be interesting to explore enantioselective sensing in a more systematic approach.

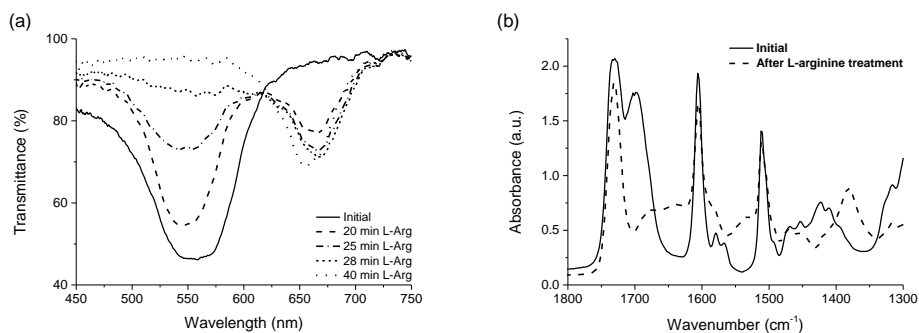
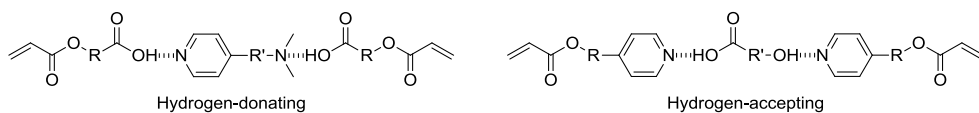


Figure 7.2 (a) UV/Vis spectra for the response of an MAA-based cholesteric coating to 10 wt% L-arginine and (b) FT-IR spectra of the initial and the L-arginine-treated coating

7.3.2 Analyte-selective sensing (molecular imprinting)

The approach presented above for the development of an enantioselective optical sensor is based on the ability of basic molecules to deprotonate carboxylic acid groups. The drawback is that materials of this kind can be cross-sensitive to various analogues of the analyte. A more elegant approach is molecular imprinting.^{11,12} In this method, a monomer mixture is polymerised in the presence of template molecules extracted from the polymer network obtained. Recognition cavities complementary to the shape, size and chemical functionality of the template molecules are then obtained. These specific properties of the cavities give rise to the selective recognition of the template molecule or structurally similar compounds. Optical sensor materials prepared by molecular imprinting are mostly based on hydrogels.



Scheme 7.2 Different kinds of analytes can be molecularly imprinted by using hydrogen-bonded amines; in the structure on the left, the polymer network has a carboxylic acid interior, while the structure on the right has a basic interior

The cholesteric coatings described in Chapters 4 and 6 are based on the response of hydrogen-bonded carboxylic acid derivatives. Those hydrogen-donating materials have an affinity to basic molecules such as amines, which disrupt these hydrogen bonds. Furthermore, hydrogen bonds between an amine and a carboxylic acid are stronger than those between two carboxylic acids. A template molecule with two

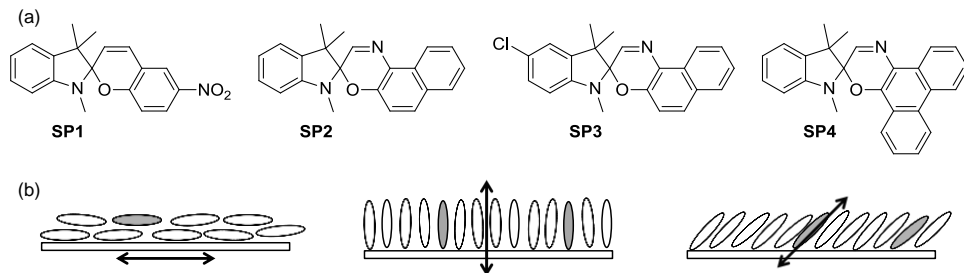
hydrogen-accepting amines will therefore be sandwiched between two carboxylic acid groups when the molar ratio is 1:2 (Scheme 7.2, structure on left). The removal of the template molecule could result in an analyte-selective sensor. Furthermore, chiral template molecules can act as a chiral dopant. In addition to materials with a hydrogen-donating interior in which basic compounds can be imprinted, polymer networks with a hydrogen-accepting interior can be prepared such as networks based on pyridine derivatives (Scheme 7.2, structure on right). Hydrogen-donating molecules such as alcohols or carboxylic acids can be imprinted in these coatings. The use of molecular imprinted (cholesteric) liquid crystal networks could open the way to a unique class of analyte-selective sensor materials.¹³⁻¹⁵

7.4 Spiropyran derivatives for other applications

In addition to using optically changing materials for sensing, various kinds of other applications could also be explored. Chapters 2 and 3, for instance, looked at the use of spiropyran for the preparation of photoresponsive materials. In this case, the corresponding colour change was used solely to analyse isomerisation behaviour. The potential application of the optical properties of spiropyran in luminescent solar concentrators and photowritable notepads will be discussed here.

A luminescent solar concentrator is a device which collects light from a large area and focuses it on a smaller area.¹⁶ These devices usually consist of an inexpensive plastic or glass sheet (a 'waveguide') doped with a dye molecule. Light emitted by this dye can be guided towards the edges of the waveguide by means of total internal reflection, where photovoltaic cells are mounted to absorb the light. Spiropyran and spironaphthoxazine derivatives are well known because they are used in photochromic sunglasses, which darken spontaneously in bright sunlight. A similar approach could be used to develop windows that can shade autonomously but also harvest energy due to the fluorescent properties of merocyanines. The emitted light can be directed towards the edges of the window by aligning the dye in a nematic liquid crystal mixture.^{16,17} When spiropyran is in its closed spiro form, the molecule is not likely to align in a liquid crystal mixture due to its non-flat molecular structure. The highly coloured, fluorescent, merocyanine molecule, on the other hand, has a relatively flat structure so that this moiety is likely to align in a liquid crystalline mixture. These anisotropic properties

could lead to the development of liquid crystal-spiropyran-based luminescent solar concentrators in which the emission of the fluorescence will be guided towards the edges of the window.^{16,18}



Scheme 7.3 (a) Derivatives of spiropyran and the similar spironaphthoxazine moiety, which were dissolved in the nematic liquid crystal mixture E7 (1 wt%). (b) Schematic representation showing chromophores (shaded grey ellipses) aligning perfectly in a planar (left), homeotropic (middle) and tilted (right) nematic liquid crystal mixture (white ellipses). The black arrow indicates the average alignment director; the optimal fluorescence emission will be perpendicular to this director.

Our initial experiments involved dissolving derivatives of spiropyran and spironaphthoxazine in the commercially available nematic liquid crystal mixture E7 (Scheme 7.3a). Planarly aligned cells were filled with these mixtures. The characteristics of these samples are listed in Table 7.1. After exposure to UV light, all samples turned bluish. Analysis of the edge emission of the cell with an integrating sphere indicated that the spiropyran derivative **SP1** is the only derivative that is fluorescent and that can be used for energy harvesting. The alignment of the LC mixture needs to be optimised to obtain the highest efficiency. A planarly aligned photochromic dye leads to optimal absorption but the emission will be guided towards the surface of the cell. Homeotropic alignment results in a directional emission towards the edges of the cell. However, in this case, the transition dipole of the chromophores is parallel to the direction of the incoming light, and so absorption is reduced. Moreover, there will be more re-absorption activity and near-homeotropic alignment is therefore expected to result in the best energy-harvesting properties (Scheme 7.3b).¹⁶

Table 7.1 Behaviour of the mixtures of E7 and spiropyran derivatives upon exposure to UV light exposure

Compound	Initial colour	Exposed to UV light ^[a]	Back-isomerisation
SP1	Colourless	Dark blue	480 sec
SP2	Colourless	Light blue	2 sec
SP3	Colourless	Light blue	5 sec
SP4	Blue	Dark blue	5 sec

[a] Illumination, using the unfiltered spectrum of an EXFO light source, was for 30 seconds

These materials could also be used as a rewritable notepad. Light pens (red, green and blue) could be used to draw or erase images in the sample depending on the wavelength used. Samples containing **SP4** are a particularly interesting candidate as they are already blue in normal conditions. Preliminary experiments showed that exposure to violet light (405 nm) leads to the darkening of the mixture, while exposure to green and red light (532 and 650 nm) reduces colour intensity. As a result, images with three different colour intensities can be produced easily.

7.5 Conclusion

This thesis described the development of a varied set of stimuli-responsive polymer coatings based on different working principles. When these materials are exposed to a specific stimulus, their functional and/or structural properties are altered reversibly. Furthermore, these coatings are very stable; after several months in storage, the response remains unaltered. Although the research in this field is still in its infancy, the materials obtained have interesting properties and they could be implemented in a wide range of applications, such as microfluidic control or the sensing of different kinds of analytes.

References

- 1 D. Diamond, F. Collins, J. Cleary, C. Zuliani and C. Fay, in *Autonomous Sensor Networks*, ed. D. Filippini, Springer Berlin Heidelberg, 2013, vol. 13, pp. 321-363.
- 2 J. Cleary, D. Maher, D. Cogan and D. Diamond, in *ICEST 2012 – the 6th International Conference on Environmental Science and Technology*, Houston, USA, 2012.
- 3 Intelesence Technologies, Web page http://www.intelesense.net/public/sc_images/products/328_large_image.jpg, (visited 24 June, 2014)
- 4 L. Florea, D. Diamond and F. Benito-Lopez, *Macromol. Mater. Eng.*, 2012, **297**, 1148-1159.
- 5 S. Sugiura, A. Szilagyi, K. Sumaru, K. Hattori, T. Takagi, G. Filipcsei, M. Zrinyi and T. Kanamori, *Lab Chip*, 2009, **9**, 196-198.
- 6 F. Benito-Lopez, R. Byrne, A. M. Raduta, N. E. Vrana, G. McGuinness and D. Diamond, *Lab Chip*, 2010, **10**, 195-201.
- 7 T. Sun and G. Qing, *Adv. Mater.*, 2011, **23**, H57-H77.
- 8 P. M. Mendes, *Chem. Soc. Rev.*, 2008, **37**, 2512-2529.
- 9 H. G. Börner and J.-F. Lutz, *Bioactive Surfaces*, Springer Berlin Heidelberg, 2011.
- 10 P. V. Shibaev, D. Chiappetta, R. L. Sanford, P. Palfy-Muhoray, M. Moreira, W. Cao and M. M. Green, *Macromolecules*, 2006, **39**, 3986-3992.
- 11 S. Xu, H. Lu, X. Zheng and L. Chen, *J. Mater. Chem. C*, 2013, **1**, 4406-4422.
- 12 Y. Ge and A. P. F. Turner, *Chem. - Eur. J.*, 2009, **15**, 8100-8107.
- 13 Y. Ishida, H. Sakata, A. S. Achalkumar, K. Yamada, Y. Matsuoka, N. Iwahashi, S. Amano and K. Saigo, *Chem. - Eur. J.*, 2011, **17**, 14693-14693.
- 14 J. D. Marty, H. Gornitzka and M. Mauzac, *Eur. Phys. J. E: Soft Matter Biol. Phys.*, 2005, **17**, 515-520.
- 15 S. Courty, A. R. Tajbakhsh and E. M. Terentjev, *Phys. Rev. Lett.*, 2003, **91**, 085503.
- 16 M. G. Debije and P. P. C. Verbunt, *Adv. Energy Mater.*, 2012, **2**, 12-35.
- 17 R. Piñol, J. Lub, M. P. García, E. Peeters, J. L. Serrano, D. J. Broer and T. Sierra, *Chem. Mater.*, 2008, **20**, 6076-6086.
- 18 P. P. C. Verbunt, A. Kaiser, K. Hermans, C. W. M. Bastiaansen, D. J. Broer and M. G. Debije, *Adv. Funct. Mater.*, 2009, **19**, 2714-2719.

Alles hat ein Ende nur die Wurst hat zwei
- Duits gezegde -

Samenvatting

Responsieve fotonische polymeren

Polymere coatings worden veelvuldig gebruikt om producten die we in het dagelijks leven gebruiken te voorzien van een beschermende of esthetische deklaag. Het merendeel van deze coatings is statisch. Dit houdt in dat de eigenschappen niet veranderen door externe factoren zoals temperatuur of licht. De verwachting is echter dat niet-statische, dynamische stimulus-responsieve coatings in de toekomst een belangrijke rol gaan spelen in bijvoorbeeld duurzame energie, gezondheidszorg en voedselveiligheid.

De ontwikkeling van responsieve materialen die op een reversibele manier reageren op externe stimuli is beschreven in dit proefschrift. Er is onderscheid gemaakt tussen licht-responsieve coatings en stimulus-responsieve fotonische coatings. Bij het eerste type coatings verandert de oppervlaktestructuur onder invloed van licht, terwijl de tweede categorie van kleur verandert als respons op een specifieke stimulus. Beide soorten coatings zijn gebaseerd op vloeibaar-kristallijne netwerken en hydrogels, waarin moleculaire veranderingen leiden tot dimensionele veranderingen in de materialen. In hoofdstuk 1 wordt een overzicht van in de literatuur gepresenteerde stimulus-responsieve fotonische coatings gegeven.

Hoofdstuk 2 beschrijft veranderingen in poly(*N*-isopropylacrylamide)-spiropyran hydrogelnetwerken onder invloed van licht. In een zuur milieu isomereert het hydrofobe spiropyran spontaan naar de hydrofiele geprotoneerde merocyanine-vorm. Met behulp van zichtbaar licht kan het molecuul weer naar de spiropyran-vorm terugschakelen. In een hydrogel leidt deze isomerisatie tot een verandering in de hydrofilititeit van het gehele netwerk, waardoor de dimensies van de hydrogel veranderen afhankelijk van de netwerkdichtheid. Met behulp van polymerisatie-gedreven diffusie kan de netwerkdichtheid in een coating gevarieerd worden. Dit leidt tot een glooiend oppervlak wanneer men de coating in een licht zuur milieu op laat zwellen. Belichting van de coating resulteert in een afname in hoogte van de oppervlaktestructuur.

In hoofdstuk 3 worden licht-responsieve hydrogels die bij neutrale pH werkzaam zijn beschreven. De hydrogel bevat acrylzuur dat als interne protonbron dient. Met behulp van polymerisatie-gedreven diffusie zijn vergelijkbare coatings als in hoofdstuk 2 verkregen. Verder zijn asymmetrische zaagtandstructuren gemaakt met behulp van een gestructureerd substraat. In deze systemen is de netwerkdichtheid in de gehele coating constant. De verandering van de oppervlaktestructuur na belichting is het resultaat van het dikteverschil van de hydrogel. De mate van vervorming is afhankelijk van de netwerkdichtheid.

In hoofdstuk 4 worden fotonische coatings, gebaseerd op waterstofgebrugde cholesterische vloeibare kristallen, behandeld. Een eigenschap van de cholesterische vloeibaar-kristallijne fase is de alternerende brekingsindex, welke resulteert in gedeeltelijke reflectie van invallend licht. Met behulp van een dubbele fotopolymerisatie-procedure zijn watergevoelige oppervlaktestructuren gemaakt met cholesterische en isotrope domeinen. De coating kan worden geactiveerd door behandeling met een alkalische oplossing, waardoor de waterstofbruggen verbroken en hygroscopische zouten gevormd worden. Als gevolg van de verschillende moleculaire organisaties hebben de isotrope gedeelten geen voorkeur voor uitzetting in een bepaalde richting, terwijl de cholesterische gebieden voornamelijk in de z-richting zwellen. Door dit verschillende zwelgedrag neemt het verschil tussen de hoogte van de twee gebieden toe wanneer de coating met water in contact komt. Bovendien zijn de isotrope gebieden kleurloos en transparant, terwijl de kleur van de cholesterische gedeelten er afhankelijk van is of de coating zich in een droge of natte omgeving bevindt. Met dezelfde techniek zijn ook dubbel-gekleurde coatings gemaakt, waarbij beide gebieden watergevoelig zijn.

Een nieuwe methode voor de productie van optische luchtvochtigheidssensoren met een breed bereik is beschreven in hoofdstuk 5. Hiervoor zijn zogenaamde interpenetrerende polymere netwerken gebruikt, waarbij cholesterische vloeibaar-kristallijne materialen met hydrogels zijn gecombineerd. Tijdens de productie neemt het cholesterisch-polymere netwerk een monomeer mengsel, gebaseerd op acrylzuur, op. Vervolgens wordt dit mengsel in het netwerk gepolymeriseerd. Met behulp van een alkalische oplossing verandert het polyacrylzuur-netwerk in hygroscopisch kaliumpolyacrylaat. Omdat dit netwerk verweven is met het cholesterische netwerk, resulteert de luchtvochtigheidsafhankelijke zwelling van

het polyacrylaat in zwelling van het gehele materiaal. De uitzetting het cholesterische netwerk veroorzaakt een kleurverandering. Verder is een interpenetrerend polymeernetwerk gemaakt, dat alternerende domeinen van kaliumpolyacrylaat en polystyreen bevat. Aangezien kaliumpolyacrylaat hygroscopisch is, maar polystyreen nagenoeg ongevoelig is voor vocht, is de oppervlaktestructuur van deze coating afhankelijk van de luchtvochtigheid.

Hoofdstuk 6 beschrijft de ontwikkeling van een waterstofgebrugde cholesterisch vloeibaar-kristallijne coating die reageert op trimethylaminegas (TMA), een stof die vrijkomt bij het rottingsproces van vis. Vergelijkbaar met de behandeling met alkalische oplossingen, deprotoneert het basische TMA de carboxylen in het materiaal, waardoor carboxylaatzouten ontstaan. Onder droge omstandigheden leidt dit tot een afname in de moleculaire orde en een afname van de intensiteit van de initieel groene reflectie. Echter, bij een hogere luchtvochtigheid zwelt de coating en wordt een kleurverandering van groen naar rood waargenomen.

Concluderend laat het onderzoek in dit proefschrift zien dat responsieve fotonische coatings gemaakt kunnen worden voor een reeks van toepassingen. In hoofdstuk 7 worden enkele interessante toepassingen nader toegelicht. De fabricage van licht-responsieve coatings is interessant voor verschillende toepassingen, van microfluidica tot celcultuur. Op het gebied van optische sensoren zijn inleidende experimenten uitgevoerd, welke de selectiviteit van de sensoren kunnen verbeteren. Verder is het gebruik van het fotochrome spiropyran voor andere toepassingen zoals slimme ramen en schrijfbaar optische materialen beschreven.

List of publications

Publications related to this thesis

Stimuli-responsive photonic polymer coatings

J. E. Stumpel, D. J. Broer and A. P. H. J. Schenning, *Chemical Communications*, 2014, Accepted manuscript.

Photoswitchable ratchet surface topographies based on self-protonating spiropyran-NIPAAm hydrogels

J. E. Stumpel, B. Ziółkowski, L. Florea, D. Diamond, D. J. Broer and A. P. H. J. Schenning, *ACS Applied Materials & Interfaces*, 2014, **6**, 7268-7274.

Optical and topographic changes in water-responsive patterned cholesteric liquid crystalline polymer coatings

J. E. Stumpel, D. J. Broer, C. W. M. Bastiaansen and A. P. H. J. Schenning, *Proceedings of SPIE 9137*, 2014, 91370U.

An optical sensor for volatile amines based on an inkjet-printed, hydrogen-bonded, cholesteric liquid crystalline film

J. E. Stumpel, C. Wouters, N. Herzer, J. Ziegler, D. J. Broer, C. W. M. Bastiaansen and A. P. H. J. Schenning, *Advanced Optical Materials*, 2014, **2**, 459-464.

Photoswitchable hydrogel surface topographies by polymerisation-induced diffusion

J. E. Stumpel, D. Liu, D. J. Broer and A. P. H. J. Schenning, *Chemistry - A European Journal*, 2013, **19**, 10922-10927.

Other publication

The mechanism of the oxidation of benzyl alcohol by iron(III)nitrate: conventional versus microwave heating

M. H. C. L. Dressen, J. E. Stumpel, B. H. P. van de Kruijs, J. Meuldijk, J. A. J. M. Vekemans and L. A. Hulshof, *Green Chemistry*, 2009, **11**, 60-64.

Acknowledgements/dankwoord

De afgelopen jaren heb ik me met veel plezier met mijn promotietraject beziggehouden. Ik heb mensen leren kennen en van sommigen ook weer afscheid genomen. Graag wil ik een aantal mensen bedanken voor hun bijdrage op verschillende gebieden.

Allereerst ben ik Albert en Dick dankbaar voor het vertrouwen dat ze in me gesteld hebben door mij in de vakgroep aan te nemen. Beste Albert, sorry dat je je af en toe zorgen hebt moeten maken vanwege mijn nonchalant-ogende houding wanneer alles niet geheel volgens planning gaat. Hopelijk ben je uiteindelijk toch tevreden met de resultaten van mijn onderzoek. Ik vond het fijn te werken met zo'n enthousiaste begeleider en wens je alle goeds met "jouw" SFD. Dick, bedankt dat je altijd tijd kan maken voor vragen van verschillende aard. Veel succes met je avonturen bij ICMS en in China.

I would like to thank the committee members, Professor D. Diamond, Dr. N. Katsonis, Professor J.M.J. den Toonder, Professor C.W.M. Bastiaansen and Dr. A.C.C. Esteves for taking the time to carefully read the manuscript and give useful comments and suggestions. Dermot, I would like to thank you, Bartosz and Larisa for your help during my stay in Dublin, which led to Chapter 3 of this thesis.

The main reason I wanted to start a doctorate project was the pleasant and informal working atmosphere that I experienced during my graduation project in Nijmegen. Many thanks to everybody for their contributions!

Hoewel het slechts een klein deel van dit proefschrift omvat, heb ik me het eerste jaar van mijn promotie voornamelijk met organische synthese op de derde verdieping bezig gehouden. Hierbij heb ik veelvuldig gebruik gemaakt van de expertise van Jef Vekemans en Johan Lub. I would also like to acknowledge the help of the analytic team from SMO (Ralf, Joost, Lou) with the characterisation of

various compounds. Sinds ik naar de begane grond verhuisd ben krijg ik dagelijks de nodige portie onzin van Michel en Rudy op mijn dak, wat ik erg op prijs stel.

I am grateful to Philippe Leclère for his AFM analysis of the cholesteric samples. Verder ben ik Anne erkentelijk voor de mooie SEM- en TEM-opnamen die ze voor me gemaakt heeft. Pauline bedank ik voor verschillende instructies. Marco wil ik bedanken voor zijn moeite om mij met röntgendiffractie te helpen.

On three occasions, I had the privilege of supervising students with their research projects. Jeroen, op de een of andere manier ben je maar niet weg te krijgen bij SFD, succes met je spiro's! Baran, although we did not obtain the results we expected, I'm glad you enjoyed your stay in Eindhoven. Dear Elda, without your help chapter 5 might not even have existed. I was amazed to see how smooth and easy the work seemed to be in your hands. Good luck with your Master's in Leuven!

I wish to thank my group members for the great atmosphere. Mike, thanks for introducing me to your passion for board games. You always took the time to listen and talk whenever I dropped by with a question and, of course, I am grateful to Audrey for her help with questions that were too difficult or stupid. Marjolijn, bedankt voor de hulp wanneer er iets geregeld moest worden of als ik bepaalde formulieren niet begreep. I thank Danqing for helping me to get acquainted with STO 0.09. Special thanks go to Nicole, Judith and Claudia for their work related to the TMA sensor. During the last year of my doctorate, a wave of new colleagues arrived and I am happy to see how you are maintaining the group spirit.

Veel van mijn vragen als promovendus kon ik onder het genot van een kop koffie kwijt bij Paul, hoewel het bij een biertje uiteraard wat beter ging. I have enjoyed the Oktoberfest with Felix, Tom, Huub and Ties and the amazing fast-one/dancing nights with Amol. I was happy to meet Ivi, with whom I've enjoyed many coffee breaks, drinks at FORT and other events. I wish you, Nico and Gabi all the best. I thank Natalala for organising great parties and introducing me to my GhettoBruder, who shares my passion for high-quality jokes. Met My, vaak het onderwerp van deze grappen, hoop ik nog vaak onbekende gerechten te gaan eten.

Laurens, nog bedankt dat je me wakker hebt gebeld waardoor ik de vlucht naar Lissabon gehaald heb. Isja bedank ik voor de keren dat ik hulp of koffie van buiten de vakgroep nodig had.

Alsof dat nog niet alles is, wil ik ook graag mijn vrienden en familie bedanken. Ik ben alle leden van ZC de OB en VV de BB dankbaar voor alles erop en eraan. Wanneer ik mijn gedachten op een rijtje wil zetten, is Igor Kowalski altijd bereid om me bij te staan in de vorm van radje draaien en mysteries. Kees, bedankt dat ik altijd bij je kan blijven slapen als ik de volgende dag moet vliegen. Jop, ik vond het leuk dat ik je getuige mocht zijn en met een sterrenteam een vrijgezellenweekend voor je geregeld heb. Verder is het altijd fijn als de Niels weer eens voor de deur staat om mijn biervoorraad te plunderen en over gewichtige zaken te praten. Met Nikki kan ik altijd kwesties van andere orde bespreken. Het afgelopen jaar heb ik veel genoten van de vakanties en het overige vertier met Kaatje, mijn leukste (en lastigste) buurmeisje ooit.

Mijn oom Pete bedank ik voor zijn zorgvuldige tekstuele controle van dit proefschrift, waarbij hij niet is vergeten dat hij zijn neef af en toe moet pesten. Tijdens mijn promotietraject ben ik zelf ook nog eens twee keer oom geworden, dankjewel Aaf! Gerebeer is verantwoordelijk voor alle hulp esthetischer wijze en de zwaarste avonden in de kroeg. Ik ben verheugd dat Woutie en mijn surrogaattweelingbroer Dave mijn paranimfen willen zijn, hun beider reacties toen ik ze vroeg spreken boekdelen.

Als laatste wil ik mijn ouders bedanken omdat ik van ze heb geleerd vooral hetgeen te doen wat ik leuk vind. Tot nu toe gaat me dat wel goed af.

Groeten,
Jelle

Curriculum Vitae

Jelle was born on 26 June 1986 in Tilburg (Schônste stad van 't laand). As a child, he was fascinated by dinosaurs and construction toys. At secondary school (the St. Odulphuslyceum, Tilburg), he was mainly interested in science and so, after obtaining his HAVO diploma, he decided to study chemistry at Avans Hogeschool (Breda), where he graduated as a Bachelor of Applied Science, specialising in organic chemistry. After an internship with Diosynth focusing on process optimisation and a graduation project “Influences of microwave irradiation on chemical reactions” at Eindhoven University of Technology, he enrolled at Nijmegen Radboud University, where he obtained his Master’s in Professor Alan Rowan’s group with the project “Tuning polymer thickness”. He then started his doctorate studies in the “Functional Organic Materials and Devices” group at Eindhoven University of Technology under the supervision of Professor Albert Schenning and Professor Dirk Broer, resulting in the thesis you have in your hands. He is currently working on the applications of responsive materials in microfluidic devices with the same research group. He received SABIC’s 2013 Innovation Challenge Award for his work on the optical amine sensor. The passion for dinosaurs got lost somewhere, but Jelle is still playing with construction toys, although on the molecular scale.

Printed by:

Uitgeverij BOXPress, 's-Hertogenbosch

Cover design by:

Geertje Stumpel & Marijn van der Zwaag